University of Cyprus

DEPARTMENT OF BIOLOGICAL SCIENCES

THE POTENTIAL ROLE OF MIR-548C-5P IN REGULATING THE TRANSCRIPTION OF FOXC2 IN DIFFERENTIATING HUMAN PODOCYTES

DOCTOR OF PHILOSOPHY DISSERTATION

ANDREA CHRISTOFIDES

2019

Department of Biological Sciences

The potential role of miR-548c-5p in regulating *FOXC2* transcription in differentiating human podocytes

Andrea Christofides

A dissertation submitted to the University of Cyprus in partial fulfilment of the requirements for the degree of Doctor of Philosophy

December 2019

VALIDATION PAGE

Doctoral Candidate: Andrea Christofides

Doctoral Thesis Title: **The potential role of miR-548c-5p in regulating *FOXC2* transcription in differentiating human podocytes**

The present Doctoral Dissertation was submitted in partial fulfillment of the requirements for the degree of Doctor of Philosophy at the Department of Biological Sciences and was approved on the ..... by the members of the Examination Committee.

Examination Committee:

Research Supervisor:

Constantinos Deltas, Professor

Committee members:

Pantelis Georgiades, Associate Professor

Paris Skourides, Associate Professor

Charalambos Spilianakis, Associate Professor

Panos Papageorgis, Associate Professor

Declaration of Doctoral Candidate

The present doctoral dissertation was submitted in partial fulfillment of the requirements for the degree of Doctor of Philosophy of the University of Cyprus. It is a product of original work of my own, unless otherwise mentioned through references, notes, or any other statements.

Andrea Christofides

Περίληψη

Τα ποδοκύτταρα είναι διαφοροποιημένα επιθηλιακά σπειραματικά κύτταρα και αποτελούν μέρος του φραγμού σπειραματικής διήθησης στο σπείραμα κάθε νεφρώνα. Ο πρώτος μοριακός δείκτης που εμφανίζεται στα ποδοκύτταρα είναι ο μεταγραφικός παράγοντας FOXC2 και είναι απαραίτητος για την έναρξη της διαφοροποίησης, αλλά και της ανάπτυξης και ωρίμανσης των ποδοκυττάρων. Τα microRNAs είναι μια εξελικτικά διατηρημένη κλάση μικρών μορίων μη μεταφραζόμενου RNA με σημαντικό ρόλο στη ρύθμιση της έκφρασης γονιδίων. Έχει αποδειχτεί η αναγκαιότητά τους στη λειτουργία των ποδοκυττάρων, αφού όταν αφαιρεθεί το γονίδιο της ενδονουκλεάσης περιορισμού Dicer σε ποδοκύτταρα ποντικών, αυτά δεν μπορούν να διατηρήσουν τη δράση τους στο φραγμό σπειραματικής διήθησης. Προβλέψεις για ακολουθίες που ενδεχομένως στοχεύουν microRNAs σε περιοχές που θεωρούνται ως προαγωγείς ή ρυθμιστικές περιοχές μεταγραφής γονιδίων (10 χιλιάδες βάσεις πριν την αρχή του 5'UTR άκρου τους), αποκάλυψαν μια ακολουθία-στόχο με πλήρη συμπληρωματικότητα ως προς το miR-548c-5p. Η ακολουθία βρίσκεται σε μια γονιδιακή περιοχή που απέχει περισσότερο από 8kb από το γονίδιο *FOXC2*. Ενδιαφέρον παρουσιάζει το ότι τόσο το miR-548c-5p όσο και η συγκεκριμένη ακολουθία στόχος απουσιάζουν από άλλους μη πρωτεύοντες οργανισμούς. Υποθέσαμε ότι η μεταγραφή του *FOXC2* κατά τη διαφοροποίηση των ποδοκυττάρων ρυθμίζεται από το miR-548c-5p μέσω αυτής της ακολουθίας-στόχου. Σε πειράματα που έγιναν σε κυτταρική σειρά ανθρωπίνων ποδοκυττάρων με πλασμίδια ελέγχου έκφρασης λουσιφεράσης στα οποία κλωνοποιήθηκε μέσα στον ενισχυτή του πλασμιδίου η ακολουθία-στόχος, επιβεβαιώθηκε η στόχευσή της από το miR-548c-5p, με μόρια μιμητές του miRNA να μειώνουν, ενώ αναστολείς-παρεμποδιστές του να ενισχύουν την έκφραση της λουσιφεράσης. Με την εισαγωγή μεταλλάξεων σε νουκλεοτίδια της ακολουθίας στόχου που αντιστοιχούν στο seed region του miR-548c-5p, βρέθηκε πως οι επιδράσεις παύουν να υφίστανται. Επιπλέον, σε καλλιέργειες ποδοκυττάρων, τα επίπεδα του mRNA και της πρωτεΐνης FOXC2 ανταποκρίνονται στα επίπεδα του miR-548c-5p συγχρονισμένα πριν και μετά την επαγωγή της διαφοροποίησης με υψηλή στατιστική σημαντικότητα. Πειράματα ανοσοκαθίζησης χρωματίνης (ChIP) με τη χρήση αντισώματος που στοχεύει όλα τα μέλη της οικογένειας πρωτεϊνών Argonaute (AGO), αποκάλυψαν την κατάληψη της DNA ακολουθίας-στόχου από το RISC σε αδιαφοροποίητα ποδοκύτταρα και την απελευθέρωσή του με την επαγωγή της διαφοροποίησης. Αυτό έχει ως αποτέλεσμα η γενωμική περιοχή που περιλαμβάνει την ακολουθία-στόχο να αλληλεπιδρά με την περιοχή του υποκινητή του *FOXC2* και να οδηγεί

σε ενίσχυση της έκφρασης του γονιδίου, όπως φαίνεται από πειράματα 3C. Συνεπώς, η γενωμική περιοχή που περιλαμβάνει την ακολουθία-στόχο είναι πιθανόν να έχει ρόλο ενισχυτή. Επιπλέον, το μοτίβο έκφρασης του *FOXC2* κατά τη διάρκεια της διαφοροποίησης των ποδοκυττάρων φαίνεται να επηρεάζεται από το miR-548c-5p. Πιο συγκεκριμένα, σε πειράματα αποτύπωσης κατά Western και ανοσοφθορισμού, όταν τα ποδοκύτταρα αφεθούν να ανακάμψουν από την επίδραση πολλαπλών συνεχόμενων διαμολύνσεων με μιμητές του miR-548c-5p, ανακτώνται τα επίπεδα των πρωτεϊνών και κατά προέκταση η πορεία της διαφοροποίησης, όπως φαίνεται και από την πυρηνική και κυτταροπλασματική έκφραση της πρωτεΐνης FOXC2. Λαμβάνοντας υπόψη όλα τα αποτελέσματα συνολικά, προτείνεται ένας μηχανισμός δράσης μέσω του οποίου το σύμπλεγμα RISC/miR-548c-5p επηρεάζει την έκφραση του *FOXC2* και κατά προέκταση τη διαφοροποίηση των ποδοκυττάρων. Τα αποτελέσματα της μελέτης αυτής, καταδεικνύουν ένα καλά οργανωμένο μοντέλο ρύθμισης της έκφρασης του *FOXC2* μέσω μιας απομακρυσμένης ακολουθίας-στόχου για το miR-548c-5p.

Abstract

Podocytes are highly differentiated epithelial cells outlining glomerular vessels. FOXC2 is a transcription factor essential for inducing podocyte differentiation, development and maturation, and is considered to be the earliest podocyte marker. It has been found that microRNAs, a class of short non-coding single-stranded RNA molecules with a prominent role in the regulation of gene expression, are essential for podocyte function, as podocyte specific dicer knockouts fail to maintain glomerular function. miRNA prediction analysis revealed a full-length target site for the primate-specific miR-548c-5p at a genomic region >8kb upstream of *FOXC2*. Interestingly, both miR-548c-5p and this specific target site are absent from non-primates. It was hypothesised that the transcription rates of *FOXC2* during podocyte differentiation might be tuned by miR-548c-5p through this target site. Experiments were performed with cultured human podocytes, transfected with luciferase reporter constructs bearing this target site region within an enhancer element of the native plasmid. The results confirmed a seed-region driven targeting potential by the miRNA, with mimics downregulating and inhibitors enhancing luciferase activity. Introducing mutations into the miRNA target seed region abolished the expected response. Moreover, also in cultured podocytes, FOXC2 mRNA and protein levels responded to miR-548c-5p abundance in a very coordinated manner before and after induction of differentiation, with high statistical significance. Ago-ChIP experiments using a Pan-Ago antibody revealed occupancy of the miRNA target site by miRNA/RISC in undifferentiated cells and its release when differentiation is initiated. The target site is thus allowed to interact with the gene's promoter region leading to amplification of *FOXC2* expression, as shown by chromosome conformation capture and qRT-PCR. Results are suggestive of an enhancing role for the region bearing the miRNA target site. Moreover, the expression pattern of *FOXC2* during podocyte differentiation seems to be affected by miR-548c-5p, as removal of miR-548c-5p results in increased FOXC2 protein levels and cells resembling those undergoing differentiation. More specifically, in Western blot and immunofluorescence experiments, allowing hPCs to recover from the effect of several sequential miRNA mimic transfections, resulted in a rescue in protein levels and resumption of differentiation by examining the nuclear or cytoplasmic localization of FOXC2. Taking everything into account, a mechanism is proposed by which the RISC/miR-548c-5p complex influences the expression of *FOXC2* and consequently affects podocyte differentiation. Collectively, results indicate a well-orchestrated regulatory model of *FOXC2* expression by a remote upstream target site for miR-548c-5p.

Acknowledgments

First and foremost, I would like to express my gratitude to my supervisor Prof. Constantinos Deltas for his continuous support, guidance and invaluable input for the completion of this PhD thesis. Without him the Molecular Medicine Research Centre would not be the supportive and stimulating environment it is today.

Secondly, I would like to thank Dr Gregory Papagregoriou, without whom this project would not have been possible. Thank you Greg for your ideas, your knowledge, your time, your support and your patience through failures and mishaps, but most of all for passing to me your determination and passion for science.

I would also like to acknowledge our collaborators, Prof. Norbert Gretz and Dr Harsh Dweep for their help with the miRWalk prediction analyses and statistics, Dr Kyriacos Felekkis for his input on experimental processes and Dr Neoklis Makrides for his help with confocal microscopy.

In addition, I would like to thank all of the lab members at MMRC, both past and present. Without you the endless hours at the lab would have been unbearable. So thank you for all the laughs that we shared together, for your friendship and support as well as your feedback and assistance whenever I needed it. I am proud to say that I can call most of you now my friends.

A big thank you goes out to my friends who have been there throughout every step of the way and have provided a shoulder to lean on whenever it was needed and great company at times good and bad.

Last but not least, I would like to thank my family. Their love and support has been imperative throughout all these years and I will never be able to fully express how grateful I am to them and how much I love and respect them for the people that they are and for the person they make me want to be. Thank you.

Contents

List of Figures and Tables

List of Abbreviations

Ago Argonaute Protein
Ago-ChIP Argonaute Protein Chromatin Immunoprecipitation
ANOVA Analysis of Variance
BAC Bacterial Artificial Chromosome
BCP Bromochloropropane
bp basepairs
cDNA complementary DNA
ChIP Chromatin Immunoprecipitation
CP Crossing Point
CRC Colorectal cancer
CSDC2 Cold-shock domain containing protein C2
DMEM Dulbecco's Modified Eagle Medium
DNA Deoxyribonucleic Acid
ds double stranded
DTT Dithiothreitol
ECL Enhanced chemiluminescence
E.coli Escherichia coli
EDTA Ethylenediaminetetraacetic Acid
ESDR End Stage Renal Disease
FBS Fetal Bovine serum
FOXC2 Forkhead Box C2
GAPDH Glyceraldehyde-3-phosphate Dehydrogenase
GBM Glomerular Basement Membrane
GFB Glomerular Filtration Barrier
HEK Human Embryonic kidney cells
HEPES 4-(2-hydroxyethyl)-1-piperazineethanesulfonic acid
hPCs Human Podocyte Cells
HRP Horseradish Peroxidase
Ig Immunoglobin
IP Immunoprecipitation
kb kilobases
LNA Locked Nucleic Acid
LncRNA Long Non-Coding Ribonucleic Acid
mActnB mouse β-Actin
MADE1 Mariner Derived Element 1
MCS Multiple Cloning Site
mFOXC2 mouse FOXC2
MITEs Miniature Inverted-repeat Transposable Elements
mMTHFSD mouse MTHFSD
mPCs Mouse Podocyte Cells
mRNA messenger RNA
MTHFSD Methylenetetrahydrofolate synthase domain-containing protein
NC Negative Control
NP-40 Nonidet P-40
NPHS1 nephrin
NPHS2 podocin
nt nucleotides
PAR promoter-associated ribonucleic acid

PBS Phosphate Buffered Saline
PCI Phenol Chloroform Isoamyl alcohol
PCR Polymerase Chain Reaction
PI Protease Inhibitor
piRNAs Piwi-Interacting RNAs
POLR3D RNA polymerase-III subunit D
PR Progesterone Receptor
pre-miRNA precursor miRNA
pri-miRNA primary miRNA
PVDF Polyvinylidene Fluoride
qRT-PCR Quantitative Real-Time PCR
RASSF3 Ras-association factor 3
RISC RNA-Induced Silencing Complex
RITS RNA-Induced Transcriptional Silencing complex
RLU Relative Light Units
rmIFN-gamma mouse recombinant Interferon gamma
RNA Ribonucleic Acid
RNAi RNA interference
RNA Pol II RNA polymerase II
RPMI Roswell Park Memorial Institute Medium
rRNA ribosomal RNA
RT Reverse Transcription
SD Standard Deviation
SDM Site-Directed Mutagenesis
SDS Sodium Dodecyl Sulfate
siRNA small interfering RNA
SYNPO synaptopodin
snoRNA small nucleolar RNA
snRNA small nuclear RNA
TE Transposable Element
TGA Transcriptional Gene Activation
TGS Transcriptional Gene Silencing
TNBC Triple Negative Breast Cancer
tncRNAs tiny non-coding RNAs
UTR untranslated region
wt wild type
WT1 Wilms' Tumor 1
3C Chromosome Conformation Capture

Chapter 1: Introduction

Over the past decades small RNA molecules have been found to be crucial modulators of gene expression in a range of different organisms including plants, animals and fungi. These small molecules represent a highly conserved ancient regulatory mechanism, as they are involved in a variety of RNA-mediated gene expression control pathways that have been preserved throughout evolution. Small RNA molecules include but are not limited to short interfering RNAs (siRNAs), tiny non-coding RNAs (tncRNAs), Piwi-interacting RNAs (piRNAs) and microRNAs (Elbashir et al., 2001, Ambros et al., 2003, Aravin et al., 2007, Lee and Ambros, 2001).

1.1 microRNAs (miRNAs)

MicroRNAs (miRNAs) are a class of short non-coding single-stranded RNA molecules, sized 21-25 nucleotides, found in plants, animals and some viruses. They comprise one of the most abundant gene families in eukaryotes with a prominent role in the regulation of gene expression (Wu et al., 2006, Filipowicz et al., 2008). Mature microRNAs are 21-23 nucleotides long and are derived from longer endogenous transcripts with a distinctive hairpin structure (Ambros et al., 2003, Bartel, 2004). These small RNAs function predominantly as downregulators of gene expression by targeting mRNA molecules for decay via deadenylation or degradation through cleavage, or by repressing translation initiation (Wu et al., 2006, Filipowicz et al., 2008). A single mRNA molecule might be targeted by more than one microRNA and inversely each microRNA might have more than one mRNA targets to which it binds through partial complementarity (Farazi et al., 2008, Lewis et al., 2003).

Generally, microRNAs regulate expression by binding to a miRNA recognition element (MRE) located at the 3' UTR of the mRNA target through a Watson-Crick base-pairing manner (Reinhart et al., 2000). MREs have also been found to be prevalent in 5'UTR sequences as well as the coding region. (Lee et al., 2009, Forman and Coller, 2010). Various experimental and bioinformatics approaches have demonstrated that target recognition and binding properties of miRNAs mostly rely on their "seed" region, representing nucleotides 2-8 from the 5'end of each miRNA (Kiriakidou et al., 2004, Chen et al., 2008). Even though base pairing of the 3'end of the miRNA with the mRNA target is neither necessary nor essential for repression, strong pairing within this region can moderately compensate for

weaker seed region binding or enhanced repression (Brennecke et al., 2005, Lal et al., 2009). In some rare cases nucleotides in the middle portion of the microRNA, ~4-15, seem to be the determinant for a strong miRNA-mRNA target binding (Grimson et al., 2007, Shin et al., 2010). Moreover, in a 2012 study by Chi et al., an additional non-canonical interaction was observed when target sites for miR-124 containing a "bulged-out" G nucleotide at position 5 or 6 were found in abundancy in the mouse brain. This mode of regulation termed as the "pivot-pairing" rule, was discovered to be the case for more than 15% of all Ago-miRNA-mRNA interactions in mouse brain and such sites were found to be evolutionarily conserved (Chi et al., 2012). Nucleation bulges were also observed in the human brain cell and have improved the search and identification of novel miRNA target sites (Boudreau et al., 2014, Stefani and Slack, 2012, Seok et al., 2016).

microRNAs have been found to be prominent regulators of gene expression in almost all tissues and cell types. More specifically, in a study performed by Landgraf et al. samples from both humans and rodents were used for isolation and sequencing of small RNAs from twenty-six cell types and organs, which revealed that miRNAs are differentially expressed in the vast majority of cell types and tissues. In addition, specific miRNAs or miRNA families were found to be greatly associated with particular samples (Landgraf et al., 2007). Thus, the distinctive combination of miRNAs found at a given time within a specific cell type or tissue might temper with the expression of the mRNAs present.

1.2 Biogenesis of microRNAs

miRNA genes can be found in intergenic regions, within the exons or introns of non-coding transcription units or within the introns of protein-coding transcriptomes either at the sense or antisense orientation (Lagos-Quintana et al., 2001, Rodriguez et al., 2004). This finding indicated that miRNAs are transcribed as distinct, autonomous transcription units, whereas miRNAs clustered together are produced from a single polycistronic primary transcript (Lee et al., 2002, Lagos-Quintana et al., 2001, Rodriguez et al., 2004). The majority of primary miRNA transcripts (pri-miRNAs) are transcribed by RNA Polymerase II (Lee et al., 2004), whereas RNA Polymerase III is used in particular cases such as the transcription of some miRNAs interspersed with Alu elements (Cai et al., 2004).

Pri-miRNAs are usually more than 1kb in length and consist of a double-stranded stem of about 33 base pairs, a terminal loop and two flanking, unstructured, single-stranded segments (Lee et al., 2002, Liu et al., 2008). Following transcription, pri-miRNAs are cleaved to form

hairpin-like structures with a length of 60-100 nucleotides called miRNA precursors or pre-miRNAs (Denli et al., 2004, Liu et al., 2008) **(Figure 1)**. Pri-miRNA cleavage is mediated by Microprocessor complexes, which are comprised of the RNAse III enzyme Drosha and the double-stranded RNA binding protein DGCR8/Pasha (Gregory et al., 2004, Han et al., 2004). The microprocessor cleaves around the hairpin-loop structure of the pri-miRNA, creating 5'monophosphate and 3' 2-nucleotide hydroxyl overhangs and thus releases the double-stranded stem from the remainder of the pri-miRNA (Lee et al., 2003). The resulting pre-miRNAs are then transported into the cytoplasm by RanGTP and a nuclear transport receptor called Exportin-5 (Bohnsack et al., 2004, Lund et al., 2004). Exportin-5 has also been implicated in the stabilisation of the pre-miRNA as depletion of this receptor results in low pre-miRNA levels both in the nucleus and cytoplasm (Yi et al., 2003). Following cytoplasmic transport, an additional RNAse III ribonuclease called Dicer cleaves the pre-miRNA leading to the formation of a mature double stranded (ds) miRNA through the removal of the terminal base pairs and the pre-miRNA loop) (Hutvagner et al., 2001, Bernstein et al., 2001, Bohnsack et al., 2004, Lund et al., 2004). Recognition and targeting of the pre-miRNA for cleavage by Dicer is thought to be due to the 5' phosphate and 3' 2-nucleotide overhang created by Drosha (Ketting et al., 2001, Bartel, 2004).

The mature ds miRNA produced also contains a 5' phosphate and 3' overhang (Bartel, 2004). However, the ds cleavage product does not exist for long as one of the two strands is degraded whereas the other remains in the cell as the mature miRNA. It has been shown that miRNA strand selection, just like in the case of siRNAs, is mainly based on sequence characteristic features (Khvorova et al., 2003). More specifically, the strands favoured for selection have a U-bias at the 5'end and are purine-rich whereas the strands least found as mature functional miRNAs have a C-bias at their 5'end and an abundance of pyrimidines (Hu et al., 2009).

Once a miRNA matures, it becomes part of the miRNA ribonucleoprotein complex (miRNP), which includes structures that closely resemble molecules containing the RNA-induced silencing complex (RISC). This takes place through the binding of the mature miRNA to an Argonaute (Ago) protein, thus forming the principal component of the miRNP effector complex, as Ago proteins are thought to mediate the cleavage of target mRNAs via an endonuclease named Slicer (Mourelatos et al., 2002, Sasaki et al., 2003). Up until now eight Argonaute proteins have been identified in humans, from which only Ago2 has been found to be catalytically active (Liu et al., 2004). In addition to the Ago proteins, the human miRNP/RISC complexes also include but are not limited to the elF2C2 protein, an Argonaute

protein homologue and the Gemin3 and Gemin4 helicases. Through the formation of the miRNP/RISC complexes, mRNA levels can be successfully regulated (Engels and Hutvagner, 2006, Peters and Meister, 2007).

Pri-miRNA cleavage mediated by Drosha is evaded in the case of "mirtrons", a subclass of miRNAs originating from short intronic hairpins (Okamura et al., 2007). Mirtron pre-miRNAs are produced by debranching and the splicing machinery and subsequently mature through Dicer cleavage (Okamura et al., 2007, Berezikov et al., 2007). A different biogenesis strategy is implemented by a subclass of miRNAs, also originating from short introns, called "agotrons" (Hansen et al., 2016). Agotron maturation is independent of Drosha, as in the case of mirtrons, nor mediation of Dicer, even though agotrons eventually associate and are stabilised by Ago proteins (Hansen et al., 2016, Cheloufi et al., 2010).

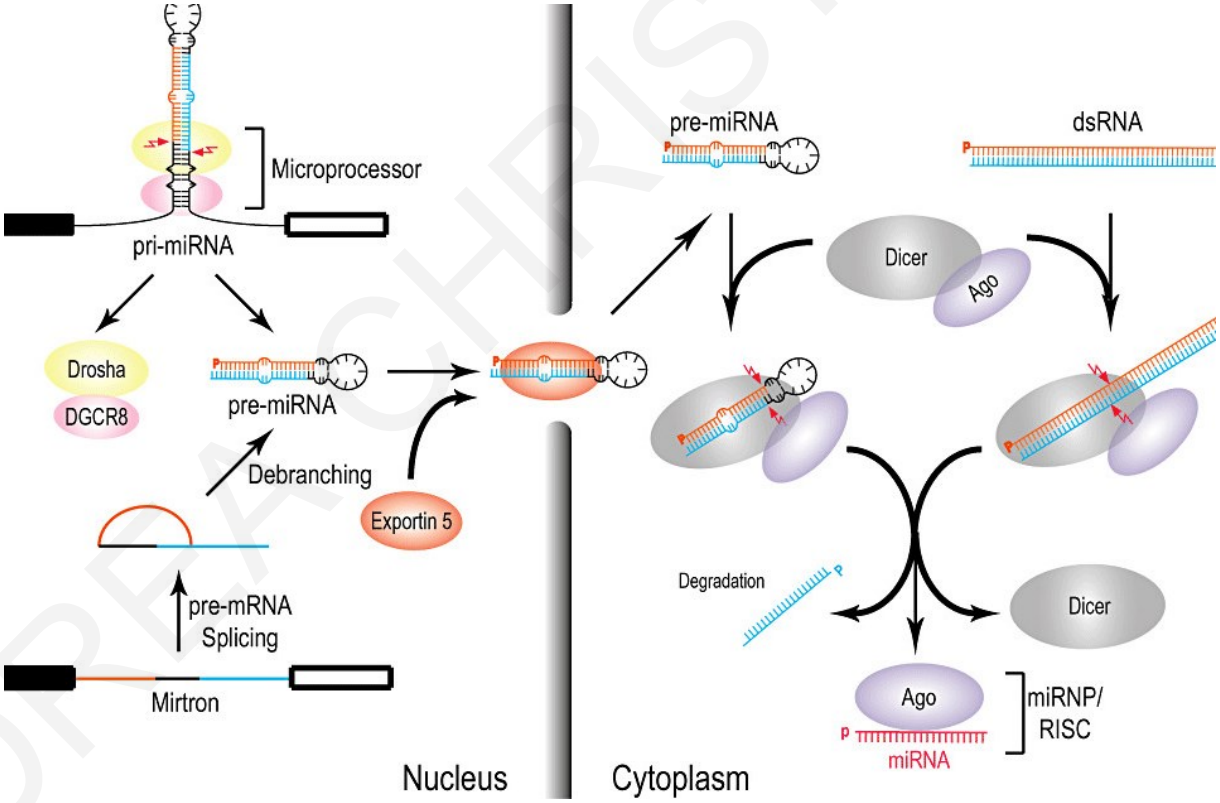

Figure 1: The miRNA biogenesis pathway. Taken from Liu et al., 2008 (Liu et al., 2008).

1.3 Nuclear functions of miRNAs

Several studies have attributed different functions for miRNAs in the nucleus. More specifically, some miRNAs have been found to post-transcriptionally regulate the

degradation of long non-coding RNAs (lncRNAs), by binding onto complementary sequences and impairing their stability and functionality (Chiyomaru et al., 2014, Zhang et al., 2013).

Moreover, miRNAs might be functionally important in the nucleolus, where they have been found to be present both in mature and pre-miRNA states (Politz et al., 2009, Bai et al., 2014). Some of these functions may include targeting of ribosome subunits and ribosomal RNA (rRNA) and thus affecting its amount in cells as well as the means by which mature ribosomes might interact with other proteins (Atwood et al., 2016). Nucleolar miRNAs might also interact with mRNAs and target them for silencing before their transport to the cytoplasm (Reyes-Gutierrez et al., 2014).

An additional role for miRNAs in the nucleus as regulators of alternative splicing has emerged following the discovery of miRNA binding sites within intronic sequences in mouse and human brain and human myocardial cells (Boudreau et al., 2014, Spengler et al., 2016). Two mechanisms have been suggested for the RISC machinery as regulators of splicing. The first one entails chromatin modifications and remodelling via miRNA, Ago1 and Ago2 recruitment at miRNA targets on both intronic and exonic sequences, whereas the second mode of action proposes hindering of the spliceosome complex recruitment by binding of the RISC complex to the nascent pre-mRNA transcript (Allo et al., 2014, Liu et al., 2015).

Finally, over the past few years a vast number of studies have examined the ability of miRNAs to act at the transcriptional level by influencing transcriptional gene activation (TGA) or transcriptional gene silencing (TGS).

1.4 miRNAs as transcriptional regulators

RNA interference (RNAi) is one of the key mechanisms of epigenetic gene silencing regulation, highly conserved in eukaryotes. More specifically, components of the RNAi machinery act at the chromatin level and drive the configuration of hetetochromatin. This particular method of transcriptional gene silencing (TGS) is governed by small non-coding RNA (Morris, 2005). Having in mind the miRNA/RISC complex, a similar complex exists for RNAi mediated TGS called the RNA-induced transcriptional silencing (RITS) complex. Examples of this mechanism of TGS are encountered in both plants and yeast. Generally, plant siRNAs, which exhibit complete complementarity with their target sequences, have

been found to alter the methylation patterns of promoter sequences at transcription start sites and thus inhibiting gene transcription (Hamilton et al., 2002). This mode of action can be seen in Arabidopsis, where siRNA mediated TGS has been primarily developed as a defence mechanism for dealing with foreign nucleic acid invasion and thus maintaining genome integrity (Matzke et al., 2004). RNAi TGS machinery in yeast also seems to have occurred for defence against extrinsic nucleic acids but also for transposable element silencing (Drinnenberg et al., 2009). It has been found that assembly of the RITS complex in yeast involves the recruitment of Ago1, which then employs other proteins such as Chp1 (a heterochromatin-associated chromodomain protein), leading to chromatin rearrangement and silencing, an event mainly observed at centromeric regions (Verdel et al., 2004). Interestingly, just as in the case of the miRNA/RISC complex, RNA polymerase II is also involved in RNAi mediated TGS, thus indicating a strong affinity between the two mechanisms (Schramke et al., 2005).

Over the past few years it has become apparent that regulation of gene transcription by small non-coding RNAs is not restricted to siRNAs. In fact, a 2010 study demonstrated that nuclear localisation of miRNAs is rather a common occurrence as deep sequencing analysis uncovered several miRNAs mainly localised in the nucleus as well as a large overlap between nuclear and cytoplasmic miRNAs, suggesting that transport of miRNAs into the nucleus is a generic event (Liao et al., 2010). In addition, several publications have shown that miRNAs are key components of gene expression control at the transcriptional level. In a 2008 study by Place et al., miR-373 was presented to increase the expression of E-Cadherin and cold-shock domain containing protein C2 (CSDC2), both genes with high sequence complementarity miR-373 target sites within the promoter (Place et al., 2008). This was the first example described of a miRNA targeting promoter sequences. Kim et al. 2008 also demonstrated that miR-320, encoded on the antisense strand within the basal promoter region of the *POLR3D* gene (RNA Polymerase III – subunit D), is acting as a cis-regulatory element of transcription by reducing the expression of that gene through binding on its complementary sequence within the promoter (Kim et al., 2008). Moreover, in a 2011 study by Younger and Corey several miRNA mimics were used to successfully impede the expression of the human progesterone receptor (PR) through binding on non-coding RNA transcripts overlapping with the promoter sequence (Younger and Corey, 2011). However, it should be noted that these studies are based on the use of artificial miRNA LNA molecules at higher concentrations than those normally encountered, which could indicate that the effects observed might not be an accurate representation of what occurs in reality.

In support of the above findings, a number of studies have established the presence of several RISC components within the nucleus including Dicer, TRBP and Ago1 and 2 (Ohrt et al., 2008). In particular, it has been shown that nuclear transport of the Argonaute proteins is facilitated by Importin-8 (Weinmann et al., 2009). Importin-8 has also been proven to mediate miRNA transport from the cytoplasm to the nucleus in an Ago2 dependent manner (Wei et al., 2014). Moreover, it has been shown that TNRC6A, the human paralog of GW182 with a prominent role in miRNA-gene silencing, can interact with Ago2 and facilitate its nuclear transportation and involvement in nuclear miRNA-mediated gene silencing, while cytoplasmic and nuclear Ago2 and TNRC6A levels seem to be interdependent (Nishi et al., 2013, Schraivogel et al., 2015). The presence of Dicer, TRBP and TNRC6A in the nucleus has also been confirmed in a 2014 study by Gagnon et al., while the absence of RISC loading and maturation factors possibly indicate differences between cytoplasmic and nuclear RISC composition and mode of action (Gagnon et al., 2014). In addition, both Ago1 and Ago2 have been associated with transcriptional gene activation or repression, either separately or together (Kim et al., 2008, Younger and Corey, 2011, Huang et al., 2013, Kim et al., 2006). The effect that this type of transcriptional gene silencing has on RNAPII levels also been established, as RNAPII has been found to be reduced in cases of transcriptional gene silencing, whereas an abundance was observed when gene expression was enhanced (Place et al., 2008, Huang et al., 2013). Furthermore, in Huang et al. 2013 a direct association between Ago1 and RNAPII is also reported, which is consistent with the RISC complex mode of action.

A number of possible ways have been suggested by which miRNAs might exert transcriptional regulation (Catalanotto et al., 2016). The first one involves alterations of the methylation status of specific sequences within the promoter region. A second premise entails affecting the transcription of genes by influencing chromatin accessibility, following the recruitment of protein inhibitory or activating complexes by the RISC complex through the recognition of miRNA target sites on the nascent RNA or non-coding promoter associated RNAs (PARs) (Matsui et al., 2013). As mentioned above, miRNAs have been found to post-transcriptionally regulate the degradation of lncRNAs. It is speculated that this could be one of the ways by which miRNAs regulate gene expression within the nucleus, as lncRNAs can epigenetically regulate gene expression through chromatin remodelling (Morris et al., 2008, Modarresi et al., 2012). Finally, it has been suggested that miRNAs have the ability to hybridise with complementary DNA sequences and promote or hinder gene expression (Corey, 2005, Younger et al., 2009).

1.5 The human glomerulus and its filtration barrier

The renal glomerulus is a knot of specialized capillaries convoluted to introduce the stream of blood to be filtered inside the kidney, surrounded by a pouch-like formation called Bowman's capsule (Greka and Mundel, 2012). The glomerular filtration barrier (GFB) is comprised by 3 main layers, the fenestrated endothelium, the glomerular basement membrane (GBM) and the visceral epithelial cells or podocytes **(Figure 2)** (Maestroni and Zerbini, 2018, Leeuwis et al., 2010).

Both the endothelium and the podocyte cells are attached to the GBM and are responsible for the maturation, maintenance and functional and structural integrity of the GBM (Abrahamson et al., 2009). Together these 3 layers as the GFB survey the mobility of the plasma ultrafiltrate towards the urinary space and prevent plasma proteins, albumin and immunoglobulins from escaping (Miner, 2012, Patrakka and Tryggvason, 2010, Abrahamson et al., 2009, Suh and Miner, 2013).

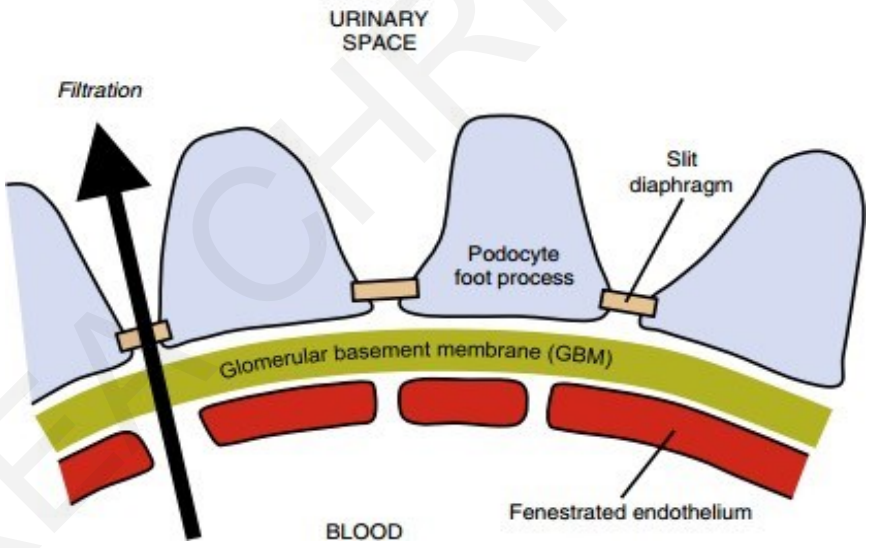

Figure 2: Schematic representation of the glomerular filtration barrier. The filtration function of the glomerulus is performed by the glomerular endothelial cells, the glomerular basement membrane GBM and the filtration slits between the podocyte cells. Taken from (Leeuwis et al., 2010).

1.5.1 Podocytes

Podocytes are highly-differentiated visceral epithelial cells and as previously mentioned are one of the three major cell types shaping up the glomerulus. They consist of a large cell body

positioned on the outer layer of the GBM as well as interdigitating primary and secondary foot processes, which expand and embrace the glomerulus and interact with the components of the GBM (Jefferson et al., 2011, Greka and Mundel, 2012, Patrakka and Tryggvason, 2010). The cell body as well as the primary and secondary foot processes, contain microtubules and intermediate filaments, i.e. vimentin and desmin, forming a dynamic cytoskeletal network, while foot processes contain long actin fibre bundles (Pavenstadt et al., 2003, Welsh and Saleem, 2011). The foot processes of adjacent podocytes are linked by a 40nm-wide network of intertwining proteins forming the glomerular slit diaphragm, which acts as the final inhibiting guard of proteins exiting and permits small molecules and water to flow through (Holthofer, 2007). Podocyte injury can cause scarring of the glomerulus, which compromises the integrity of the glomerular filtration barrier and thus leads to a variety of disorders including Alport syndrome and steroid-resistant nephrotic syndrome (Quaggin and Kreidberg, 2008, Takemoto et al., 2006).

One of the main protein components of the slit diaphragm is nephrin (NPHS1), which acts as a linker between other slit diaphragm proteins and thus is essential for controlling the escape of circulating proteins (Philippe et al., 2008). Nephrin was the first slit-diaphragm protein to be discovered and is a member of the immunoglobulin (Ig) superfamily of cell adhesion molecules (Kestila et al., 1998). Nephrin is an important modulator of the podocyte cytoskeleton and the key regulator of podocyte intracellular signalling, controlling the activation of several pathways, including the MAP kinase and phosphoinositide 3-OH kinase-PKB pathway and appears to be the first podocyte protein to be altered or downregulated during the early stages of most conditions characterised by proteinuria (Welsh and Saleem, 2010, Li et al., 2013, Zhu et al., 2008).

An additional key component of podocytes and the glomerular slit diaphragm is podocin (NPHS2), a hairpin-like membrane-attached protein of the stomatin family, almost exclusively expressed in the glomerular podocytes (Boute et al., 2000). Podocin is exclusively localized at the cytoplasmic face of the slit diaphragm and it has been shown to be vital for the localization and function of nephrin (Nishibori et al., 2004, Godel et al., 2013). Moreover, podocin knockout mice have been presented to die within the first weeks of life because of kidney failure, which further demonstrates the importance of this protein for the integrity and function of the glomerular filter (Roselli et al., 2004).

Synaptopodin is another protein found to be highly expressed in podocytes and more specifically their foot processes (Garovic et al., 2007, Sugimoto et al., 2003). It has been found to be associated with actin and has a significant role in cross-linking between actin

filaments and polarisation of foot processes, while presence and stable expression of synaptopodin in podocytes is an indication of cell type preservation (Djinovic-Carugo et al., 1999). Moreover, loss of synaptopodin leads to the formation of aberrant, non-polarised foot processes, while recovery of cells following injury is severely compromised as seen in studies conducted in synaptopodin depleted mice (Yanagida-Asanuma et al., 2007, Asanuma et al., 2005).

The establishment of human and rodent podocyte cell lines in addition to the recent identification in Drosophila melanogaster of podocyte-like cells, enabled the study of podocyte biology *in vivo* and *in vitro* (Cheng and Harris, 2010). Two of the most widely used podocyte cell lines are the AB8/13 conditionally immortalised human podocyte cell line (hPC), originating from primary cell cultures transfected with a temperature-sensitive SV40 gene construct and developed by Dr Moin A. Saleem and his team, and the mouse podocyte cell line (mPC) originating from the "immortomouse" with the use of a temperature-sensitive SV40 under the control of a γ-interferon inducible promoter developed by Dr Peter Mundel and his team (Saleem et al., 2002, Mundel et al., 1997). Both cell lines have proven to be invaluable *in vitro* models for understanding the formation and modulation of podocytes as well as the role of various components in the establishment of the slit diaphragm and the glomerular filtration barrier both under normal and pathological conditions.

1.6 miRNAs in kidney disease

The role of miRNAs in kidney disease has been well described (Harvey et al., 2008, Papagregoriou, 2015, Ho et al., 2008, Shi et al., 2008). The general involvement of miRNAs in the maturing mammalian kidney was established by the podocyte-specific inactivation of Dicer in mice, leading to depletion of podocyte foot processes followed by apoptosis, with animals developing albuminuria, glomerulosclerosis and tubule-insterstitial fibrosis, while mice died after 6-8 weeks (Harvey et al., 2008, Shi et al., 2008, Ho et al., 2008). It is important to note that even though Dicer inactivation results to the reduction of proteins important for podocyte function such as nephrin and podocin, it did not affect WT1 (Wilms' tumor 1), a transcription factor essential for podocyte differentiation. Thus, it can be deduced that miRNAs are not imperative for podocyte differentiation to occur but have an essential role in the regulation and completion of the process. Similar findings were obtained in Drosha-depleted mouse podocytes where end stage renal disease (ESRD) clinical features were recorded, further emphasising the importance of miRNAs for podocyte function

(Zhdanova et al., 2011). Renal cell type identity has also been associated to miRNAs, as human parietal epithelial cells were found to be transdifferentiated to podocytes under the influence of miR-193a (Kietzmann et al., 2015). It is thus suggested that miRNA function is of great importance for the maintenance of the glomerular filtration barrier.

1.7 miR-548c-5p, FOXC2 and Podocyte Differentiation

The mammalian kidney glomerulus is a greatly dynamic, complex structure, which acts as a filtration barrier by permitting the passage of small molecules such as water, sugars, electrolytes and small proteins, while disallowing passage of cells and high molecular weight proteins in circulation (Quaggin and Kreidberg, 2008). As mentioned above, podocytes, the visceral epithelial cells of the glomerulus, are one of the three major cell types from which the glomerulus is composed.

One of the most important podocyte markers identified is FOXC2 (Forkhead box protein C2), a member of the forkhead/winged-helix family of transcription factors, which are of great importance for cell fate determination, proliferation and differentiation of multiple tissue and organs (Rascle et al., 2007). In general, FOXC2 has been associated with developmental and tumour angiogenesis by mediating the transcription of protein agents required for endothelial cell migration, such as CXCR4 and integrin β3 (Kume, 2008, Kume, 2012). In addition, mutations in *FOXC2* cause the autosomal dominant lymphedema distichiasis syndrome (Fang et al., 2000). In the kidney, overexpression of *FOXC2*, following ischemia/reperfusion-initiated differentiation of renal tubular cells, promotes injury recovery and re-differentiation from a transitional mesenchymal type to epithelial cells (Hader et al., 2010). FOXC2 also has a proven role in podocyte differentiation and GBM maturation (Rascle et al., 2007). In *FOXC2* knock-out mice expression of *NPHS2* is reduced and kidneys appear hypoplastic with less glomeruli and dilated capillaries (Takemoto et al., 2006). In *Xenopus* the functional association between *FOXC2*, *WT1* and Notch signalling, is essential for podocyte development (White et al., 2010).

It has been shown that FOXC2, in addition to WT1, is one of the most important podocyte markers with great significance for early kidney development (Kreidberg et al., 1993). In human kidney organoids, *FOXC2* was found to be expressed in early podocytes and nephron progenitors (Subramanian A, 2019). As the earliest podocyte marker, it has a prominent role in the differentiation, development and maturation of podocytes, through the regulation of a

variety of different genes such as podocin, the loss of which leads to extensive proteinuria and nephrotic syndrome, the transcription factor *Mafb* and podocyte marker *Cdkn1c* (Grahammer et al., 2013) (Takemoto et al., 2006, Rascle et al., 2007, Boute et al., 2000). More specifically, in *Foxc2* knockout mice in addition to the downregulation of several podocyte markers such as the ones mentioned above, a substantial decrease of the mature glomerular basement membrane (GBM) collagens Col4α3, Col4α4 and Col4α5 was observed indicating failure in the maturation of the GBM. Overall, the *Foxc2* knockout podocytes failed to develop foot processes and a slit diaphragm and were instead connected via adherence junction-like structures, all features found in immature podocytes, thus indicating failure to differentiate (Takemoto et al., 2006). Moreover, in mice knockout models the absence of both *Foxc2* alleles causes severe podocyte injury and dysregulation of several genes, some of which are essential for podocyte integrity (Motojima et al., 2017). Therefore, it can be deduced that regulation of *FOXC2* expression is of utmost importance for correct cellular functions in podocytes. It is important to note that FOXC2 protein localisation changes according to the differentiation state of the cells. More specifically, in differentiating podocytes FOXC2 levels are increased in the cytoplasm, whereas in proliferating podocytes FOXC2 is mainly found in the nucleus (Datta et al., 2015, Hader et al., 2010).

As mentioned above, one of the possible ways by which miRNAs exert transcriptional regulation is by binding to complementary DNA sequences and causing repression or enhancement of gene expression (Corey, 2005). While searching for miRNA target sites on known genes, preliminary bioinformatic analysis uncovered high complementarity between certain miRNAs and gene promoter regions. A specific miRNA, miR-548c-5p, was of particular interest, as it appeared to have a target region corresponding to its full length (22/22 nucleotides) at more than 8kb upstream the *FOXC2* gene transcription start point. Notably, in cultured podocytes, miR-548c-5p has been characterised as cell-type specific, while it has been shown to regulate the expression of PTPRO through a 3'UTR target site, a proteinuria and nephrotic syndrome associated protein (Wang et al., 2018, Müller-Deile et al., 2017).

The miR-548c-5p belongs to the miR-548 family (MIPF0000317), which is comprised of 121 primate specific miRNAs (81 found in humans and 40 in other primate species) and is believed to have originated from Transposable Elements (TEs) and more specifically MADE1 type elements (Mariner Derived Element 1) (Kozomara and Griffiths-Jones, 2013, Piriyapongsa and Jordan, 2007). These elements are short miniature inverted-repeat

transposable elements (MITEs) of 80bp in length and consist of two 37bp terminal inverted repeats that flank an internal 6bp internal region. It is presumed that these sequences have been integrated into the genome at various locations during primate evolution and could have important regulatory roles. Made1-related structures are recognised by the RNA interference enzymatic machinery and are processed to form mature miRNA sequences, a process thought to have evolved as a defence mechanism against the detrimental nature of the TEs (Piriyapongsa and Jordan, 2007). Several members of the miR-548 family share high sequence similarity with some miRNAs being completely identical while others only differ by one or two bases. In the case of miR-548c-5p, two other miRNAs, miR-548am-5p and miR-548o-5p share its mature sequence but all three miRNAs are derived from separate premature transcripts.

The extended complementarity observed particularly between miR-548c-5p and its suspected target site at 8kb upstream the *FOXC2* gene transcription start point, has led to the hypothesis that the transcription rates of *FOXC2* during podocyte differentiation might be influenced by miR-548c-5p, through its interaction with this predicted target site located >8kb upstream *FOXC2*.

Chapter 2: Scientific hypothesis and specific aims

It has been previously proposed that miRNAs might have the ability to control gene expression by acting at the transcriptional level. Several possible mechanisms have been suggested by which this could be possible, including miRNA hybridisation to complementary DNA sequences (Corey, 2005). Moreover, preliminary bioinformatics analysis revealed the presence of extended complementarity between certain miRNAs and target sites found in upstream promoter regions. In particular, a full-length target site of the primate-specific miR-548c-5p was revealed at a genomic region >8kb upstream *FOXC2* in the human genome (hg19). Hence, it is speculated that miRNAs exert transcriptional repression or enhancement of genes through DNA target sites located on extended genomic regions upstream of gene transcription start points. More specifically, **it is hypothesised that the transcription rates of *FOXC2* during podocyte differentiation, are tuned by miR-548c-5p through a target site located >8kb upstream the gene's transcription start point. Consequently, the differentiation of podocytes might be affected.**

There are specific aims needed to be addressed based on the above hypothesis:

1. **Prediction analysis of miRNA targets on extended promoter sequences**
   The presence of miRNA binding sites was investigated in the extensive genomic region of 10kb upstream the 5'UTR of known human genes, by using the miRWalk prediction algorithm. Filtering of the results was based on the degree of complementarity between the target site and the respective miRNA as well as the distance of the site from the 5'UTR of the gene. Targeting predictions for miR-548c-5p identified many putative target sites having complete complementarity to the mature miRNA, within the 10kb upstream region. *FOXC2* was selected for further investigation, due to its significance in podocyte differentiation.
2. **Examination of the miRNA/gene promoter coupling ability using luciferase reporter constructs**
   Luciferase reporter constructs were used to examine the recognition of the predicted miRNA/DNA target site and explore the seed-region properties of the selected miRNA towards the putative DNA target site. These constructs are commonly used in the investigation of the interaction between transcription factors and promoter enhancer elements. The target site of miR-548c-5p was cloned in the pGL4.27 vector, which has its multiple cloning site upstream the basal promoter of the luciferase gene. The vector was then transfected in the AB8/13 human podocyte cell line (hPCs)

together with miRNA mimics and inhibitors. Alterations in the levels of the luciferase gene expression reflect the ability of the miRNA to bind to the DNA target site cloned in the vector and thus affect the transcription of the luciferase gene.

3. **Investigation of the miRNA effect on the endogenous *FOXC2* mRNA levels in podocytes**

   hPCs were transfected with miR-548c-5p mimics and inhibitors and the *FOXC2* expression pattern was followed throughout a differentiation time-course. This was necessary for establishing coordinated responses between the miRNA and the gene's transcriptional rates throughout differentiation and how these responses affect podocyte differentiation, as *FOXC2* is vital for the differentiation, development and maturation of podocytes (Takemoto et al., 2006).

4. **Exploration of the enrichment of miR-548c-5p in the nucleus and the involvement of the RISC complex in targeting the predicted DNA site by Ago-Chromatin Immunoprecipitation (Ago-ChIP) experiments**

   An important step towards the verification of the hypothesis was the use of a modified Chromatin Immunoprecipitation (ChIP) protocol for immunoprecipitating the RISC complex and isolating the endogenously expressed miR-548c-5p, together with its predicted target sequences upstream the *FOXC2* transcription start point. It is assumed that this interaction is facilitated by components belonging to the RISC complex, thus a PanAgo antibody was used to immunoprecipitate the DNA region in question. Enrichment of both miRNA and target site provides strong indications of the interaction that takes place between the two.

5. **Functional assessment of the miR-548c-5p DNA target region, by investigation of its mobility towards the *FOXC2* promoter**

   Chromosome Conformation Capture **(**3C) is a technique used for the *in vivo* study of the spatial organization of genomic regions with a length of up to several hundred kilobases and has been proven extremely beneficial in genomes where distal regulatory elements are involved in gene regulation. In this case 3C was used to examine the possibility of the miR-548c-5p target site having a regulatory effect on the expression of *FOXC2*, determined by its mobility towards the *FOXC2* promoter.

6. **Establishment of miR-548c-5p effect on FOXC2 localisation and protein levels in selected differentiation time-points**

   It was important to assess how miR-548c-5p levels affect FOXC2 expression and localisation within hPCs throughout differentiation, to establish any effect that this may have on their differentiation course. For this, hPCs were treated with miR-548c-

5p mimics or inhibitors for an extended time frame and the effects of these transfections were assessed during hPC differentiation. Following these transfections, cells were left to recover, and the state of the cells and podocyte markers were reassessed with regards to their differentiation state.

Chapter 3: Methods

3.1 miR-548c-5p target prediction analysis and result filtering

Prediction analysis for targets of hsa-miR-548c-5p and other mir-548 family members was performed by using miRWalk2.0 database (mirwalk.uni-hd.de) (Dweep and Gretz, 2015, Dweep et al., 2011). The 5' and 3'UTR, the coding sequence as well as the promoter region (defined as 10kb upstream of a gene's transcription start site) of 20,728 genes were considered for the predictions. For this study, we focused on hits concerning gene promoter sequences and used the other gene regions as means of comparing the frequency of which predicted sites appear among them. To evaluate the statistical significance on the mean values of binding sites among different members of the miR-548 family, analysis of variance (ANOVA) was firstly applied to test the null hypothesis (i.e., H0: all means are equal) followed by the multiple comparison using one-way ANOVA with 5% level of significance ($p \leq 0.05$).

Results returned for promoter regions were filtered in further. As miR-548 family of miRNAs are derived from a specific type of transposable elements, the lengthier predicted target sites were screened for palindromicity to eliminate sites that are possibly transcribed. Hence, MADE-1 type palindromic motifs/sequences were identified using RepeatMasker (http://www.repeatmasker.org/cgi-bin/WEBRepeatMasker) (Smit et al., 2013-2015). Briefly, a file containing the promoter sequences of the lengthier target genes in fasta format was uploaded to RepeatMasker, followed by the default search parameters, such as - Search Engine: abblast, Speed/Sensitivity: default, DNA source: Human and Return Format: tar file. The output files were downloaded to study RepeatMasker's findings. Filtering of target sites was solely based on the degree of complementarity to MADE1-type elements translated as the number of conserved nucleotides, which would depict or imply palindromicity. Sequences that had 50 or less base matches, were considered as non-palindromic, hence having a low chance of being transcribed to a miRNA by shaping up an RNA loop if being transcribed.

3.2 Cell Culture

The AB8/13 conditionally immortalised human podocyte cell line (hPC), originating from primary cell cultures, was supplied by Dr Moin A. Saleem, while the mouse podocyte cell

line (mPC) originating from the "immortomouse" was supplied by Prof. Tobias Huber. hPCs were cultured in RPMI medium supplemented with 10% Fetal Bovine Serum (FBS), 1% of 100 units/ml Penicillin/Streptomycin and 1% Insulin-Transferrin-Selenium (all by Invitrogen, CA, USA), whereas proliferating mPCs were cultured in RPMI medium with L-Glutamine (ThermoFisher Scientific, MA, USA) supplemented with 10% FBS (Invitrogen, CA, USA) and 15U/ml Interferon gamma, mouse recombinant (rmIFN-gamma) (Biomol, Germany) (Saleem et al., 2002, Mundel et al., 1997). Podocytes are dividing when cultured at 33^{o}C with 5% CO_2. By switching to 37^{o}C, podocytes stop dividing and start to differentiate. The HEK293T human embryonic kidney cell line was cultured in DMEM medium supplemented with 10% Fetal Bovine Serum (FBS), 1% of 100units/ml Penicillin/Streptomycin (all by Invitrogen, CA, USA), and incubated at 37°C with 5% CO_2. Lipofectamine®2000 Transfection Reagent (Invitrogen, CA, USA) was used for all transfections, with 0.1 ng of vectors and 25 nM of locked nucleic acid (LNA) molecules (mimics, inhibitors, negative control, QIAGEN, West Sussex, UK) per transfection. All cell lines were kept at low passages and discarded after a few splits to prevent alterations in their nature.

3.3 Luciferase expression reporter system constructs

3.3.1 Cloning of the miRNA target site into the pGL4.27 luciferase vector

Target site binding of miR-548c-5p was validated through the Dual-Luciferase® Reporter Assay System (Promega, WI, USA), comprised of the pGL4.27 firefly luciferase vector bearing a multiple cloning site (MCS) within an enhancer element upstream the basal promoter of the fLuc gene and the pGL4.74 renilla luciferase normalization vector **(Supp. Figure 1).**

A 386 bp DNA fragment containing the predicted target site of miR-548c-5p upstream of *FOXC2* was cloned into the pGL4.27 enhancer (pGL4.27-wt) **(Figure 13A)** after testing different sized constructs to achieve a baseline expression **(Figure 12)**. The fragment was cloned with the use of PCR primers bearing restriction sites for enzymes *Nhe*I and *Hind*III, following initial subcloning of the fragment in the pGEM-T Easy vector (Promega, WI, USA) **(**Error! Not a valid bookmark self-reference.**)**.

Table 1: Primer pairs used for insert cloning in the pGL4.27 firefly luciferase vector and their resulting product size.

Cloning	Forward Primer	Reverse Primer	Product size
pGL-548c-5p-SiteOnly	atagttgctagcGCAAAAACCGCAATTACTTTTaagcttgcggcg	cgccgcaagcttAAAAGTAATTGCGGTTTTTGCgctagcaactat	
pGL-386bp	atagttgctagcTGGAAGGAATAGCGTAGA	cgccgcaagcttGAAAATAACAATGCCCACAG	386
pGL-235bp	atagttgctagcCGTGGCTCTGAATCTCCAA	cgccgcaagcttAATCTGGCAACCTCTAATGTG	235
pGL-149bp	atagttgctagcTTCTCCGAAACTACATCCA	cgccgcaagcttAATTCTTCAAATACCTTTTCAGTT	149
pGL-80bp	atagttgctagcGCTTCAGTTATACTTTCAATCTACA	cgccgcaagcttATTTTGTTAAGTTGGTTGGTG	80

The pGL-548c-5p-SiteOnly primers were designed being complementary and included the miRNA target site flanked by *Hind*III and *Spe*I restriction sequences. The site-only vector was created with the use of a site-directed mutagenesis modified protocol. More specifically, 2 separate PCR reactions one for each primer were performed with the use of the Pfu Polymerase (Agilent, CA, USA) on 100ng of an empty pGL4.27 template under the following conditions for 5 cycles: 30 seconds denaturation at 98 °C, 5 cycles of 95 °C for 30 seconds, 55 °C for 1 minute and 7 minutes at 68 °C. This was followed by a joint PCR reaction using as template 25μl from each of the 2 separate primer reactions with Pfu Polymerase and the same conditions as above for 18 cycles. The reaction products were then treated with *DpnI* for one hour at 37 °C followed by a 20-minute deactivation period at 80°C.

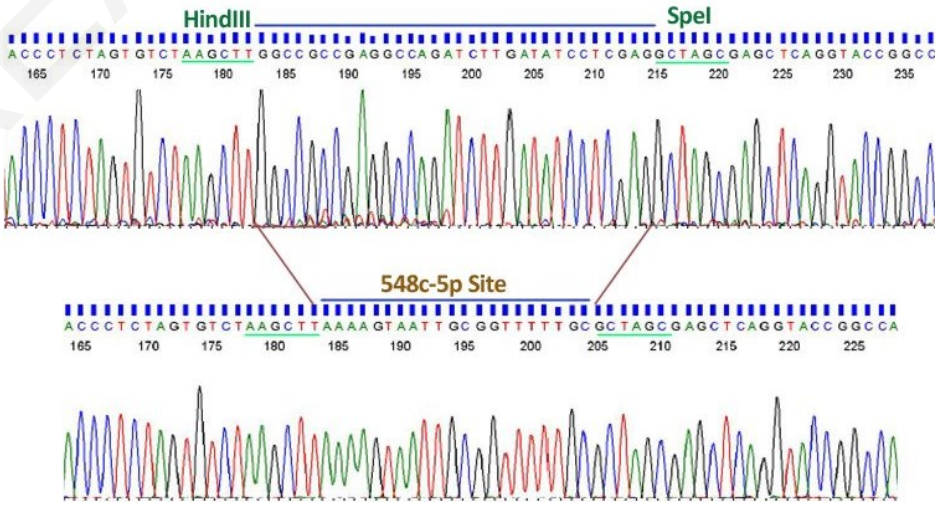

Figure 3: Insertion of the miR-548c-5p target site into pGL4.27 flanked by HindIII and SpeI.

The NucleoSpin Extract II kit (Macherey-Nagel, Germany) was then used for the purification of the PCR product as per the manufacturer's protocol, followed by ligation with the T4 DNA ligase for one hour at room temperature and transformation into DH5α *E. coli* competent cells (Invitrogen, CA, USA). Colonies were purified with the use of the Nucleospin Plasmid Mini kit (Macherey-Nagel, Germany) and verified with sequencing analysis. Subsequently, the insert was digested with the *Spe*I and *Hind*III enzymes and purified with the Nucleospin Extract kit II. The purified insert was then cloned into a fresh pre-digested and purified pGL4.27 vector **(Figure 3)**.

3.3.2 Site Directed Mutagenesis (SDM)

Seed-region significance was tested by introducing sequential point mutations on the target site cloned in the pGL4.27 vector by engineered PCR primers (**Table 2**). The PCR reactions were performed on a subcloning vector bearing the 386 bp insert (pGEM-T Easy System, Promega, WI, USA) and validated by Sanger Sequencing (using BigDyeV3.1 on AB3130*xl*, Applied Biosystems, CA, USA).

Table 2: Primers used for the introduction of point mutations on the predicted target site sequence of the vector bearing the 386bp insert

SDM	Forward Primer	Reverse Primer
548c-SDM-P2	GCAAAAACCGCAATTACTTgTGCACCAACCAACTTAACAAAATGC	GCATTTTGTTAAGTTGGTTGGTGCAcAAGTAATTGCGGTTTTTGC
548c-SDM-P23	GCAAAAACCGCAATTACTggTGCACCAACCAACTTAACAAAATG	CATTTTGTTAAGTTGGTTGGTGCAccAGTAATTGCGGTTTTTGC
548c-SDM-P234	GCAAAAACCGCAATTACaggTGCACCAACCAACTTAACAAAATG	CATTTTGTTAAGTTGGTTGGTGCAcctGTAATTGCGGTTTTTGC
548c-SDM-P2345	GCAAAAACCGCAATTAtaggTGCACCAACCAACTTAACAAAATG	CATTTTGTTAAGTTGGTTGGTGCAcctaTAATTGCGGTTTTTGC

PCR reactions were carried out on 50 ng template by using the Pfu Polymerase (Agilent, CA, USA) under the following conditions: 2 minutes denaturation at 95 °C, 20 cycles of 95 °C for 50 seconds, 60 °C for 50 seconds and 4 minutes at 68 °C and a final step of a 7-minute incubation period at 68 °C. The reaction products were then treated with *Dpn*I for one hour at 37 °C followed by a 20-minute deactivation period at 80°C. The NucleoSpin Extract II kit (Macherey-Nagel, Germany) was then used for the purification of the PCR products as per the manufacturer's protocol, followed by ligation with the T4 DNA ligase for one hour at

room temperature and transformation into DH5α *E. coli* competent cells (Invitrogen, CA, USA). Colonies were selected and inoculated in 5ml LB supplemented with ampicillin for 16h at 37°C using a shaking incubator. Plasmids were then extracted with the use of the Nucleospin Plasmid Mini kit (Macherey-Nagel, Germany) and verified with sequencing analysis. Subsequently, the inserts were digested with the *Nhe*I and *Hind*III enzymes and purified with the Nucleospin Extract kit II. The purified inserts were then cloned into the pre-digested and purified pGL4.27 vector. Four constructs were created each one bearing sequential mutations at the nucleotides corresponding to the miRNAs seed region: position 2, positions 2 + 3, positions 2 + 3 + 4, positions 2 + 3 + 4 + 5 **(Figure 4)**.

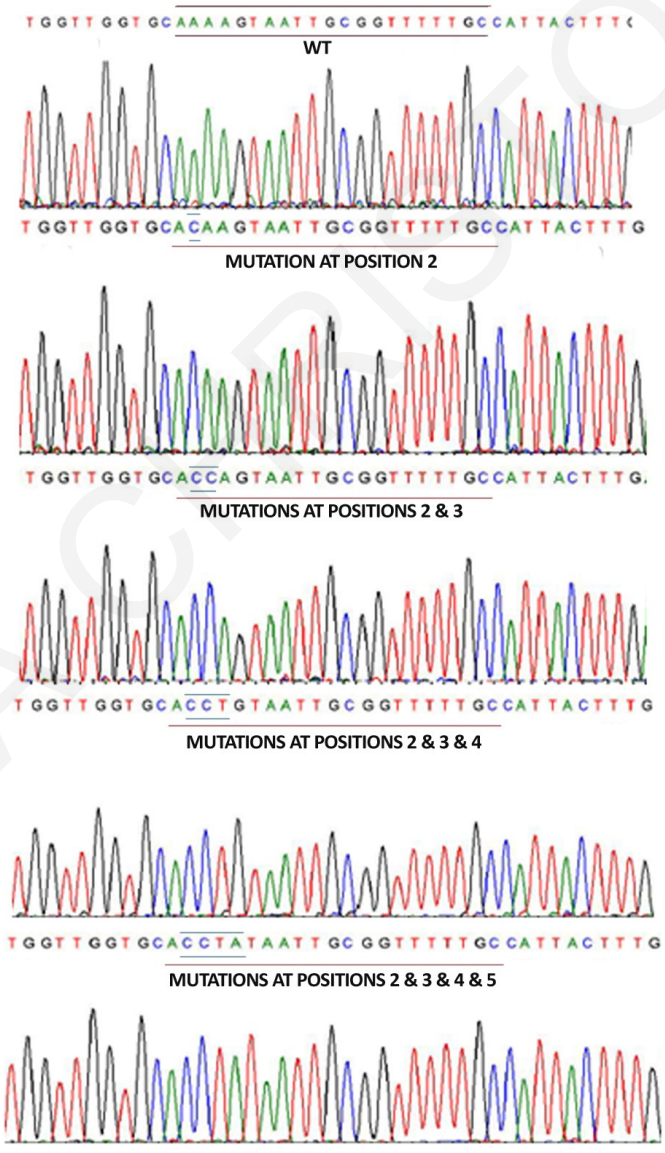

Figure 4: Sequencing results of the sequential point mutations introduced on the target site cloned in the pGL4.27 vector used in the luciferase reporter assays. Four constructs were created each one bearing sequential mutations at the nucleotides corresponding to the miRNAs seed region: position 2, positions 2 + 3, positions 2 + 3+ 4, positions 2 + 3 + 4 + 5.

3.3.3 Transfection of the AB8/13 hPCs and the luciferase reporter constructs

hPCs were transfected using Lipofectamine ®2000 Transfection Reagent (Invitrogen, CA, USA) with 0.1 ng of vectors and 25 nM of LNA molecules each time in triplicates: miR-548c-5p mimic, inhibitor, or the AllStars Negative Control (NC) (all from QIAGEN, West Sussex, UK). Cells were harvested by lysis 16 hours post transfection with the use of the 5X Passive Lysis buffer (Promega, WI, USA) and luciferase levels were determined on an automated luminometer (Sirius, Berthold Detection Systems, Germany). Results were analysed for trend significance using one-way ANOVA with Tukey post-testing.

Table 3: Primer Sequences for evaluation of the mRNA levels for the genes of interest

mRNA qPCR	Forward Primer	Reverse Primer
FOXC2-RT	CGGCTGGGGATTGAGAAC	CTGCGTGGCGATAGAGAG
MTHFSD-RT	CCTGGGGCAACTAAAGAC	CGATTCTCCAGCCTTTTTC
bACTN-RT	CCACCACAATGAAGATCAAGATCA	TAGTCCGCCTAGAAGCATTTGC
mFoxc2-RT	GCA CCA AAT ACT GAG GCT GTC	GCT TTC CGT CGC TTT CTG
mMthfsd-RT	GTG ACC TGG ACT CAG CCT T	GAG CCT GCG TCC CTC AGT
m-bActn-RT	GGCTGTATTCCCCTCCATCG	CCAGTTCGTAACAATGCCATGT
FLJ30679-RT	TACGCAGGAGGCAACAGA	GGACACCACATAGGAAGAGAGA
RP11-463O9-RT	ATGCCGTTCAAGGTTTCC	CATTTTCGTCTTCTGTTCTTTTATTG

3.4 Endogenous miR-548c-5p, *FOXC2* and *MTHFSD* mRNA levels in hPCs during differentiation

Undifferentiated hPCs at 60% confluency were cultured as described above and incubated at 37 °C with 5% CO2 for a period of fourteen days until complete differentiation. Cells were harvested and RNA was extracted with the use of TRIzol® Reagent (Life Technologies, CA, USA). Briefly, cells from 12-well plates were harvested with TRIzol® and collected in RNase free tubes, followed by the addition of Bromochloropropane (BCP) (Sigma-Aldrich, MI, USA) at 1/5 of TRIzol® volume. Samples were vigorously shaken and left at room temperature for 10 minutes. Following a 15-minute centrifugation at 12000 rpm, the upper aqueous RNA phase was collected. Equal volume of isopropanol was then added and after mixing gently, tubes were left at room temperature for 10 minutes. Samples were

centrifuged at 12000 rpm for 20 minutes and the supernatant was discarded. The RNA pellet was then washed twice with 70% ethanol and was left to dry for 5-10 minutes. Each RNA pellet treated with DNase by being resuspended in 10 μl of the following: 10xDNase Buffer, DNase (2000U/ml) and dH2O (all from New England BioLabs, MA, USA), and incubated for 10 minutes at 37 oC. EDTA 0.05M was added to deactivate the enzyme. The levels of both miR-548c-5p and FOXC2 and MTHFSD mRNA at predetermined time points were assessed through quantitative Real-Time PCR (qRT-PCR) using specific primers **(Table 3)**.

These time points were: day (-1) (undifferentiated dividing cells), day 1, day 2, day 3, day 4, day 7, day 10, day 13 and day 16 (mature differentiated podocytes). Time point day1 corresponds to a harvest 24 h after switching cultures to 37 ºC to initiate differentiation, time point day 2 to 24 hours after day 1 and so forth. The total RNA fraction per day was reversely transcribed using the ProtoScript® First Strand cDNA synthesis kit (New England BioLabs, MA, USA) following the manufacturer's guidelines, whereas the miScript II Reverse Transcription Kit (QIAGEN, West Sussex, UK) was used for miRNA assessment. Following the RT reaction, gene expression levels were determined by quantitative Real-Time PCR (qRT-PCR) using the Fast SYBR® Green Master Mix on the ViiA™ 7 Real-Time PCR System (Life Technologies, CA, USA), with β-actin as a reference gene. Cycling started with an activation step of 20 seconds at 95ºC, followed by 40 cycles of denaturation at 95ºC for 1 second and the annealing and extension step for 20 seconds at 60ºC, followed by a melting curve step. miR-548c-5p levels were quantified using the miScript™ SYBR Green PCR Kit (QIAGEN, West Sussx, UK), using *SNORA37* as a reference gene using commercially available primers (QIAGEN, West Sussex, UK). Cycling started with an initial activation step at 95 ºC for 15 minutes and 40 cycles of denaturation at 94 ºC for 15 seconds, annealing at 55 ºC for 30 seconds and extension at 70 ºC for 35 seconds, followed by a melting curve step.

3.5 Effect of miRNA mimics and inhibitors on endogenous mRNA expression in hPCs and mPCs

To evaluate miR-548c-5p effect on *FOXC2* mRNA levels, hPCs were transfected on day 1 and day 7 with 25 nM of mimics or inhibitors and harvested 24h post-transfection (day 2 and day 8 respectively). To study the role of the miRNA in undifferentiated hPCs, cells were transfected twice, once in every 24h, with miRNA mimics or inhibitors (25 nM per transfection), to enforce and amplify ongoing interactions. Cells were harvested 24h after the second transfection. Untransfected cells treated with Lipofectamine (Invitrogen, CA,

USA) were used as controls. Moreover, as mouse podocytes are a natural knock-out of both the miRNA and its genomic target region **(Figure 7B, Figure 7C)**, undifferentiated mPCs were treated in the same way to investigate the effect of miR-548c-5p on *mFOXC2* normalized on *β-Actin*. For all experiments, RNA was extracted with TRIzol® Reagent (Life Technologies, CA, USA) and *FOXC2* and *MTHFSD* mRNA levels were assessed with qRT-PCR as described above. Results were compared using one-way ANOVA with Tukey post-testing.

3.6 Ago-Chromatin Immunoprecipitation (Ago-ChIP)

Monoclonal anti-Pan-Ago antibodies, the anti-PanAgo (clone 2A8) antibody (Millipore, Germany) and the anti-PanAGO antibody sc-376696 (B-3) (SantaCruz Biotechnology, TX, USA) were used to immunoprecipitate the RISC complex in crosslinked nuclear fractions of cultured hPCs at various time-points. Through this assay, the simultaneous collection of RISC-associated miRNAs acting in the nucleus and DNA regions bound on the RISC, was made possible. Experiments were carried out based on the ChIP-assay protocol (PROT11) by the EPIGENOME Network of Excellence (Kouskouti and Kyrmizi, 2005), with modifications. The same protocol was used for experiments carried out in a non-differentiating cell line HEK293T.

3.6.1 Crosslinking and lysis

Cells were cultured in 150 mm plates as described above and differentiation was induced at 60% confluency ($5x10^6$ cells). Cells were crosslinked with 3% PFA for 10 minutes at room temperature, followed by the addition of 10X Glycine. The plates were then placed on ice and washed twice with ice cold 1X PBS, followed by the addition of 2 ml 1X PBS containing 0.5 mM of Protease Inhibitors (PIs) (Roche, Switzerland) and scraping of the cells into 2 ml sterile tubes. Cells were then centrifuged and the supernatant was discarded, followed by lysis in 1ml homemade Swelling (Lysis) Buffer containing 25 mM Hepes pH 7.8, 1.5 mM $MgCl_2$, 10 mM KCl, 0.1% NP-40, 1 mM DTT and 0.5 mM of PIs. 30 μl of the sample lysate were saved in order to validate that the nuclei isolated remain intact during this step through light microscopy. After centrifugation, pelleted nuclei were resuspended in 800 μl Sonication buffer (50 mM Hepes pH 7.8, 140 mM NaCl, 1 mM EDTA, 1% Triton X-100, 0.01% Na-deoxycholate, 0.1% SDS and 0.5 mM PIs) for nuclear lysis and aliquoted in 0.5 ml sterile PCR tubes (100 μl per tube). 20 μl of sample was saved in order to test sonication

efficiency and the size range of DNA fragments following DNA shearing by sonication, by either gel electrophoresis or the Bioanalyzer 2100 instrument.

3.6.2 Isolation of nuclei and DNA shearing by sonication

The Diagenode® Pico Bioruptor (Diagenode, Belgium) was used for DNA shearing of the crosslinked samples, which were sonicated in 10 cycles: 15 seconds of High Power sonication followed by 90 seconds of rest, while briefly spinning down the samples after cycle 5. Samples were constantly rotated in circulating cold water for maintaining uniform conditions. Following sonication, the samples were centrifuged at 10 000 rpm at 4 °C to remove insoluble material. At this point, 20 μl of sonicated lysate was removed for comparison with the unsonicated sample previously kept, through agarose gel electrophoresis. Sonication was deemed successful if a DNA smear with a molecular weight of 100-200 bp appeared on the gel, whereas any unsonicated DNA could be seen at around 10 kb. Moreover, the ability to successfully isolate nuclei and subsequently retain the nuclear fraction and dispose of the cytoplasmic debris was tested via western blot. For nuclear fraction identification a rabbit antibody against Lamin A/C sc-20681 (1:1000) was used, while a mouse β-tubulin antibody sc-55529 (1:2000) concentration was used for detection of the cytoplasmic segment of the samples (SantaCruz Biotechnology, MA, USA). Proteins were released through de-crosslinking of the sonicated samples with the addition of 8 μl 5 M NaCl in 200 μl lysate and overnight incubation at 65°C. Non-treated cell lysates as well as lysates that were not decrosslinked served as controls. Heightened Laminin A/C levels and minimal β-tubulin levels in sample lysates, compared to the controls, depicted successful isolation of the nuclear fraction of the lysate. Successfully sonicated lysates were prepared for immunoprecipitation by being diluted in homemade IP dilution buffer (0.01% SDS, 1.1% Triton X-100, 1.2 mM EDTA, 16.7 mM Tris-HCl pH 8.0, 150 mM NaCl and 0.5 mM PIs) to a final volume of 1 ml. 10 μl of each sample was retained to be used as the "Input" control in subsequent qRT-PCR experiments.

3.6.3 Immunoprecipitation

As mentioned above, immunoprecipitation was carried out with 2 different anti Pan-Ago antibodies, whereas an Anti-RNA Polymerase II antibody (sc-47701) and a normal mouse anti-IgG antibody (sc-2025X) (SantaCruz Biotechnology, MA, USA) were used as positive and negative control respectively **(Table 4)**. 2 μg of each antibody was diluted in 200 μl PBS/Tween® (0.02%) and incubated with 20 μl Dynabeads® Protein G (Life Technologies,

CA, USA) for 1 h at room temperature on a rotating platform, for the antibody to bind to the beads. The supernatant was then discarded and prepared lysates were incubated with the antibody-bound beads on a rotating platform for 3 h at 4°C.

Table 4: Antibodies used for Immunoprecipitation in ChIP experiments

Antibodies	Company/PN Code	Concentration
Anti-PanAgo (B-3)	Santa Cruz Biotechnology/sc-376696	2μg
Anti-PanAgo	Millipore/MABE56	2μg
Anti-Normal mouse IgG	Santa Cruz Biotechnology/sc-2025X	2μg
Anti-RNA Polymerase II	Santa Cruz Biotechnology/sc-47701	2μg

Following supernatant removal, each IP was washed once in Low Salt Immune Complex Wash Buffer (50 mM Hepes pH 7.8, 140 mM NaCl, 1 mM EDTA, 1% Triton-X 100, 0.1% Na-deoxycholate, 0.1% SDS, 0.5 mM PIs), once in High Salt Immune Complex Wash Buffer (50 mM Hepes pH 7.9, 500 mM NaCl, 1 mM EDTA, 1% Triton-X 100, 0.1% Na-deoxycholate, 0.1% SDS and 0.5 mM PIs), once in LiCl Immune Complex Wash Buffer (20 mM Tris pH8.0, 1 mM EDTA, 250 mM LiCl, 0.5% NP-40, 0.5% Na-deoxycholate and 0.5 mM PIs) and twice in TE buffer (50 mM Tris pH 8.0, 1 mM EDTA and 1% SDS). Samples were incubated with each one of the wash buffers for five minutes at room temperature on a rotating platform.

3.6.4 Elution of Protein/DNA/miRNA complexes

Freshly prepared Elution Buffer (10 μl 20% SDS, 20 μl 1M $NaHCO_3$ and 170 μl ddH_2O) was used for the elution of the protein/DNA/miRNA complexes. IP samples were eluted in two steps, both of which were comprised of the addition of 100 μl elution buffer to the sample, to a final volume of 200 μl. The first elution was carried out at room temperature and the second at 70°C. 200 μl of elution buffer were also added to all Input samples. Elution was followed by de-crosslinking of all samples with the addition of 8 μl 5 M NaCl and an overnight incubation at 65°C. Samples were then incubated with 1μl 10mg/μl Proteinase K solution for 2 hours at 37°C. DNA was extracted from samples by using the NucleoSpin® Gel and PCR Clean-up kit (Macherey-Nagel, Germany) using the NTB buffer alternative protocol developed for samples containing SDS, as per the kit manufacturer's protocol. The miRNA fraction of the samples was extracted with the NucleoSpin® miRNA Kit for

Isolation of small and large RNA (Macherey-Nagel, Germany), following the kit manufacturer's protocol.

3.6.5 Enrichment analysis of miR-548c-5p and its DNA target site

Enrichment analysis of DNA regions and selected miRNA was performed by qRT-PCR using appropriate primers **(Table 5)**.

Table 5: Primer sequences and product sizes used in ChIP enrichment analysis.

Region	Forward Primer	Reverse Primer	Product Size
P0	GAATCTCCAAGCTGTGTTCC	ACATTTTGTTAAGTTGGTTGGT	152
PA	CACATCACTTTTCCCCTTATCT	GCAGCCTCATACTGTCTTTCC	169
PB	CCGTCTCAACAACAACAGGA	TACAGAAGCGGGTGGGTAGT	137
PC	GGTTAGAAAAAGAGCCCAGAA	CCAATAAAAGAACAGAAGACGA	155
PD	GCCTCCTGGTATCTCAACCAC	CGGCGTGGATCTGTAGGG	192
GAPDH-Pro	TACTAGCGGTTTTACGGGCG	TCGAACAGGAGGAGCAGAGAGCGA	166

qPCR primers for mature miRNA sequences were supplied by QIAGEN, West Sussex, UK. ChIP efficiency was tested using primers amplifying the GAPDH promoter region in RNA-Polymerase ChIP preps. Primer pairs were designed to encompass the miRNA target site and then at every ≈2 kb, towards *FOXC2* **(Figure 5)**. P0 corresponds to a product containing the miR-548c-5p target site, while PD is placed within the *FOXC2* gene.

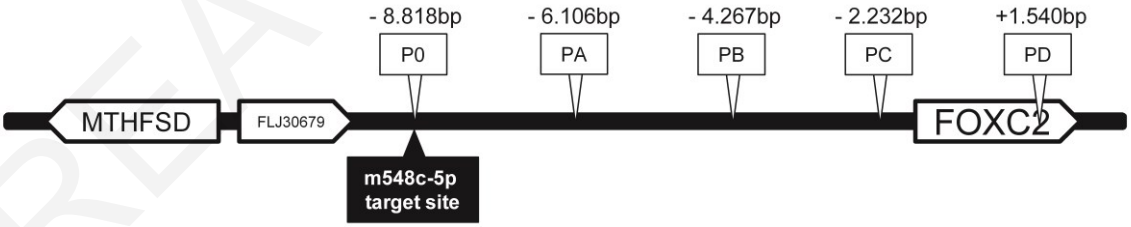

Figure 5: The five regions examined for enrichment in ChIP experiments and their position in relation to the miR-548c-5p target site and the FOXC2 gene. Primer set P0 amplifies a region containing the miR-548c-5p target site, whereas PD is specific for a region located within the *FOXC2* gene. The schematic is not in scale.

The enrichment of miR-548c-5p in in ChIP preps of undifferentiated hPCs was compared to the podocyte specific miR-23b, the nuclear miR-29c and the active in podocytes miR-30d-3p (Liao et al., 2010, Ho et al., 2008, Shi et al., 2013, Liu et al., 2016, Hwang et al., 2007).

The SYBR® Select Master Mix (Life Technologies, CA, USA) was used for the reaction, which took place using the ViiA™ 7 Real-Time PCR System (Life Technologies, CA, USA). Cycling started with an activation step of 2 minutes at 50 ºC and 2 minutes at 95 ºC followed by 40 cycles of denaturation at 95ºC for 15 seconds, annealing at 57 ºC for 15 seconds and extension for 1 second at 72 ºC and a final melting curve step. Results are depicted as Fold Change, where the Cps obtained were calculated as an enrichment fraction to the 10% input sample, while noise between experiments was deducted by further normalizing values over mock % input IP (mIgG or beads) values. Results were analysed using one-way ANOVA with Dunnett's post-testing comparing P0 to all other primer pairs for hPCs at day (-1) and HEK293T cells, while Tukey post-testing was used for evaluating target site fraction enrichment at progressing differentiation time points and miRNA enrichment.

3.6.6 Ago-ChIP on the pGL4.27 vector constructs in mPCs following transfections

Double transfections in mPCs, using Lipofectamine®2000 Transfection Reagent (Invitrogen, CA, USA), took place with the pGL4.74 vector containing the WT miR-548c-5p target site (pGL4.27-wt) or the vector with seed-region mutations at positions 2 + 3 and 25 nM of either a miRNA mimic or NC (QIAGEN, West Sussex, UK). The ChIP protocol was carried out as previously explained and immunoprecipitated DNA fractions were analysed with qRT-PCR and relevant primers as described above while one-way ANOVA with Tukey post-testing was used for their evaluation.

3.7 Chromosome Conformation Capture (3C)

The 3C protocol was carried out as described in Naumova et al. 2012 (Naumova et al., 2012) to explore the possible mobility of the genomic region bearing the miR-548c-5p target site towards the promoter of *FOXC2* in hPCs during different differentiation time points: day (-1), day 1 (24 h after initiating differentiation), day 2 and day 7. In brief, protein-bound DNA in lysed cells was digested with *EcoR*I and restriction fragments were ligated with the Instant Sticky-end Ligase Master Mix (New England Biolabs, MA, USA). Ligation products were purified and analysed by qRT-PCR using primers with reverse orientation towards *FOXC2* and a reverse docking primer on the fragment bearing the miRNA target site **(Table 6)**. The bacterial artificial chromosome (BAC) clone RP11-1017A18 [BACPAC Resources Center] stored in DH10B cells was used as the control non-interacting sample for regions tested. A

random genomic region shared by both the BAC clone and included in the ligation products of interest (ChIP primer set PC) was amplified with regular primers and used as a reference region to normalize for template concentration. To further explore the effect of miR-548c-5p abundancy on DNA conformation dynamics, hPCs were transiently transfected with mimics or inhibitors and 3C was performed as described in detail below, 24 h post-transfection at day (-1) and day 1. Moreover, cells were transfected twice, once in every 24 h, with miRNA mimics or inhibitors and harvested at day 2, followed by 3C.

Table 6: Primer sequences and product sizes for 3C

3C	Forward Primer	Reverse Primer	Product Size
3C-5R	-	CAGTTTCCCCGACCTCAAG	-
3C-6R	-	CACATTAGAGGTTGCCAGAT	131
3C-7R	-	CACCTCGGGCAGAAAGACA	139
3C-89R	-	GCTACCTTCCCCTCTATGC	151
3C-10R	-	GATGTGGGTTTTGTTTCCTGTA	134
Reference Primer (PC)	GGTTAGAAAAAGAGCCCAGAA	TCGTCTTCTGTTCTTTTATTGG	

3.7.1 Crosslinking and Cell Lysis

For 3C template preparation hPCs were trypsinised and resuspended in fresh cell medium. The cells were then crosslinked with the addition of 10% formaldehyde and a 10 minute incubation on a rotating platform at room temperature. Formaldehyde was deactivated with glycine 2.5 M at room temperature for 5 minutes with rotation and the cell pellet was resuspended in Lysis buffer (50 mM glucose, 10 mM EDTA pH 8.0, 25 mM Tris/HCl pH 8.0 and 0.5 mM Protease Inhibitor Cocktail (Roche, Switzerland). A dounce homogeniser was used for cell lysis, the cells were placed on ice for 15 minutes and the process was repeated. The lysate was then pelleted and supernatant was discarded.

3.7.2 Digestion of crosslinked lysate

A 6-cutter restriction enzyme, *Eco*RI, was selected to achieve an optimal resolution in 3C, as multiple and evenly distributed *Eco*RI restriction sites exist around the miR-548c-5p target site and throughout the 10 kb region upstream *FOXC2*. Moreover, *Eco*RI was selected as it is an enzyme highly suitable for 3C assays with at least 70% digestion efficiency at each restriction site. Therefore, the cell lysate pellet was resuspended in 10 µl 10X NEB3 (New

England Biolabs, MA, USA) and 66 μl dH_2O, followed by the addition of 10% SDS and a 10 minute incubation at 65 °C for the removal of proteins that were not crosslinked to the DNA. Prior to the addition of the restriction enzyme, 10% Triton X-100 was added for quenching the SDS. The digestion reaction took place following the addition of 400 units *EcoR*I and 100X BSA overnight at 37 °C.

3.7.3 Ligation of digested products

The digested products were then ligated with the use of Instant Sticky-end Ligase Master Mix (New England Biolabs, MA, USA) and a one-hour incubation period at room temperature.

3.7.4 Decrosslinking of cells and DNA purification

Cells were decrosslinked with the addition of 20 mM NaCl and overnight incubation at 65°C. For the removal of the protein fraction of the sample 5 mg Proteinase K (10 mg/ul) were then added and the sample was incubated at 37°C for three hours. This was followed by the addition of 1μl RNase 10 μg/μl, one-hour incubation at 37°C and finally 4 μl EDTA 0.5 M for deactivation of the RNase. The sample was then purified using UltraPure™ Phenol:Chloroform:Isoamyl Alcohol (PCI) (25:24:1) (Invitrogen, CA, USA) pre-made solution. An equal volume of PCI to the sample was added; the tubes were shaken vigorously and centrifuged at 11.000 rpm for 10 minutes. The upper aqueous phase (~200 μl) was then transferred to a clean tube, followed with the addition of 1:10 volume 3 mM of NaAC pH 5.2 and 2.5 volumes ice cold 100% Ethanol and incubation for one hour at -80°C. Samples were then centrifuged for 20 minutes at 12.000 rpm at 4°C. The supernatant was removed and samples were washed with 70% ice cold ethanol. After centrifugation at 12.000 rpm for 15 minutes at 4°C, the supernatant was removed and the pellet was left to air-dry for ~15 minutes. Once all residual ethanol was removed, the pellet was resuspended in dH_2O.

3.7.5 BAC control preparation

For this set of experiments the Bacterial Artificial Chromosome (BAC) clone RP11-1017A18 [BACPAC Resources Center] was used as a negative linear (no interactions/non-specific interactions) control, stored in DH10B cells. The BAC clone contains a region of 16q24 starting from 86434189bp to 8631166bp and includes both the miRNA target site region (86558539bp – 86558560bp) and *FOXC2* (86600857bp – 86602537bp). After plating

the cells and culturing the clone containing bacteria in Luria Broth supplemented with 2.5 µg chloramphenicol (30 µg/ml), cells were pelleted and resuspended in Lysis buffer (50 mM glucose, 10 mM EDTA pH 8.0 and 25 mM Tris/HCl pH 8.0) with 4.5 µl of 10 mg/ml RNase and the sample was incubated for five minutes on ice. 400 µl 0.2 M NaOH with 1% SDS were then added and the sample was incubated on ice for five minutes, followed by addition of 300 µl of 3 M KOAc pH 5.0 and a 15-minute incubation on ice. The sample was then centrifuged for 15 minutes at 11.000 rpm and the supernatant was transferred to a clean microcentrifuge tube. An equal volume of isopropanol was added, followed by centrifugation and washing of the resulting pellet with 70% ethanol. Following centrifugation, the ethanol was removed and the pellet was left to air-dry at room temperature for 15 minutes. Once all residual ethanol had been removed, the pellet was resuspended in 40 µl dH_2O. 10 µg of isolated BAC were then digested in a 500 µl reaction with 400 units *EcoR*I and 100X BSA (New England Biolabs, MA, USA) in a rotating chamber overnight at 37°C. The digestion products were then cleaned, ligated and purified following the protocol guidelines found in Naumova et al. 2012 (Naumova et al., 2012). Briefly, clean-up and purification was performed using UltraPure™ Phenol:Chloroform:Isoamyl Alcohol (PCI) (25:24:1) (Invitrogen, CA, USA) pre-made solution, as described above **(3.7.4)**, whereas ligation was performed using the Instant Sticky-end Ligase Master Mix (New England Biolabs, MA, USA) and a one-hour incubation period at room temperature.

3.7.6 Detection and Quantification via Real-Time PCR

The Power-UP SYBR® Green Master Mix (Life Technologies, CA, USA) was used for the reaction, which took place using the ViiA™ 7 Real-Time PCR System (Life Technologies, CA, USA). Cycling started with an activation step of 2 minutes at 5 ^{o}C and 2 minutes at 95^{o}C followed by 40 cycles of denaturation at 95^{o}C for 15 seconds, annealing at 57^{o}C for 15 seconds and extension for 1 second at 72^{o}C and a final melting curve step. Detection primers were designed around the restriction sites of the experimental template in the reverse direction (**Figure 21, lower panel**). Thus, a product was detectable only in the case of chromatin rearrangement and looping and interaction between two regions **(Supp. Figure 2)**. The BAC template described above was used as the reference sample. For normalisation of the sample concentration a region within the 10 kb region upstream *FOXC2* was used and quantified with forward and reverse primers.

3.8 Protein expression

We examined the influence of prolonged treatments with miR-548c-5p mimics on FOXC2 and WT1 protein levels in podocytes entering differentiation and their recovery two days post-transfection. Expression levels of podocyte markers podocin (NPHS2), nephrin (NPHS1), p57 and Synaptopodin (SYNPO) were also examined. Results were normalized on β-tubulin. hPCs were serially transfected with miRNA mimics at day (-1) and day 1 and harvested 30 h or 48 h after the second transfection directly with 2x Laemmli sample buffer (4% SDS, 20% glycerol, 10% 2-mercaptoethanol, 0.004% bromphenol blue and 0.125 M Tris HCl, pH approx. 6.8) (Sigma-Aldrich, MI, USA), brought to 95ºC prior to use. Cells transfected with the AllStars Negative Control (NC) (QIAGEN, West Sussex, UK) were used as controls. Lysates were homogenized with a 2 ml syringe and denatured at 95ºC for five minutes and equal volumes were subsequently analysed by Western blotting according to standard procedures. More specifically, samples were ran on pre-cast 1.5mm 3-8% or 4-12% gels (Invitrogen, USA) and following a short incubation in 20% ethanol, were transferred to a PVDF membrane using the iBlot apparatus for 7 minutes in variable voltage. Membranes were blocked with 5% milk or BSA, both in PBS/Tween 0.01%, followed by overnight incubation with the primary antibody at 4ºC. Membranes were washed 3x10 minutes with PBS/Tween 0.01% and incubated with the secondary antibody for 1 hour at room temperature, followed again by 3x10 minutes washes and protein detection. The following antibodies were used for protein detection: podocin sc-22296 1:500, nephrin sc-28192 (1:200), synaptopodin sc-21537 (P-19) (1:1000), WT1 sc-192 (1:300), FOXC2 sc-515234 (1:300), β-tubulin sc-55529 (1:2000), p57 sc-8298 (1:500) all from Santa Cruz Biotechnology, TX, USA) **(Table 7)**.

Table 7: Antibodies used in Western Blot experiments

Primary antibodies	Company/PN Code	Working Dilution
Anti-FOXC2	Santa Cruz Biotechnology/sc-515234	1:300
Anti-β-Tubulin	Santa Cruz Biotechnology/sc-55529	1:2000
Anti-Nephrin (NPHS1)	Santa Cruz Biotechnology/sc28192	1:200
Anti-p57	Santa Cruz Biotechnology/sc-8298	1:500
Anti-Podocin (NPHS2)	Santa Cruz Biotechnology/sc-22296	1:500
Anti-Synaptopodin (P-19)	Santa Cruz Biotechnology/sc-21537	1:1000
Anti-WT1	Santa Cruz Biotechnology/sc-192	1:300
Secondary antibodies	**Company/PN Code**	**Working Dilution**
Anti-mouse	Santa Cruz Biotechnology/sc-516102/sc-2005	1:2000
Anti-rabbit	Santa Cruz Biotechnology/sc-2354/sc-2020	1:2000
Anti-goat	Santa Cruz Biotechnology/sc-2357/sc-2004	1:4000

The Enhanced ChemiLuminescence (ECL) Plus Blotting Detection system (Amersham Biosciences, UK) or the SuperSignal West Femto Maximum Sensitivity Substrate (Pierce, USA) were used for protein detection through the ChemiDoc™ XRS+ System (BioRad, CA, USA). Band density was defined by ImageJ software [http://imagej.nih.gov/ij], with band normalization over b-tubulin expression. Results were analysed using one-way ANOVA with Tukey post-testing or t-test.

3.9 FOXC2 localization in hPCs

FOXC2 localisation and expression during hPC differentiation was recorded in a time-course starting from day (-1) and following the thermal switch from 33ºC to 37ºC on day 1 to day 7. Moreover, the effect of prolonged transfections with miRNA inhibitors or mimics on FOXC2 localisation was also investigated, to examine whether it can potentially influence hPC differentiation dynamics through FOXC2 localisation. In differentiating hPCs, FOXC2 localisation was studied both on day 5, 12 h after 5 consecutive transfections with miRNA mimics, and day 8, following a recovery period of 3 days. In addition, in undifferentiated hPCs (day (-1)), where the miRNA has a higher expression, FOXC2 localisation was examined after 5 serial transfections with miR-548c-5p inhibitors and mimics. In all cases, hPCs were seeded on coverslips and transfected every 24 h with Lipofectamine®2000 (Invitrogen, CA, USA), as described above in section **3.3.3**. Cells transfected with the AllStars Negative Control (NC) (QIAGEN, West Sussex, UK) were used as controls. Cells were fixed with 4% paraformaldehyde in PBS for 10 minutes, followed by 3x5 minute washes with PBS. Cells were then permeabilised using 0.5% Triton X-100 in PBS for 2 minutes, followed by 3x5 minute washes with PBS and blocking in 2% BSA for one hour. Incubation with the primary antibody for FOXC2 sc-31734 (1:35) (Santa Cruz Biotechnology, TX, USA) at 4°C, took place overnight and was followed by incubation of the secondary antibody in PBS for 1 hour at room temperature. Nucleus staining was performed with the use of TO-PRO®-3 Iodide (ThermoFisher Scientific, MA, USA) (1:1000) for 15 minutes at room temperature according to the manufacturer's guidelines. Finally, transfected cells were mounted with fluorescence mounting medium (DAKO, USA). A detailed observation of the slides was conducted using a TCSL confocal microscope (Leica SP5, IL USA) and the images were obtained using the Leica LCS Software. To obtain quantitative results, the laser power and exposure was adjusted to avoid oversaturation as well as the PMT voltage, frame averaging, pinhole aperture size, scan speed, and zoom magnification remained constant in all images presented. Antibodies and

reagents are listed below in **Table 8**.

Table 8: Antibodies and reagents used in immunofluorescence experiments

Antibodies and Reagents	Company/PN Code	Concentration
Anti-FOXC2	Santa Cruz Biotechnology/sc-31734	1:35
TO-PRO®-3 Iodide	ThermoFisher Scientific	1:1000
Fluorescence mounting medium	DAKO	N/A

Densitometry of confocal microscopy images was performed using ImageJ. The Wright Cell Imaging Facility (WCIF) version of ImageJ was downloaded from http://www.uhnresearch.ca/facilities/ wcif/fdownload.html and was used in all analyses. For nuclear localisation analysis, images of FOXC2 and TO-PRO nuclear staining were imported into ImageJ and were processed using the Colocalisation Highlighter plug-in, using the standard parameters (Ratio: 50%, Threshold channel 1/FOXC2/Red: 50, Threshold Channel 2/Nuclei/TO-PRO: 50, Display value: 255). Regions with evident colocalisation were displayed in a new 8-bit monochrome image generated by ImageJ and Integrated Density was measured. Values were plotted and analysed using one-way ANOVA with Tukey post-testing by GraphPad Prism. To calculate the total intensity of FOXC2, images were imported into ImageJ, despeckled to remove background spots and their threshold was adjusted until the areas of FOXC2 presence were distinct from background fluorescence. Integrated density was measured by the software, limiting values to the threshold set previously. Values were plotted and analysed using one-way ANOVA with Tukey post-testing by GraphPad Prism.

Chapter 4: Results

4.1 miR-548c-5p has a full-length predicted target site upstream the *FOXC2* gene

The miRWalk2.0 algorithm was used to examine the frequency of predicted miRNA target sites at the 5'UTR, coding sequence, 3'UTR and extended promoter regions, which were defined as 10kb upstream the transcription start sites of genes, for miRNAs belonging to the MIR-548 family (MIPF0000317). Impressively, the analysis revealed a high frequency of unusually lengthy target sites, most of them spanning ≥15nt **(Figure 6A)** within the 10 kb promoter region. Overall predicted target sites on gene promoters outnumbered other regions with 43.56% of predicted sites, compared to 34.29% found in the 3'UTR, 16.54% in the coding sequence and 5.61% in the 5'UTR **(Figure 6B)**. Target sites were defined by their complementarity against the mature sequences of miRNAs and were only included in the results if they had a pValue≤0.05 following automatic statistical analysis by the miRWalk2.0 algorithm.

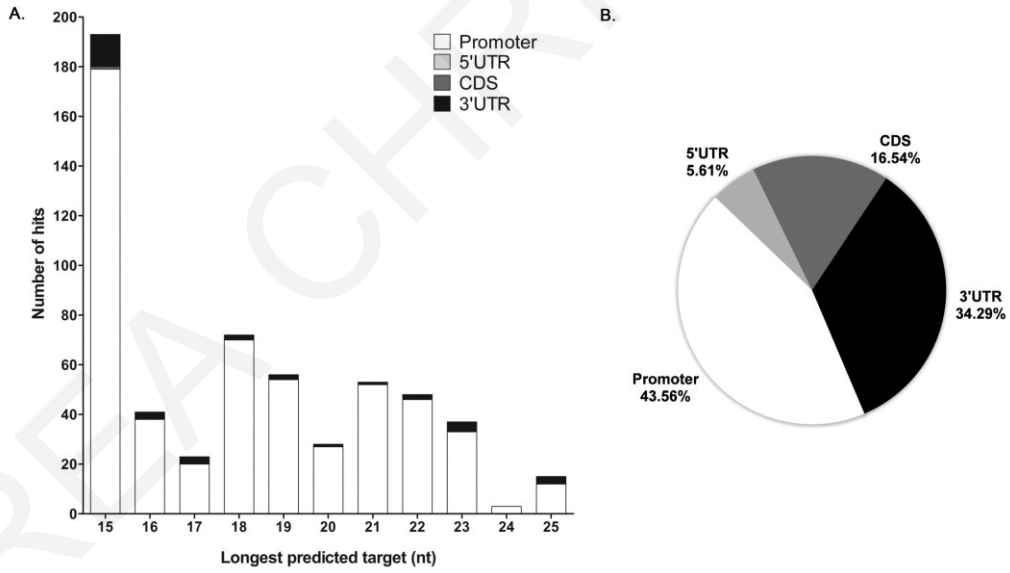

Figure 6: Target predictions by MiRWalk2.0 and target site region conservation. A. Distribution of predicted lengthier target sites for family MIR-548. Prediction results demonstrated an apparent enrichment of lengthy target sites located within the 10 kb promoter regions. Target sites were defined by their complementarity against the mature sequences of miRNAs and were only included in the results if they had a pValue≤0.05 following automatic statistical analysis by the miRWalk2.0 algorithm, **B. Percentage of total predicted binding sites.** Target predictions for MIR-548 family members were performed by miRWalk2.0 at the promoter, 5'UTR, coding sequence (CDS) and 3'UTR of all available genes. Target sites at the distant upstream promoter region were represented in 43.56% of total results, outnumbering hits in every other region, including the 3'UTR.

Upon comparing the mean values of the total predicted binding sites of 56 miRNAs belonging to MIR-548 family within gene promoter regions, sites predicted to be targeted by miR-548l were found to be significantly enriched ($p<0.001$; Oneway-ANOVA) in 45 different pair-wise comparisons. Interestingly, miR-548c-5p closely followed miR-548l and appeared to have a significantly ($p<0.001$) higher mean value of binding sites when compared with the mean values of 44 other members of MIR-548 family, reflecting a preferential appearance of predicted target sites upstream candidate genes possibly affecting transcriptional rates. Target prediction analysis for miR-548c-5p at the 10 kb upstream regions of genes, identified many lengthy target sites **(Table 9)**.

Table 9: Predicted target sites for miR-548c-5p on the 10 kb promoter region of different genes. Start and end values are defined as the position within the 10 kb input sequence ending at the transcription start point of associated genes. Seed region starts at either the 1st or the 2nd nucleotide of the mature miRNA sequence. Fourteen genes have perfect complementary (22 nt long site) site for the miR-548c-5p sequence within the promoter region.

Associated gene	miRNA	Target Complementarity (nt)	Start	End	Pvalue	Seed Region Start (nt)
FOXC2	hsa-miR-548c-5p	22	1310	1289	0	1
ANXA3	hsa-miR-548c-5p	22	9753	9732	0	1
C1orf94	hsa-miR-548c-5p	22	8984	8963	0	1
CDC23	hsa-miR-548c-5p	22	3638	3617	0	1
FGF23	hsa-miR-548c-5p	22	140	119	0	1
GPR141	hsa-miR-548c-5p	22	1914	1893	0	1
NR0B1	hsa-miR-548c-5p	22	4273	4252	0	1
NSUN5	hsa-miR-548c-5p	22	3064	3043	0	1
OR2T8	hsa-miR-548c-5p	22	2955	2934	0	1
PLAC1	hsa-miR-548c-5p	22	8757	8736	0	1
PSTPIP2	hsa-miR-548c-5p	22	9230	9209	0	1
RBP4	hsa-miR-548c-5p	22	2623	2602	0	1
UBQLN2	hsa-miR-548c-5p	22	8296	8275	0	1
ZNF418	hsa-miR-548c-5p	22	9269	9248	0	1
ASB5	hsa-miR-548c-5p	21	6948	6928	0	1
ATHL1	hsa-miR-548c-5p	21	7462	7442	0	1
CLYBL	hsa-miR-548c-5p	21	7613	7593	0	2
GRP183	hsa-miR-548c-5p	21	1569	1549	0	2
LBP	hsa-miR-548c-5p	21	3246	3226	0	1
NLRP11	hsa-miR-548c-5p	21	3015	2995	0	1
ORM1	hsa-miR-548c-5p	21	336	316	0	2
C11orf65	hsa-miR-548c-5p	20	8063	8044	0	1
SSH1	hsa-miR-548c-5p	20	4831	4812	0	1
ACSM2A	hsa-miR-548c-5p	19	3269	3251	0	1
ACSM2B	hsa-miR-548c-5p	19	3291	3273	0	1
AOX1	hsa-miR-548c-5p	19	9533	9515	0	1
HRK	hsa-miR-548c-5p	19	212	194	0	1
PTER	hsa-miR-548c-5p	19	9157	9139	0	1

RepeatMasker MADE1-type motif search of the lengthier predicted target sites (19-22 nt) was used to evaluate sites in further and many of them were highly similar to MADE1 sequences and shared their palindromic nature. Sequences that had 50 or less base matches, were considered as non-palindromic, hence having a low chance of being transcribed to a miRNA.

Among filtered hits, miR-548c-5p appeared to have a full-length target site at a region located >8 kb upstream and in *cis* with the *FOXC2* transcription start point, at 16q24 between genes *MTHFSD* and *FOXC2* **(Figure 7A)**.

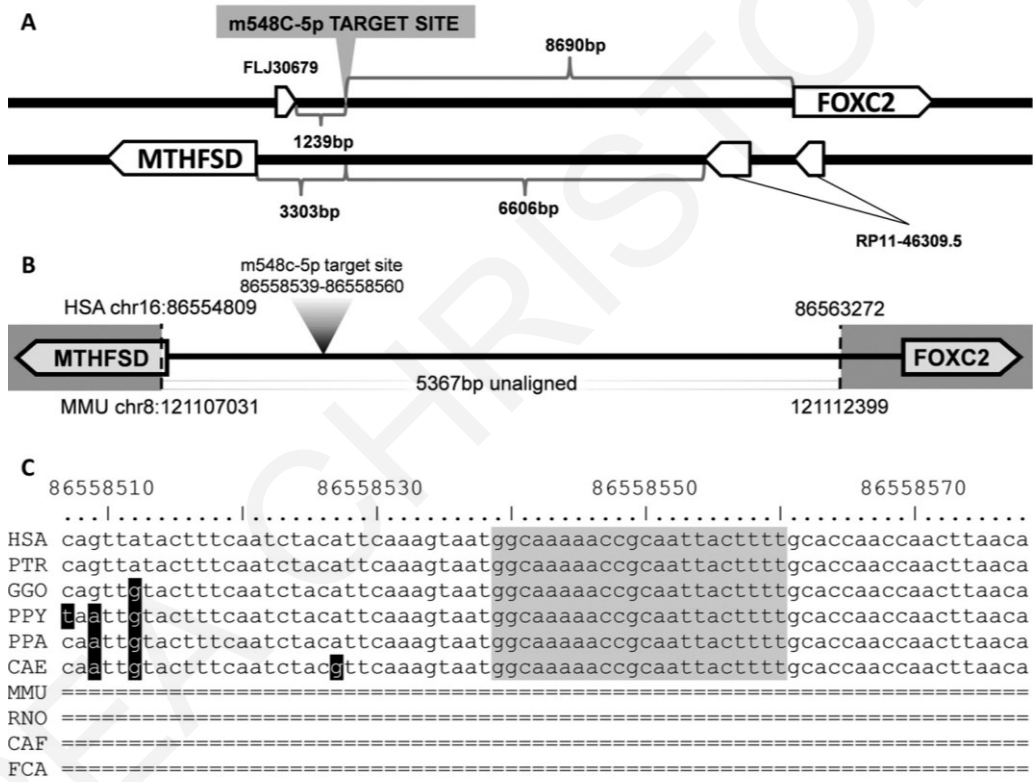

Figure 7: **A. *FOXC2*-associated miR-548c-5p target site topography**. The predicted site is placed 8.6 kb upstream of the *FOXC2* transcription start point in an intergenic region and does not participate in any transcripts. *MTHFSD* is placed 3.3 kb further upstream from the miRNA target site, encoded in the opposite direction (head-to-head with *FOXC2*). **B. Schematic alignment of human vs mouse synteny of the miRNA target region**. Head-to-head arrangement of *MTHFSD* and *FOXC2* in mouse chromosome 8 corresponds to (or is syntenic to) human chromosome 16. The intergenic region containing the miRNA predicted target site remains different in mice. The hatched pattern signifies conservation between human and mouse, while 5367 bp are different and unaligned to the human reference genome. **C. Multiple alignment of the miRNA target site region, between primates and other mammals**. Primates have a high degree of conservation for the site and flanking sequence while the same region is absent from other mammals. Data were retrieved from multiple alignments performed by multiz and other tools displayed in USCS genome browser, considering the default parameters of basewise conservation (phyloP) and element conservation (phastCons). Human (HSA), Chimp (PTR), Gorilla (GGO), Orangutan (PPY), Baboon (PPA), Green monkey (CAE), Mouse (MMU), Rat (RNO), Dog (CFA), Cat (FCA).

This site only shared 44/80 nt of the MADE1 consensus, thus it was considered as non-palindromic. As FOXC2 is a very important podocyte transcription factor and is highly involved in podocyte differentiation, we sought to prove whether this target site has a functional significance over *FOXC2* expression in a human podocyte cell line, which follows a gradual differentiation course, remaining undifferentiated when cultured at 33ºC and starting to differentiate when switched to 37ºC. Notably, while in primates both miR-548c-5p and this predicted target region are highly conserved, they are completely absent from mice, even though the genomic head-to-head arrangement of genes *MTHFSD* and *FOXC2* is maintained **(Figure 7B, Figure 7C)**. Hence, mPCs can be considered as a natural knock-out system for both the miRNA and its target site.

```
                ....|....| ....|....| ....|....| ....|....| ....|....| ....|....|
                    5          15         25         35         45         55
FOXC2-Target    CATAGTTCTC CGAAACTACA TCCAGTAGCT TCAGTTATAC TTTCAATCTA ---CATTCAA
miR-548c-5p     ---------- ---------- ---------- ---------- ---------- ----------
MADE-1          ---------- ---------- TTAGGTTGGT GCAAAAGTAA TTGCGGTTTT TGCCATTACT

                ....|....| ....|....| ....|....| ....|....| ....|....| ....|....|
                    65         75         85         95        105        115
FOXC2-Target    AGTAATGGCA AAAACCGCAA TTACTTTTGC ACCAACCAAC TTAACAAAAT GTAAGATTGT
miR-548c-5p     ------GGCA AAAACCGCAA TTACTTTT-- ---------- ---------- ----------
MADE-1          TTYAATGGCA AAAACCGCAA TTACTTTTGC ACCAACCTAA ---------- ----------

                ....|....| ....|....| ....|....| ....|....| ....|....| ....|....|
                   125        135        145        155        165        175
FOXC2-target    TTAATAAGCT AATAACTGAA AAGGTATTTG AAGAATTCTT TCCCTCACAT TAGAGGTTGC
miR-548c-5p     ---------- ---------- ---------- ---------- ---------- ----------
MADE-1          ---------- ---------- ---------- ---------- ---------- ----------
```

Figure 8: **Alignment of *FOXC2* target region with the miR-548c-5p target sequence, the MADE-1 consensus and the pri-miRNA sequence.**

4.2 Expression patterns of *FOXC2* and miR-548c-5p in differentiating hPCs suggest a dynamic relationship

The expression levels of *FOXC2* and miR-548c-5p were examined in hPCs at nine day-points during cell differentiation: day (-1) (D-1, corresponding to undifferentiated and dividing cells cultured at 33 ºC), day 1 (D1, 24h after switching to 37ºC), day 2 (D2), day 3 (D3), day 4 (D4), day 7 (D7), day 10 (D10), day 13 (D13), and day 16 (D16).

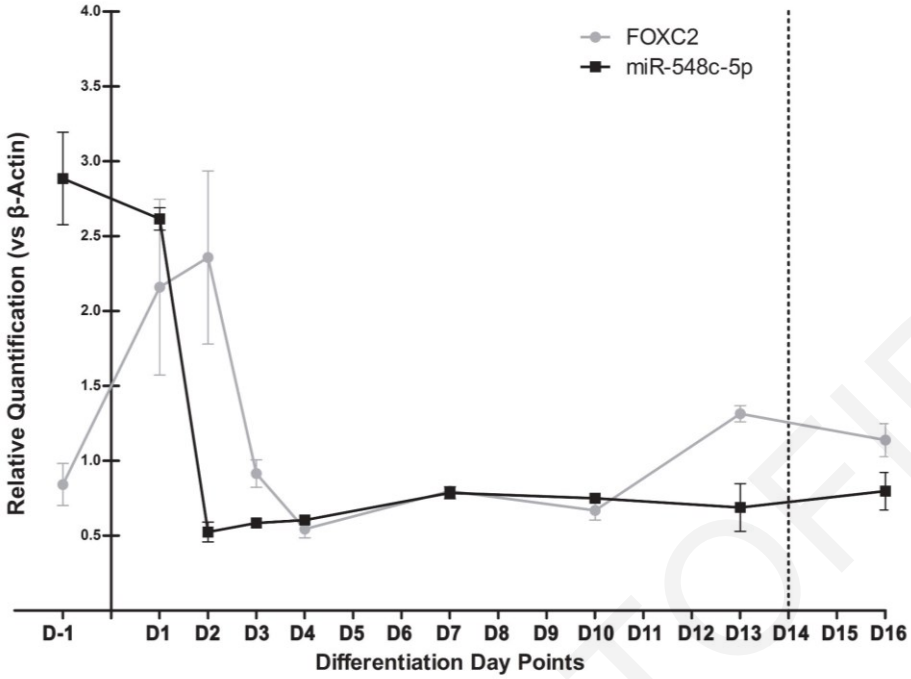

Figure 9: Endogenous mRNA expression levels of *FOXC2* and miR-548-5p at hPC differentiation time points. At day (-1) where cells proliferate, *FOXC2* levels are kept low and are elevated upon differentiation induction at day 1. By day 4 they return to previous baseline levels. miR-548c-5p is expressed in high levels at day (-1) and its levels are reduced dramatically as differentiation initiates to reach a low level of expression by day 2. Results are suggestive of an interplay between *FOXC2* and the miRNA, as they follow opposite patterns of expression to eventually return to baseline levels. (SEM, n=3 per condition in 3 technical replicates).

Results demonstrate an interchange between *FOXC2* and miR-548c-5p pattern of expression. More specifically, *FOXC2* is expressed at basal levels in undifferentiated cells. During initiation of, and early differentiation, *FOXC2* expression is increased, followed by a decrease to the same baseline as in undifferentiated cells, after a peak at day 2. miR-548c-5p follows the exact opposite pattern of expression; it is highly expressed in undifferentiated hPCs and its levels drop as differentiation initiates and is diminished at day 2 **(Figure 9)**. Accordingly, the pattern of FOXC2 protein expression in hPCs during differentiation was also investigated and correlated with data on mRNA expression **(Figure 10)**; cells at early days of differentiation show stronger FOXC2 staining.

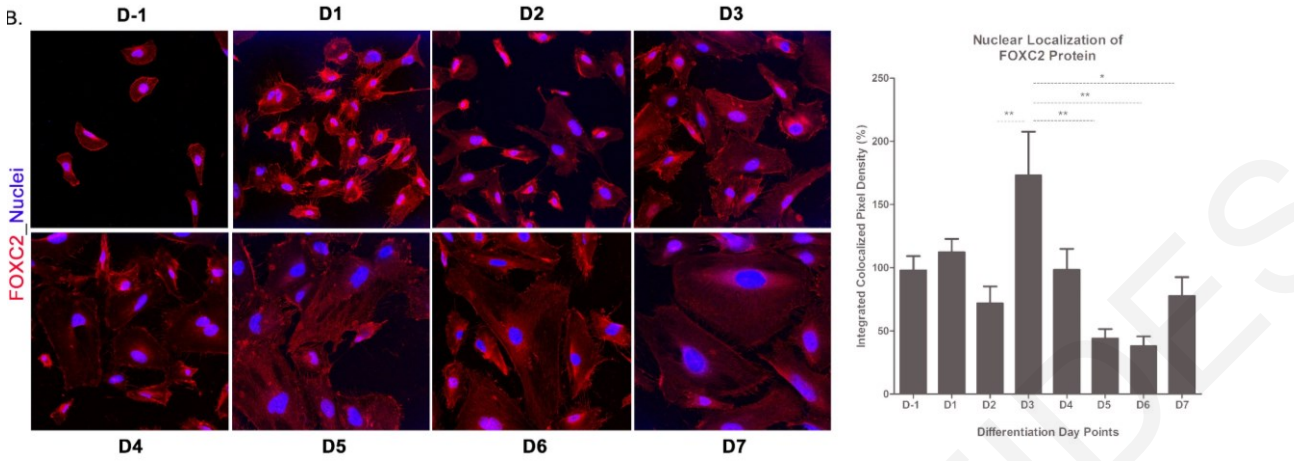

Figure 10: FOXC2 localisation during the differentiation time-course of hPCs. Images show representative confocal imaging of merged profiles from nuclei (blue) and FOXC2 (red). FOXC2 is mainly found in the nucleus of proliferating cells. As differentiation initiates FOXC2 nuclear localisation peaks at day 3 and gradually migrates from the nucleus to the cytoplasm as cells become larger and wider by day 7 (63x magnification). Result groups were analysed by one-way ANOVA with Tukey post-testing (*: $p<0.05$, **: $p<0.01$, ***: $p<0.001$, $n\geq5$ from independent slide preparations).

These patterns of expression indicate an interdependent functional relationship during the crucial first days of differentiation between miR-548c-5p and *FOXC2*, in response to the increasing needs for FOXC2 as hPCs enter differentiation. Expression measurements were performed for evaluating the response of the *MTHFSD* gene, coding for methenyltetrahydrofolate synthetase domain-containing protein whose function remains unknown, located further upstream of the miRNA target site. It was observed that *MTHFSD* expression does not seem to correlate to miR-548c-5p levels as it peaks at both day 1 and day 7 **(Figure 11)**. Thus, these results do not suggest a meaningful interdependence of *MTHFSD* and miR-548c-5p expression during differentiation. However, the effect of miR-548c-5p on MTHFSD levels was investigated in subsequent experiments to rule out any possible association between the two. Similarly, the expression levels of *FLJ30679,* a long-non coding RNA, and *RP11-46309.5*, whose function remains unknown, did not seem to be affected by the differentiation timeline **(Figure 11)**.

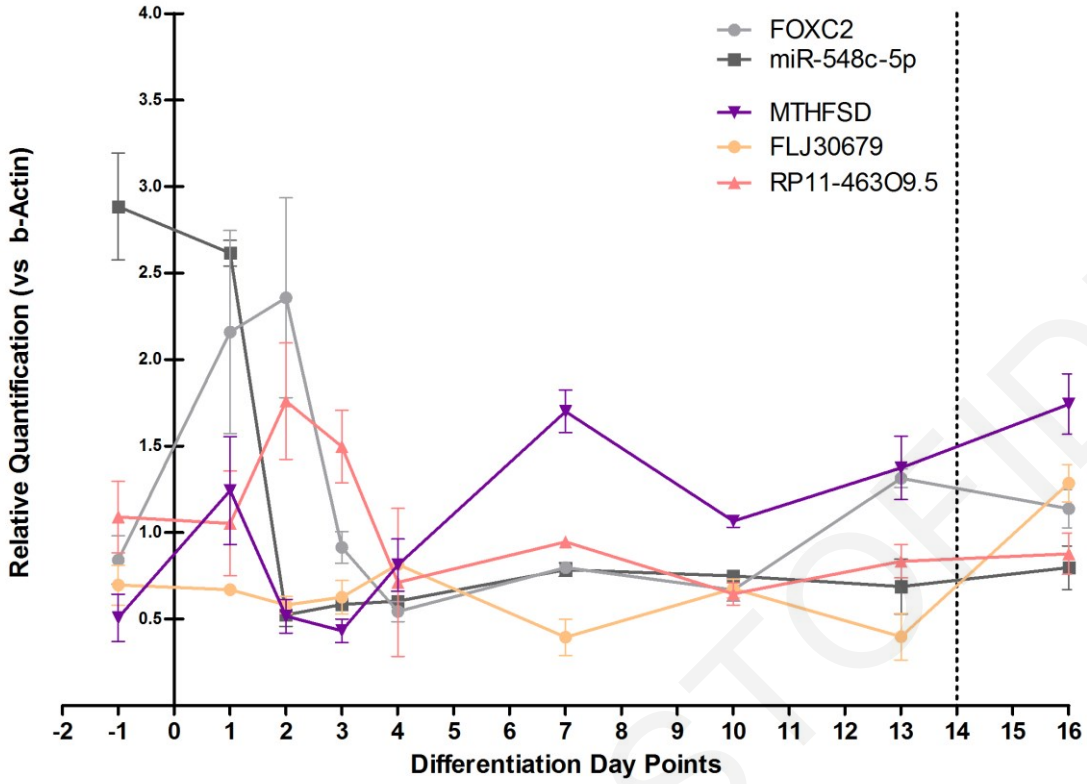

Figure 11: Endogenous mRNA expression levels of *MTHFSD*, *FLJ30679* and *RP11-46309.5* in relation to FOXC2 and miR-548-5p at hPC differentiation time points. *MTHFSD* expression levels are low in d (-1) hPCs, peak at day 1 and then again at day 7. As far as the expression of the other two genes, there seems to be a small increase in the expression of *RP11-46309.5* during day 2 of differentiation but other than that expression levels are maintained stable throughout all the time course points studied. (SEM, n=3 per condition in 3 technical replicates).

4.3 miR-548c-5p recognizes the predicted DNA target sequence with seed-region specificity

The ability of miR-548c-5p to recognise the predicted target site was investigated in cell culture luciferase construct experiments. The pGL4.27 vector expressing firefly luciferase (having an MCS within an enhancer element) was used to insert a 386 bp PCR product bearing the predicted wild type miR-548c-5p target site plus flanking sequences into the pGL4.27 vector (pGL4.27-wt). The size of the insert cloned into the pGL4.27 vector was determined by comparing the Relative light unit (RLU) values of pGL4.27 vectors containing inserts of different sizes with the RLU value obtained for the empty vector **(Figure 12)**.

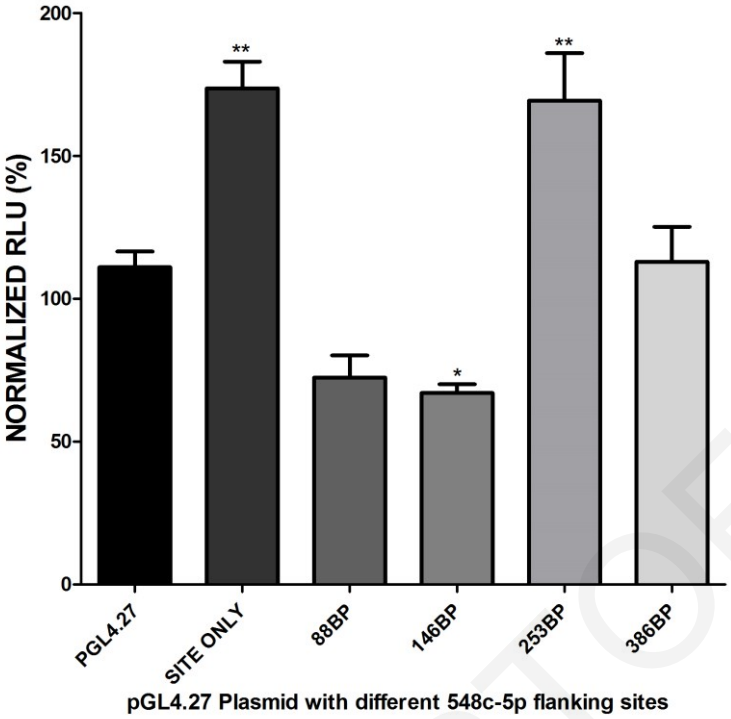

Figure 12: Relative light unit (RLU) values for pGL4.27 plasmids expressing renilla luciferase bearing inserts of variable length. The construct selected was the one having a 386bp insert containing the miR-548c-5p target site with flanking region, as it demonstrated similar expression to the empty vector (n=3 per construct).

Basal expression of luciferase was significantly diminished by 30% (p=0.011) when co-transfecting dividing hPCs with miRNA mimics and the pGL4.27-wt vector and was induced by 40% when removing endogenously expressed miR-548c-5p by co-transfection with miRNA inhibitors (p=0.018), compared to the control **(Figure 13B)**.

To test the specificity of the DNA target site towards miR-548c-5p seed region, serial mutations were introduced by site-directed mutagenesis to the miRNA's seed region from positions 2-5. When mutating position-2 (p.2) of the seed-region, luciferase was still induced by inhibitors, presumably owing to a strong effect of the endogenous miR-548c-5p **(Figure 13C, left panel)**. All binding effects were lost when adding more mutations at positions 2-5, as a result of seed-region alterations **(Figure 13C)**. This behaviour is reminiscent to how miRNAs identify target sites on 3'UTRs. Collectively, these results demonstrate regulation of luciferase gene expression by miR-548c-5p through a DNA target region at the enhancer element of the pGL4.27 vector, exhibiting a miRNA function pattern with seed-region influenced target recognition. The control in this set of experiments represents transfections with the AllStars NC scrambled sequence LNA (QIAGEN, West Sussex, UK).

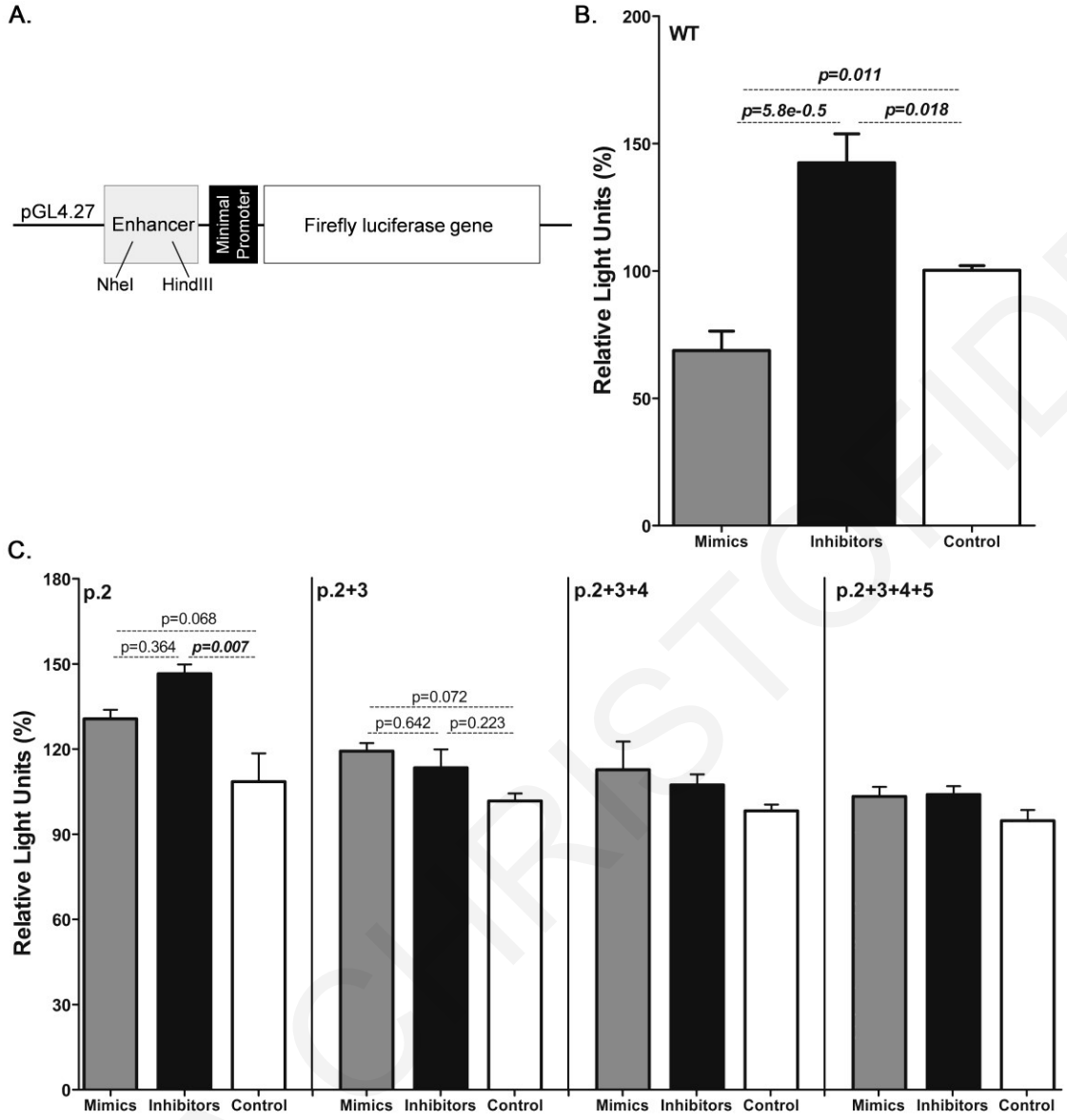

Figure 13: Reporter assay experiments demonstrate a regulation of luciferase expression by miR-548c-5p with seed-region specificity. A. Schematic representation of the pGL4.27 vector. The pGL4.27 vector used contains a multiple cloning site within the enhancer element (Enhancer) upstream the minimal promoter of the firefly luciferase gene. A 386 bp genomic fragment containing the miR-548c-5p target site was cloned into the enhancer using the *NheI* and *HindIII* restriction sites. **B. Luciferase expression levels in hPCs transfected with the pGL4.27-wt vector and miR-548c-5p mimics or inhibitors.** miR-548c-5p mimics significantly diminished luciferase levels (p=0.011), whereas inhibitors enhanced them (p=0.018) when compared to the control. (SEM, n=6 per LNA) **C. Luciferase levels after introducing sequential mutations on the nucleotides corresponding to the miRNA's seed region.** In the presence of the vector containing a mutation at position 2 of the target site, naturally transcribed endogenous miR-548c-5p is still active and is abolished by the inhibitor resulting in increased luciferase expression compared to the control, whereas miRNA mimics fail to cause a significant change (p. 2 with p=0.007). This effect is further attenuated with the introduction of consecutive mutations at nucleotides 3, 4 and 5 (p. 2 + 3, p. 2 + 3 + 4 and p. 2 + 3 + 4 + 5). The nucleotides replacing the seed region nucleotides have been selected at random. (SEM, n=3 per plasmid/LNA).

4.4 *FOXC2* mRNA levels are influenced by miR-548c-5p in hPCs

Consistent with the luciferase construct transfection results, persistent presence of miRNA mimics in two serial transfections of undifferentiated hPCs reduced *FOXC2* mRNA levels by 30%, while the removal of the highly expressed miR-548c-5p with inhibitors increased expression by 40% compared to control transfections **(Figure 14A)**. *MTHFSD* mRNA levels were boosted when adding miRNA inhibitors, while miRNA mimics have no effect on its expression **(Figure 15A)**. Importantly, in mouse PCs (mPCs), a natural knock-out for both miR-548c-5p and the miRNA binding site, neither mimics nor inhibitors affect *mFoxc2* or *mMthfsd* mRNA levels **(Figure 14B, Figure 15B)**. This finding lends confidence to the results with hPCs.

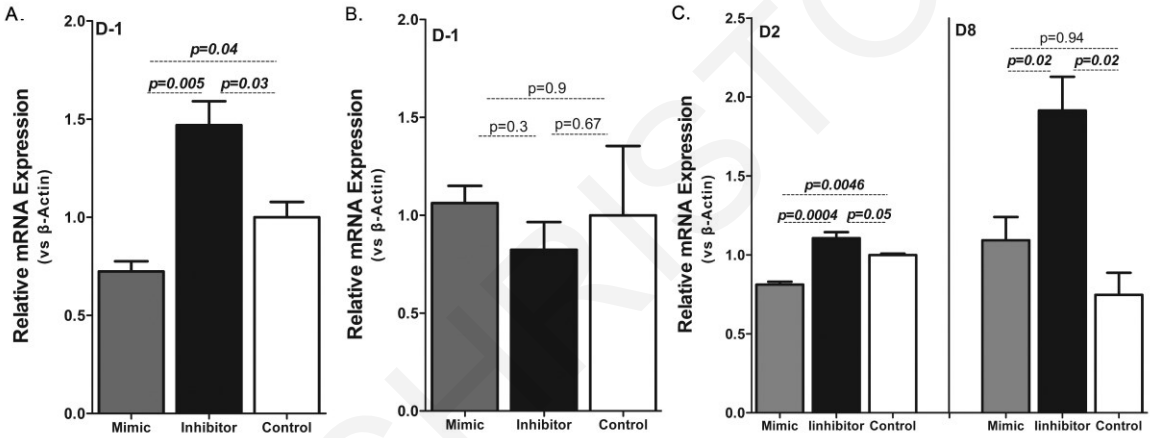

Figure 14: Influence of miR-548c-5p on endogenous *FOXC2* mRNA levels. A. *FOXC2* mRNA levels in undifferentiated hPCs transfected with miRNA mimics or inhibitors. Two sequential transfections were performed in undifferentiated hPCs with either miRNA mimics or inhibitors. *FOXC2* levels were decreased by 30% (p=0.04) with the addition of miRNA mimics and increased by 40% with miRNA inhibitors (p=0.03). (SEM, n=3 per condition in 3 technical replicates) **B. *mFoxc2* mRNA levels in undifferentiated mPCs transfected with miRNA mimics or inhibitors.** Two sequential transfections were performed in mPCs, which lack both miR-548c-5p and its target site, with either miRNA mimics or inhibitors. Transfections had no effect on the expression levels of *mFoxc2*. (SEM, n=3 per condition in 3 technical replicates) **C. *FOXC2* mRNA levels at days 2 and 8 of differentiation following transfections of hPCs with miRNA mimics or inhibitors.** Cells at day 1 and day 7 were transfected with miR-548c-5p mimics/inhibitors and harvested 24 h later. miRNA inhibitors cause a significant increase in *FOXC2* mRNA levels in both day 2 and day 8 (p=0.05 and p=0.02). However, miRNA mimics significantly reduced *FOXC2* levels only at day 2 (p=0.005), whereas at day 8 miR-548c-5p mimics fail to induce a reduction (p=0.94), possibly due to prior satiety of the target site. (SEM, n=3 per condition in 3 technical replicates).

During hPC differentiation, cells transfected at day 1 and day 7 with miR-548c-5p mimics/inhibitors and harvested 24 h later (day 2 and day 8 respectively), *FOXC2* mRNA levels followed the same pattern in both settings and are in agreement with results at day (-1), thus demonstrating a specific effect of the miRNA on *FOXC2* expression **(Figure 14C)**. This is suggestive of a dynamic system involving the abundance of miR-548c-5p and

FOXC2 mRNA in response to hPC course of differentiation. More specifically, at day 2, when miR-548c-5p endogenous expression levels are reduced and *FOXC2* levels are increased **(Figure 9)**, miRNA mimics repress *FOXC2* levels in a setting resembling undifferentiated cells; i.e. miRNA levels are high while *FOXC2* expression is low. Inhibitors on the other hand cause a significant increase in *FOXC2* levels at day 2. Moreover, at day 8, even though miRNA inhibitors cause an increase in the levels of *FOXC2,* miRNA mimics do not act correspondingly. This could possibly be due to a failure to exert an effect on an already saturated system, when the need for *FOXC2* by the cell is low and all available endogenous miR-548c-5p expressed at baseline levels is engaged on the target site.

Regarding *MTHFSD,* its mRNA levels appear to be unaffected by miRNA inhibitors at day 2 **(Figure 15C)**. Keeping in mind the time-course results, where at day (-1) miR-548c-5p is elevated and *MTHFSD* expression is lower compared to day 1 **(Figure 9)**, it was observed that mRNA levels were increased rather than decreased by mimics as expected. Moreover, at day 8 miRNA inhibitors also boost *MTHFSD* mRNA levels. Hence, results suggest an unpredictable and non-specific behaviour by *MTHFSD* in relation to miR-548c-5p.

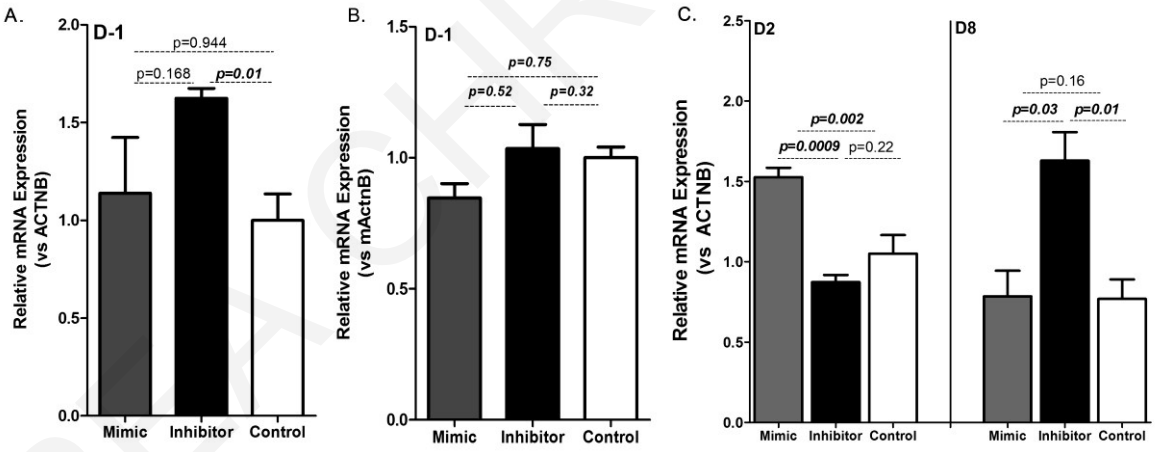

Figure 15: Influence of miR-548c-5p on endogenous *MTHFSD* mRNA levels. A. *MTHFSD* mRNA levels in undifferentiated hPCs transfected with miRNA mimics or inhibitors. *MTHFSD* levels were enhanced with the addition of miRNA inhibitors (p=0.01) while miRNA mimics had no significant effect. (SEM, n=3 per condition in 3 technical replicates) **B. *mMthfsd* mRNA levels in undifferentiated mPCs transfected with miRNA mimics or inhibitors.** Two sequential transfections were performed in mPCs, which lack both miR-548c-5p and its target site, with either miRNA mimics or inhibitors. Transfections had no effect on the expression levels of *mMthfsd*. (SEM, n=3 per condition in 3 technical replicates) **C. *MTHFSD* mRNA levels at days 2 and 8 of differentiation following transfections of hPCs with miRNA mimics or inhibitors.** *MTHFSD* mRNA are enhanced when transfecting cells with mimics at day 1 (p=0.002) and are unaffected by miRNA inhibitors at the same time-point. Moreover, an effect similar to day (-1) findings for *MTHFSD* expression is evident at day 8, as miRNA inhibitors enhance its mRNA levels (p=0.01), thus indicating that *MTHFSD* expression is independent from miRNA dosage. (SEM, n=3 per condition in 3 technical replicates).

4.5 The RISC is bound on the miR-548c-5p DNA target region at day(-1) and day7

Ago-ChIP experiments were performed in hPCs at day (-1) (undifferentiated cells). The DNA sequence encompassing the miR-548c-5p target site was found to be significantly enriched compared to other genomic regions towards and into the *FOXC2* gene. Amplicon P0 **(Figure 5)** showed a highly statistically significant consistent enrichment over all other amplicons (amplicons PA-PD in **Figure 16A)**. The same samples were tested for the nuclear enrichment of miR-548c-5p. Compared to control miRNAs that included miR-23b, a podocyte specific miRNA, miR-29c, a miRNA previously identified to mainly act in the nucleus (Hwang et al., 2007, Liao et al., 2010) and miR-30d-3p, also active in podocytes (Shi et al., 2013, Liu et al., 2016), miR-548c-5p was significantly enriched in immunoprecipitated samples at day (-1) **(Figure 16B)**. Quite importantly, repetition of these experiments with a different anti-Ago antibody (Millipore, Germany) produced a similar enrichment when comparing P0 to PC **(Figure 17)**.

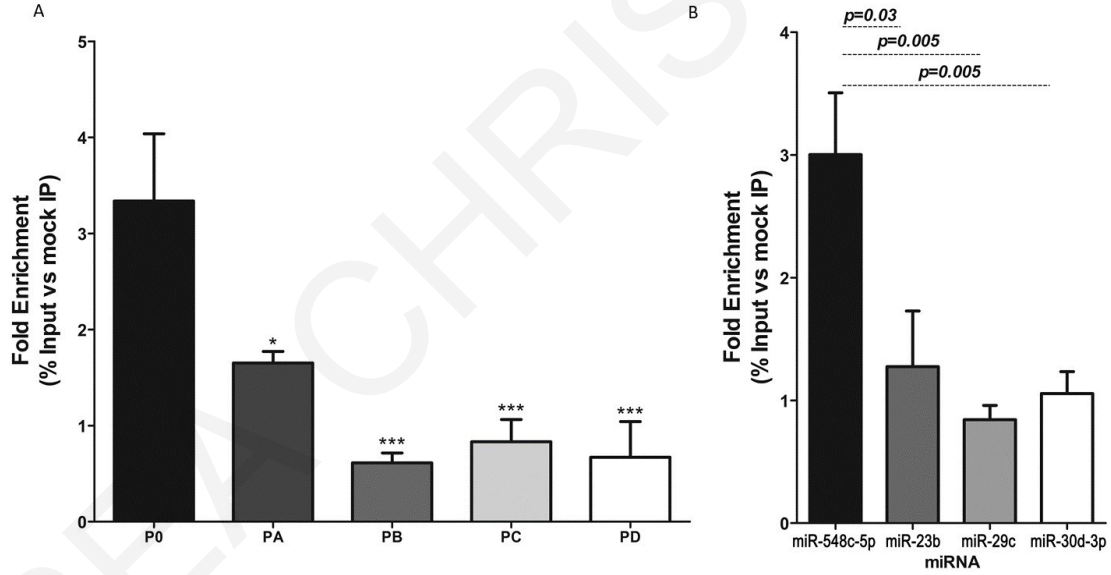

Figure 16: DNA target site and miR-548c-5p relative enrichment after Ago-ChIP experiments in undifferentiated hPCs. A.DNA target site relative enrichment following Ago-ChIP experiments: P0 was found to be significantly enriched compared to every other region examined while walking closer to the *FOXC2* gene ($p<0.05$ compared to region PA and $p<0.001$ compared to regions PB, PC, PD). Results are depicted as fold change: The Cps obtained were calculated as enrichment to the input sample (10%). Baseline was defined by further normalizing values over mock (mIgG or beads) % input IP values. (SEM, $n\geq3$ per primer set in 3 technical replicates). **B. miR-548c-5p relative enrichment following Ago-ChIP experiments** miR-548c-5p was also significantly enriched when compared to the podocyte specific miR-23b ($p=0.03$), the predominantly nuclear miR-29c ($p=0.005$) and miR-30d-3p ($p=0.005$), also found in abundance in podocytes. Results are depicted as fold change: The Cps obtained were calculated as enrichment to the input sample (10%). Baseline was defined by further normalizing values over mock (mIgG or beads) % input IP values. (SEM, $n\geq3$ per primer set in 3 technical replicates).

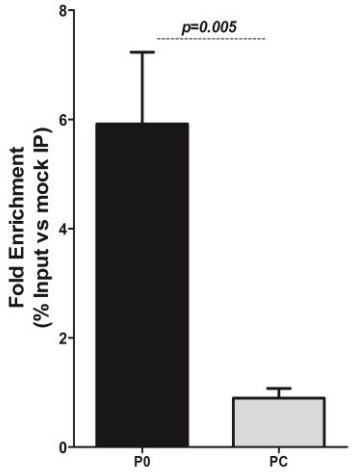

Figure 17: DNA target site relative enrichment in proliferating hPCs using a different anti-Ago antibody. A different anti-Ago antibody was used for verification purposes. Results are consistent with previous experiments as region P0 was significantly enriched compared to region PC ($p=0.006$). Results are depicted as fold change: The Cps obtained were calculated as enrichment to the input sample (10%). Baseline was defined by further normalizing values over mock (mIgG or beads) % input IP values (SEM, n=3 per primer set in 3 technical replicates).

In another setting, P0 had comparable enrichment in non-differentiating HEK293T cells **(Figure 18)**. Collectively, results suggest that the RISC complex is bound at this region in both undifferentiated hPCs and HEK293T, presumably guided by miR-548c-5p, which is highly enriched in hPC nuclei.

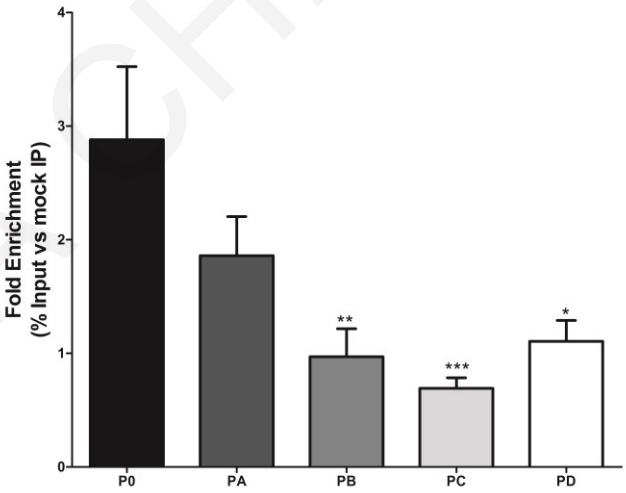

Figure 18: Target site relative enrichment after Ago-ChIP experiments in HEK-293T cells. P0 was significantly enriched compared to regions PB ($p<0.01$), PC ($p<0.001$) and PD ($p<0.05$), demonstrating a similar trend with undifferentiated hPCs. Results are depicted as fold change: The Cps obtained were calculated as enrichment to the input sample (10%). Baseline was defined by further normalizing values over mock (mIgG or beads) % input IP values. (SEM, n=3 per primer set in 3 technical replicates).

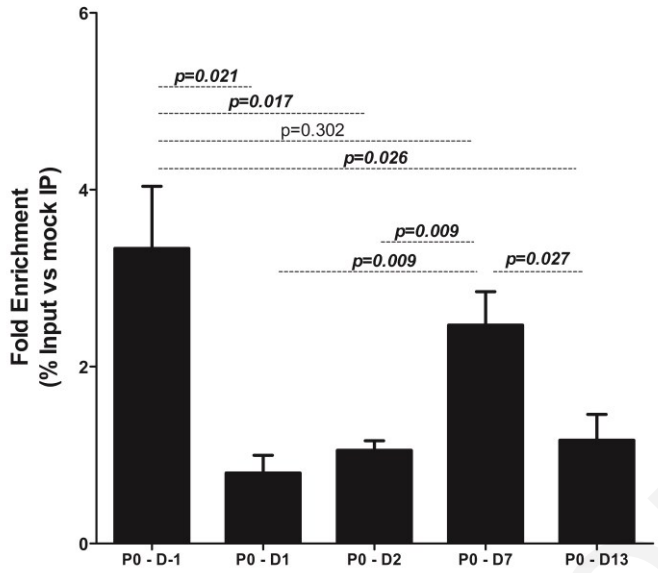

Figure 19: Relative enrichment of the P0 amplicon in selected hPC differentiation time points. P0 was significantly immunoprecipitated in day (-1) and day 7 hPCs, suggesting an association between *FOXC2* expression levels and target site occupancy by the RISC. Results are depicted as fold change: The Cps obtained were calculated as enrichment to the input sample (10%). Baseline was defined by further normalizing values over mock (mIgG or beads) % input IP values (SEM, n≥3 per primer set in 3 technical replicates).

Different time-points in differentiating hPCs demonstrated occupation of the target site fragment P0 by RISC at day (-1) and day 7 **(Figure 19)**, corresponding with the baseline expression pattern of *FOXC2* during differentiation **(Figure 9)**.

Target site occupancy by miR-548c-5p and target sequence specificity was evaluated by Ago-ChIP experiments using undifferentiated mPCs, an absolute negative control for both the miRNA and its target site, transfected with the pGL4.27 vectors used in luciferase experiments and mimics or NC. Results revealed an enrichment of the target site fragment in mPCs transfected with the pGL4.27-wt construct and miR-548c-5p mimics **(Figure 20)**. Enrichment was lost when a plasmid mutated (P-Mut-m548c-5p) at seed-region nucleotides (positions 2 and 3) was used.

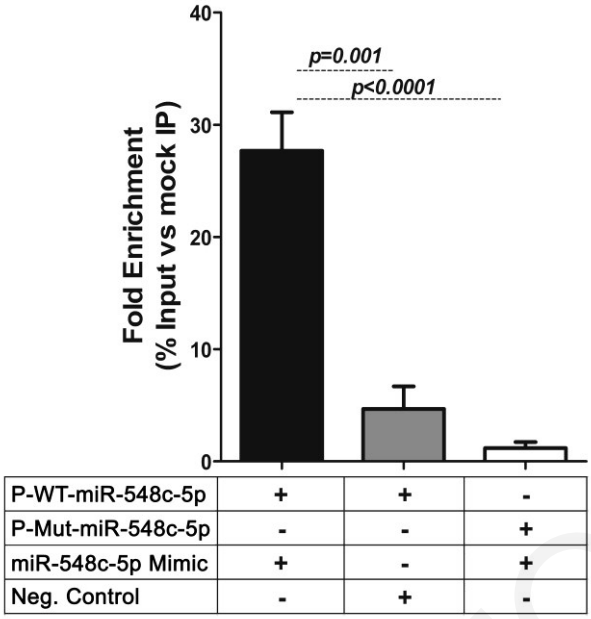

Figure 20: Ago-ChIP experiments performed in mPCs transfected with plasmids containing the WT or mutated miRNA target site in the presence or absence of miR-548c-5p mimics. mPCs represent a knock-out both for miR-548c-5p and its target site. When transfected with the pGL4.27 vector bearing the WT target site (P-WT-m548c-5p) and miRNA mimics, an enhanced enrichment of the target site fragment (p=0.001) was observed. This effect was lost when cells were transfected with a plasmid containing point mutations at positions 2 and 3 (P-Mut-m548c-5p) of the miRNA seed-region (p<0.0001). Results are depicted as fold change: The Cps obtained were calculated as enrichment to the input sample (10%). Baseline was defined by further normalizing values over mock (mIgG or beads) % input IP values (SEM, n=3 per condition in 3 technical replicates).

4.6 Evidence for mobility of miR-548c-5p target site region towards the FOXC2 proximal promoter when hPC differentiation initiates

Results as far demonstrated an association between miR-548c-5p and *FOXC2* mRNA expression and highly supported an interaction of the miRNA with its target site upstream of *FOXC2*. Equally importantly, Ago-ChIP results indicate occupancy of the miR-548c-5p target site region by RISC at two specific time-points. Taken together, these results were suggestive of an enhancing effect by the DNA target region under study, possibly exerted due to DNA conformational changes causing its mobility and juxtaposition against the proximal *FOXC2* promoter sequences. To investigate the occurrence of such interactions, 3C experiments were performed at four hPC differentiation day-points **(Figure 21)**.

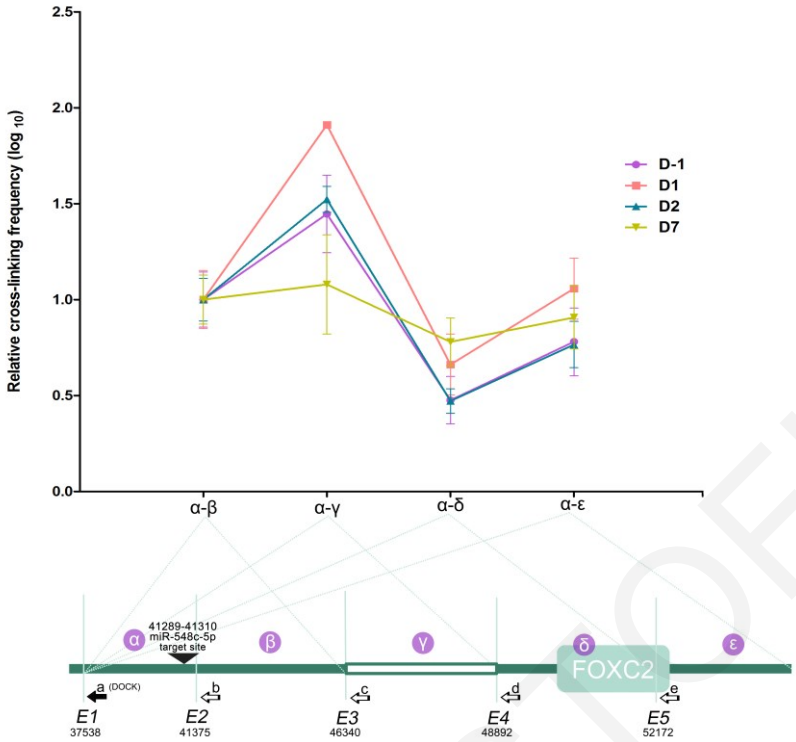

Figure 21: miR-548c-5p target site region interacts with the *FOXC2* promoter upon differentiation induction in hPCs. 3C experiments were performed at four hPC differentiation time points (day (-1), day 1, day 2, day 7). Ligation products were quantified by qRT-PCR. Amplicons were amplified by using a reverse docking primer (black arrow - A) at the DNA fragment containing the miR-548c-5p target site (α) and different reverse primers (B-E) each representing a fragment generated after *EcoR*I digestion at specific sites (*e1-e5)* of crosslinked DNA. Position of *EcoR*I restriction sites are noted by numbering relevant to the BAC clone used as a control. Region α was designated as the region between positions *e1* and *e2* of *EcoR*I digestion, which includes the miR-548c-5p target site, region β between positions *e2* and *e3*, region γ containing the *FOXC2* promoter between *e3* and *e4*, region δ between *e4* and *e5* including part of the *FOXC2* gene, region ε after position *e5*. The lower panel schematic is not in scale. The interaction between region α and the four other regions was determined. The relative cross-linking frequency of the fragment α-β, was set as the starting point to evaluate interactions. It was observed that the target site fragment α mobility towards fragment γ was enriched at day1 compared to other day points and every interaction was diminished by day 7. (SEM, n=3 per condition in 3 technical replicates).

Evidently, cells at day 1 demonstrate a notable enrichment of the resulting fragment α-γ, which signifies the interaction between the miRNA target site region and the promoter region of *FOXC2*, while the effect attenuates in the remaining fragments. Day (-1) and day 2 follow a similar but less prominent effect for fragment α-γ, with the effect being completely lost by day 7. In greater detail, the relative crosslinking frequency between α-γ at day (-1) is lower than the one seen at day 1, which signifies reduced interaction between fragment α containing the target site and fragment γ (*FOXC2* promoter).

This correlates with the enrichment of fragment P0 in Ago-ChIP experiments at day (-1) **(Figure 19)** as the RISC appears to be bound on the target site and thus hinders the interaction of fragments α-γ. Considering how FOXC2 mRNA levels rise when

differentiation initiates **(Figure 9)**, RISC appears to be released from region P0 when the mobility of the target site fragment towards the promoter of *FOXC2* is more pronounced at day 1 to boost expression levels. At day 7, the target site region appears enriched in Ago-ChIP experiments **(Figure 19)**, hence no interactions were expected to take place at the chromosomal level, while FOXC2 mRNA levels are at baseline. Moreover, following transfection of hPCs with miR-548c-5p mimics and inhibitors, the relative cross-linking efficiency of fragment α-γ was affected.

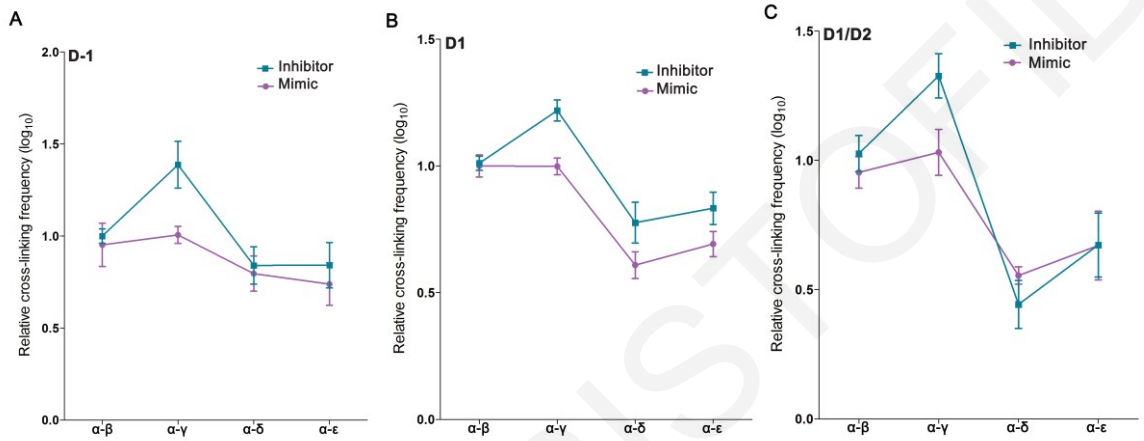

Figure 22: miR-548c-5p effect on fragment interactions in 3C experiments. Interactions were altered after transfection of hPCs with miR-548c-5p mimics and inhibitors at day (− 1). Cells transfected with miRNA mimics at day (− 1) presented a marked loss of α–γ enrichment, while inhibitors kept this interaction at high levels. Dynamics in hPCs at day 1 were altered by miRNA mimics. In line with results of cells transfected at day (− 1), the relative cross-linking efficiency of fragment α–γ appeared also to be compromised by miRNA mimics at day 1 of differentiation. Sequential transfections of hPCs at days 1 and 2 with miRNA mimics or inhibitors result in similar effects. Mimics introduced in differentiating cells were able to reduce interactions between fragments α and γ, while inhibitors enhanced interactions. The enrichment of fragment α–δ by inhibitors appeared markedly low compared to α–γ to signify a strong interaction of the site with the promoter region of *FOXC2*. Ligation products were quantified by qRT-PCR. (SEM, n=3 per condition in 3 technical replicates).

Mimics introduced at day (-1) diminished all interactions, while inhibitors demonstrated enrichment of α-γ fragments **(Figure 22, left panel)**. The same results were observed in hPCs transfected at day 1 **(Figure 22, middle panel)**. To investigate interactions in further, cells were transfected with mimics and inhibitors for two consecutive days (day 1 & day 2) before harvesting. In this case, the pattern of α-γ enrichment was much stronger with inhibitors and appeared to have a distinct difference compared to all other fragments **(Figure 22, right panel)**. Results are suggestive of a coordinated mobility configuration of the target site region towards the promoter of *FOXC2* and chromosomal dynamics seem to be specifically influenced by miR-548c-5p abundancy in the cell. These interactions suggest the presence of a yet unknown enhancer element related to the miR-548c-5p target site

region, which seems to remain constrained in undifferentiated hPCs at day (-1) and differentiating cells at day 7, when *FOXC2* remains at baseline expression levels.

4.7 Increased miR-548c-5p affects FOXC2 protein levels

Cells entering differentiation experience a drop in miR-548c-5p expression during the first days, to reach baseline levels at later time-points **(Figure 9)**. To study the effect of high miR-548c-5p levels on protein expression of FOXC2, WT1 and other podocyte markers, hPCs were transfected with mimics and scrambled NC and switched to 37ºC to initiate differentiation. Cells were transfected at two consecutive time-points, day 1 and day 2, and were either harvested after 30 h to study the effects caused by the elevation of miR-548c-5p, or after 48 h to see how protein levels recover. At 30 h post transfection, FOXC2 protein levels were significantly reduced compared to controls **(Figure 23)**. Moreover, as the cells were let to recover for 48 h after the last transfection time-point, FOXC2 protein expression was significantly increased compared to controls. In line with data on FOXC2 mRNA expression **(Figure 14C)**, high levels of miR-548c-5p during the first days of differentiation cause a delay in FOXC2 protein expression, an effect which implies that the general differentiation course of podocytes might also be affected by miRNA mimics. Accordingly, the expression of WT1, the most important transcription factor and a specific marker of podocytes, known to succeed FOXC2 in podocyte differentiation, is also down regulated in transfected cells and its levels remain low in recovering cells **(Figure 23)**. The increase in FOXC2 levels 48 h post transfection and four days into differentiation could indicate a delayed initiation of differentiation, also reflected by WT1 reduced levels. Nephrin levels remain lower in both transfected and recovering cells, while podocin expression seems unaffected with a slight (but not statistically significant) increase in expression in recovering cells **(Figure 23)**. Synaptopodin remains stably expressed indicating the preservation of cell type identity. Moreover, a great increase in p57 expression, known to induce cell cycle arrest (Harvey et al., 2008, Koutroutsos et al., 2014) was observed 30 h post-transfection, possibly demonstrating the end of the proliferating stage, while in recovering cells p57 levels have no difference between cells treated with mimics and the control **(Figure 23)**.

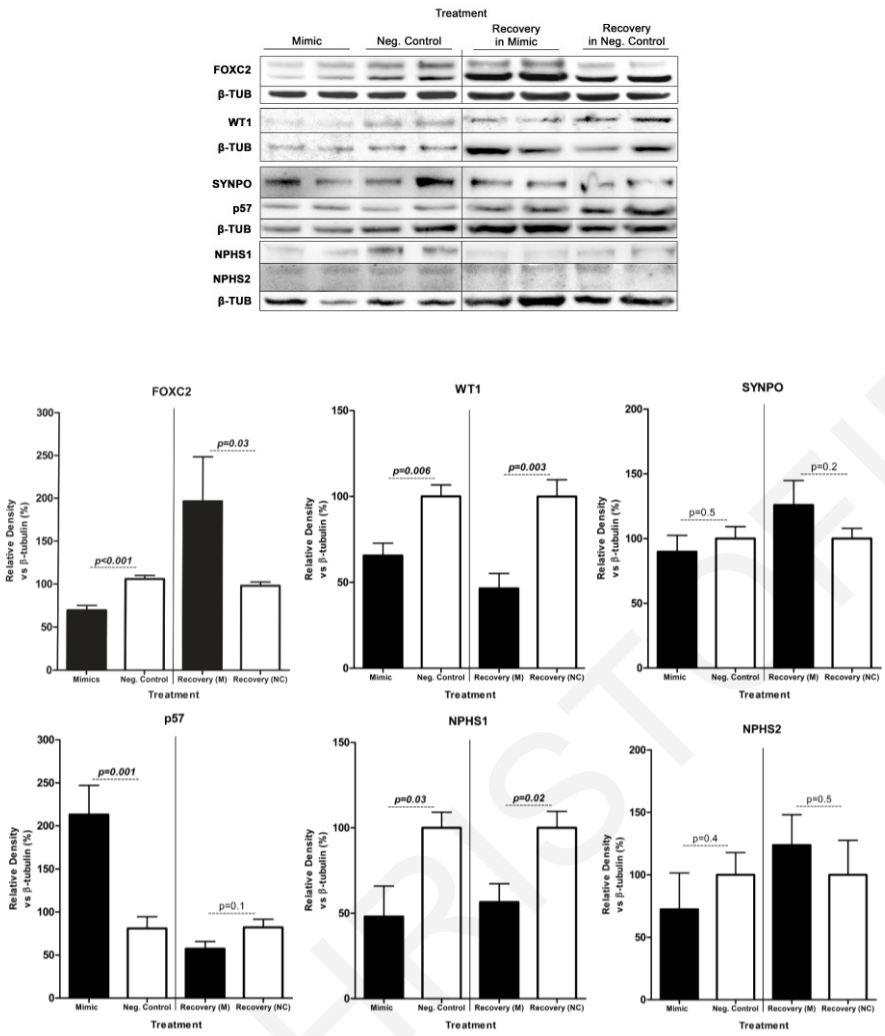

Figure 23: Podocyte protein levels are influenced by miR-548c-5p mimics. hPCs were serially transfected at day (-1) and day 1 with miR-548c-5p mimics (M) or negative control LNAs (Neg. Control) and harvested 30 h after the second transfection or 48 h post the second transfection (Recovery). FOXC2, WT1 and NPHS1 protein levels were significantly reduced in cells harvested 30 h post-transfection compared to control samples. On the contrary, a substantial increase in the expression of p57 was observed (p=0.001), whereas NPHS2 and synaptopodin levels did not differ significantly from control samples (SEM, n=3 per LNA), In recovery cells, harvested 48 h post transfection, FOXC2 levels were increased, whereas WT1 levels were reduced compared to the control samples. NPHS1 levels remain low, whereas NPHS2, p57 and synaptopodin remained unaffected. (SEM, n≥3 per LNA).

4.8 Localisation of FOXC2 in differentiating hPCs is affected by miR-548c-5p mimics

In undifferentiated human podocytes, FOXC2 accumulates in the nucleus, while in differentiated cells it becomes mainly perinuclear. On day 3 of differentiation when FOXC2 levels are high, its nuclear localisation is more pronounced **(Figure 10)**. This result is in line with the data on *FOXC2* mRNA expression **(Figure 9)**, where *FOXC2* appears to peak at day 1 and day 2 and returns to basal levels later, while high protein levels are retained until

day 3, in accordance with its longer half-life. Previous publications also support that podocytes overexpressing FOXC2, have a stronger nuclear staining (Datta et al., 2015, Hader et al., 2010). More specifically, small-sized undifferentiated hPCs keep FOXC2 in the nucleus, while cells entering differentiation have strong nuclear staining which gradually moves mostly around the nucleus and the cytoplasm, accompanied by FOXC2 reduction and marking cell differentiation **(Figure 9)**.

In parallel to Western blot data, to study the effect of high miR-548c-5p concentration in hPCs on FOXC2 localisation, differentiating hPCs were transfected with miR-548c-5p mimics for 5 consecutive days. Cells were then either harvested 12 h post-transfection (day 5) or after they were left to recover for 72 h (day 8). In controls at day 5 FOXC2 expression in hPCs, is low and has a cytoplasmic or perinuclear localisation, as expected. Image analysis corroborates this also for cells transfected with miRNA mimics. However, in recovering cells (miR-548c-5p Mimics day 8), FOXC2 has a stronger nuclear staining and significantly higher expression, as seen by densitometry analysis **(Figure 24A).** Recovering cells resemble cells undergoing differentiation at day 3 in terms of FOXC2 profile **(Figure 10)**, although they appear large and differentiated-like similar to day 7 cells. Hence, this mixed phenotype in hPCs suggests that the miRNA abundance, at differentiation time-points were the endogenous miR-548c-5p is low, appears to influence FOXC2 expression dynamics. The abundance of miR-548c-5p was also studied in undifferentiated hPCs at day(-1), which express the miRNA at high levels **(Figure 9)**. By knocking-down miR-548c-5p in proliferating undifferentiated hPCs with inhibitors for 5 consecutive days, FOXC2 was found to be strongly expressed. It appears to stain both inside and around the nucleus, with nuclear staining being significantly higher compared to the control and cells transfected with miRNA mimics **(Figure 24B)**. Again, this appearance is reminiscent of differentiating cells at day 3, while cells are smaller in size **(Figure 10)**.

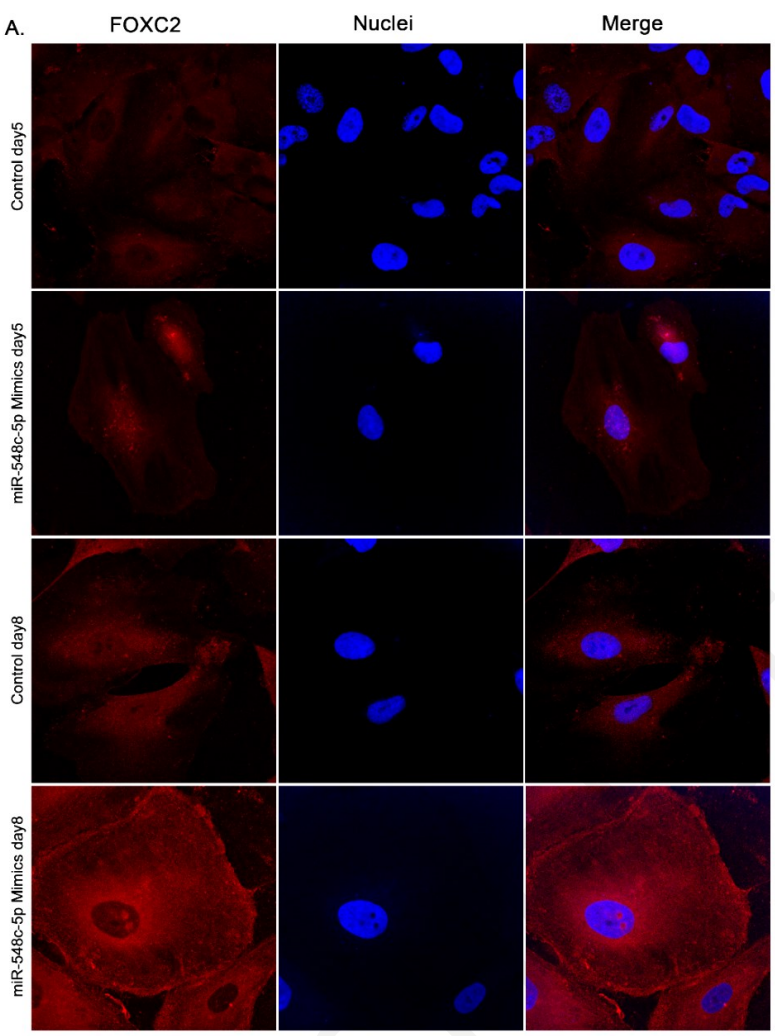
A.
FOXC2
Nuclei
Merge
Control day5
miR-548c-5p Mimics day5
Control day8
miR-548c-5p Mimics day8

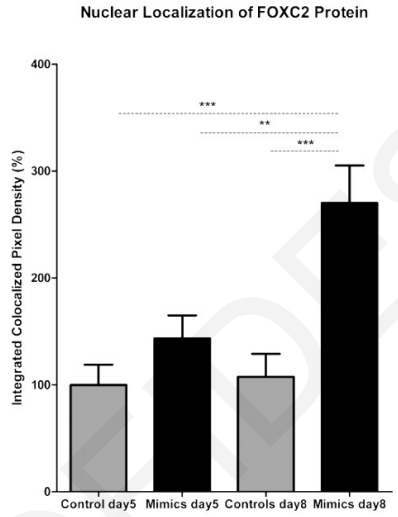
Nuclear Localization of FOXC2 Protein
Integrated Colocalized Pixel Density (%)
400
300
200
100
0
***
**
***
Control day5
Mimics day5
Controls day8
Mimics day8

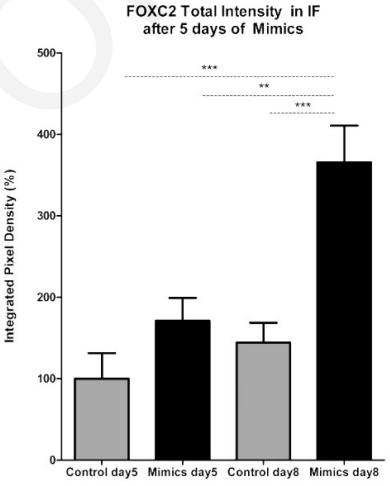
FOXC2 Total Intensity in IF
after 5 days of Mimics
Integrated Pixel Density (%)
500
400
300
200
100
0
***
**
***
Control day5
Mimics day5
Control day8
Mimics day8

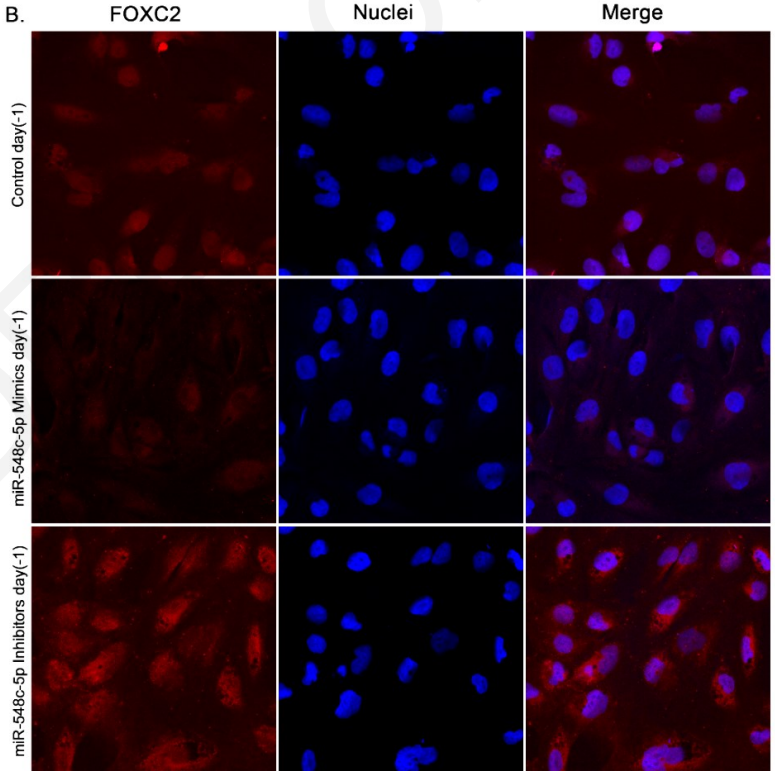
B.
FOXC2
Nuclei
Merge
Control day(-1)
miR-548c-5p Mimics day(-1)
miR-548c-5p Inhibitors day(-1)

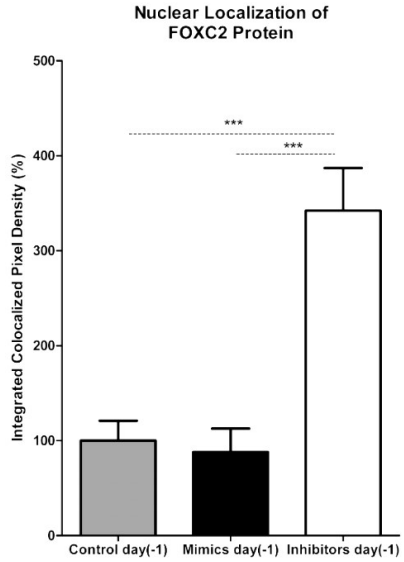
Nuclear Localization of
FOXC2 Protein
Integrated Colocalized Pixel Density (%)
500
400
300
200
100
0
***
***
Control day(-1)
Mimics day(-1)
Inhibitors day(-1)

Figure 24: FOXC2 localisation in hPCs in response to miR-548c-5p. Loss of miRNA expression induces expression of FOXC2. Densitometry analysis was performed by ImageJ and all result groups were analysed by one-way ANOVA with Tukey post-testing (**: $p<0.01$, ***: $p<0.001$, $n\geq5$ from independent slide preparations). **A. miR-548c-5p mimics effect on FOXC2 in differentiating podocytes.** Representative confocal imaging of differentiating hPCs transfected with miR-548c-5p mimics for 5 consecutive days and harvested 12 h (day 5) and 72 h (day 8) post transfection. In cells harvested at day 5 (miR-548c-5p Mimics day 5) FOXC2 displayed a similar cytoplasmic localisation to the control. In cells let to recover for three days after mimic transfections (miR-548c-5p Mimics day 8), FOXC2 had a stronger expression compared to controls and was also localised in the nuclei of cells, resembling cells in the early stages of differentiation (63x magnification). **B. Effect of miR-548c-5p inhibition in undifferentiated hPCs on FOXC2 localisation.** Representative confocal imaging of undifferentiated hPCs at day (-1), transiently transfected with miR-548c-5p inhibitors (miR-548c-5p Inhibitors day (-1)) and mimics (miR-548c-5p Mimics day (-1)) for 5 consecutive days. miRNA inhibitors resulted in stronger FOXC2 staining in the cytoplasm and nuclear localisation of FOXC2 was more pronounced. Contrastingly, FOXC2 expression appears to weaken by miRNA mimics compared to inhibitors (63x magnification).

Chapter 5: Discussion

During the last few years several studies have demonstrated the importance of miRNAs in the regulation of gene transcription, a feature complementing their well-established action in fine-tuning mRNA translation. The aim of this study was to demonstrate that the expression of *FOXC2*, the earliest podocyte marker with a prominent role in differentiation, development and maturation of podocytes, is influenced by miR-548c-5p through a target site located more than 8kb upstream the gene's transcription start site.

Prediction analyses using the miRWalk2.0 platform revealed interesting results in regards to MIR-548 family members and miR-548c-5p in particular. According to miRbase (Kozomara and Griffiths-Jones, 2013), the miR-548 family is comprised of 121 mature miRNAs, 81 of which are found in humans and 40 are primate specific. Impressively, miR-548 family members appeared to have an enrichment of predicted target sites on genomic sequences upstream transcription start sites (termed here as "promoters"), compared to the 5'UTR, the coding sequence and the 3'UTR. Specifically, targets in the region upstream the transcription start sites represent 43.56% **(Figure 6A, Figure 6B)**. These target sites were much lengthier compared to other genomic regions – at times reaching up to the full length of a given miRNA. The abundance and length of these target sites can be well explained by their origins; such MADE1-type sequences originating from transposable elements are spread out in the human genome and are presumably more frequently placed in non-coding regions. It is worth noting that the RNA interference pathway has primarily been evolved as part of the cell's need of a protection mechanism against TEs (Obbard et al., 2009).

To document the existence of an interaction between a MIR-548 member and an extensive in length predicted target site on a DNA promoter region, we focused on miR-548c-5p due to the optimal pValues this miRNA gave when evaluating its putative targeting properties by miRWalk2.0. As the MIR-548 family of miRNAs emerged from MADE1-type transposons as previously mentioned, the ability of any given miR-548c-5p target sequence predicted by miRWalk2.0 to be transcribed was examined by evaluating the existence of palindromes at the genomic sequence adjacent to the predicted target sites. A site located upstream the transcription start site of *FOXC2*, deemed non-palindromic, was eventually selected.

Several members of the MIR-548 family share high sequence similarity, with some of them

being identical while others only differing by one or two bases. Moreover, several miRNAs of the MIR-548 family seem to have complementary sequences. This can be easily explained, as for any given miRNA both a 3p and 5p strand emerge from the same RNA hairpin premature molecule and thus partial complementarity exists between the two strands. Regarding miR-548c-5p, the same mature sequence is shared with two other miRNAs, miR-548am-5p and miR-548o-5p. However, it is important to note that all three miRNAs are derived from separate loci, which could be signifying the importance in dosage of this mature miRNA sequence and the possible need to be transcribed in abundance or in response to specific molecular stimuli. On the contrary, miR-548z has a mature sequence complementary to that of miR-548c-5p and it is transcribed from intron 1 of the *RASSF3* gene (Ras-association factor 3), the same transcript that gives rise to miR-548c-5p. *RASSF3* is a possible tumor suppressor that induces apoptosis and cell cycle arrest through p53 (van der Weyden and Adams, 2007). This is suggestive of a common regulatory role for the two miRNAs, probably involving the transcriptional activation of their host gene *RASSF3* and might be implicated in common or competitive roles pertaining to *RASSF3* or the miRNAs themselves.

We sought to demonstrate that the expression of *FOXC2*, the earliest podocyte marker with a prominent role in differentiation, development and maturation of podocytes, is influenced by miR-548c-5p through a target site located >8 kb upstream the gene's transcription start site **(Figure 7A)**. To explore the binding properties of miR-548c-5p onto its predicted DNA target sequence, we encompassed a number of luciferase constructs, bearing the target site along with flanking sequence on an enhancer element upstream a basal promoter placed before the renilla luciferase gene. This particular vector is mainly used in studies examining promoter enhancer elements by bearing a MCS right upstream the basal promoter of the luciferase gene. Constructs demonstrated an enhancer activity for the DNA region bearing the miR-548c-5p target site, as luciferase expression was significantly enhanced when transfecting cells with miRNA inhibitors and lowered with miRNA mimics **(Figure 13B)**. The site appeared to act as a "regular" miRNA binding site, since the regulation by miRNA mimics/inhibitors was gradually lost when introducing serial mutations on the nucleotides corresponding to positions 2 to 5 of the miRNA's seed region **(Figure 13C)**. A similar functional pattern was shown by Meng et al., when small activating RNA molecules were generated and found to target a region located 1.6kb upstream the promoter of the progesterone receptor gene (Meng et al., 2016). Such interactions are suggestive of preservation in miRNA properties that are not restricted to the cytoplasm but also expanding

to the nucleus to finely regulate gene transcription. This is the first study exhibiting transcriptional regulation of a gene by a miRNA through such a distal DNA target site. It is likely that many other miRNAs and especially other members of the MIR-548 family might also have similar properties. As previously mentioned, members of the miR-548 family exhibit high sequence similarity for sequences located at the promoter region of genes. Therefore, their main mode of action could be confined to the nucleus and be of great importance in transcriptional regulation as fine-tuners of gene expression.

FOXC2 and miR-548c-5p expression levels in differentiating hPCs strongly indicate the presence of a dynamic system involving the abundance of the miRNA and *FOXC2* mRNA towards cell differentiation **(Figure 9)**. *FOXC2* mRNA levels respond to miRNA abundancy in both undifferentiated and differentiating hPCs **(Figure 14A, Figure 14C)**. Alternating expression levels of miR-548c-5p and *FOXC2* might be the driving force to generate interactions between the miRNA's target site region and the promoter of the gene. The specific association between the miRNA and *FOXC2* is exemplified by the fact that *MTHFSD*, a gene located upstream the target region, does not seem to have consistent responses to stimuli occurring by the absence or over-representation of miR-548c-5p in the cell. The specificity of the association is further supported by the lack of changes in the expression of the other two genes, FLJ30679 and RP11-46309.5 located in close proximity to the target site, with regards to miR-548c-5p levels in podocytes.

In 3C experiments, the interaction between the miRNA's target site region and the promoter of *FOXC2* appears to be enhanced upon induction of hPC differentiation and subsequently fades out **(Figure 21)**. The effect on DNA conformation dynamics was lost when miR-548c-5p mimics were introduced in hPCs, while inhibitors enhanced this interaction **(Figure 22)**. The possibility that an enhancer element, still undefined, is present at the target site region cannot be excluded. This interaction seems to occur when the expression of miR-548c-5p drops and *FOXC2* mRNA levels are boosted at day 1 and day 2 (**Figure 9**), thus allowing the hypothesis that there is an association between the miRNA/RISC target site occupancy and gene expression data.

In support to this notion, data generated by Ago-ChIP experiments, with primer walking from the target site towards *FOXC2*, demonstrate a significant enrichment of the target site fragment and endogenous nuclear miR-548c-5p in undifferentiated dividing hPCs **(Figure 16)**. In mouse podocytes transfected with miR-548c-5p mimics and the P-WT-m548c-5p luciferase reporter vector, the target site is significantly enriched, whereas enrichment is lost

in the plasmid containing a mutated target site P-Mut-m548c-5p **(Figure 20)**, signifying that the effect observed is directly related to the miRNA. These data further support the notion of a dynamic relationship between the miRNA and its target site in the context of coordinating with podocyte differentiation influenced by *FOXC2* induction. Such interactions between miRNAs and DNA target sites near or far away from transcribed genes, might naturally occur in other cells as well and could be a mechanism with a wider application; a non-differentiating cell system such as the HEK293T line also demonstrated enriched Ago-target site interactions **(Figure 18)**. Hence, it is possible that such target sites are active throughout the genome and they remain to be identified.

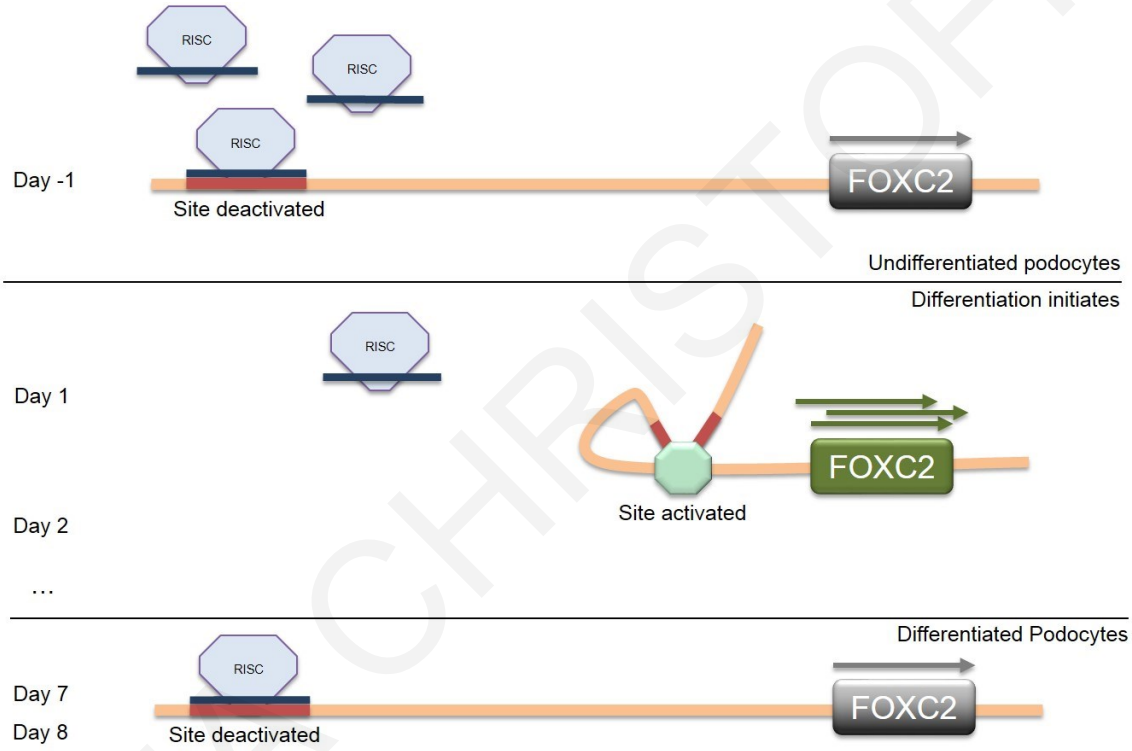

Figure 25: Proposed mechanism. In undifferentiated podocytes at day (-1), miR-548c-5p directs the RISC complex to its specific target site and thus the region becomes occupied, moderating its interaction with the *FOXC2* promoter. Enhancement of gene expression is hindered, but certainly not expected to be silenced completely. When the RISC/miR-548c-5p complex is no longer bound onto the target site, the region is released and interacts with the gene's promoter region, thereby increasing *FOXC2* transcription rate and inducing differentiation. It is possible that the target site is part of a yet unknown distal enhancer element. As differentiation progresses and FOXC2 is inessential for podocyte differentiation, interaction of the enhancer element with the promoter is no longer needed for gene expression enhancement and thus the site becomes deactivated. By day 7 the RISC complex is found to be bound on the target site, but not as abundantly as in proliferating podocytes, which could indicate an attempt to restrain but not diminish FOXC2 levels in the podocyte.

Considering all data presented herein, a mechanism is proposed by which the RISC/miR-548c-5p complex modifies the levels of *FOXC2* with regards to hPC course of differentiation **(Figure 25)**. It is hypothesised that the target site region behaves as part of a distal enhancer element, which during the proliferating stage is occupied by the RISC complex guided by miR-548c-5p and thus DNA-DNA interactions are impeded rendering *FOXC2* expression at basal levels. However, when demands for FOXC2 increase, the RISC-miR-548c-5p complex is no longer bound onto its target site and the pressure is relieved, which allows the interaction between the target site region and the *FOXC2* promoter and subsequently marks induction of differentiation. This is accompanied by a considerable reduction in miR-548c-5p levels as differentiation initiates. The RISC complex in this case acts as a molecular "paper weight" driven by the miRNA and holds interacting DNA regions away from each other. Differentiation initiates when cells are drained of miR-548c-5p and the target region is released.

As differentiation progresses and FOXC2 is no longer essential for podocyte differentiation, interaction of the enhancer element with the promoter is no longer needed for gene expression enhancement and *FOXC2* expression returns to basal levels. By day 7 the miR-548c-5p-RISC complex is found to be bound on the target site, but not as abundantly as in proliferating podocytes as indicated by ChIP data, which could indicate an attempt to restrain FOXC2 levels in the podocyte during later differentiation but not diminish them. Cells undergoing differentiation are trying to keep a balance between miRNA and *FOXC2* expression levels. This force keeps interactions harmonized; when cells reach day 7 the low miR-548c-5p expression can modulate the limited or basal need for *FOXC2* expression, while the cell needs higher amounts of miRNA to keep FOXC2 from being induced while they remain undifferentiated at day (-1). miR-548c-5p keeps with the general notion of miRNA action; it fine-tunes gene expression, instead of silencing or drastically increasing the expression levels of its target gene. A different line of investigations is required to further examine this hypothesis in a direct fashion.

To delve further into the role of the miRNA-*FOXC2* relationship in hPC differentiation, the effect of miRNA abundance in hPCs on the protein levels of FOXC2 and other podocyte relevant proteins was explored. In every occasion when miR-548c-5p, either endogenous or transfected with miRNA mimics, was removed from the system, FOXC2 levels increased. More specifically, in immunofluorescence experiments, differentiating cells recovering from mimics **(Figure 24A)** and cells serially transfected with inhibitors **(Figure 24B)**, resembled cells undergoing differentiation that overexpress FOXC2. Moreover, in Western blot

experiments WT1 expression was delayed in cells recovering from miRNA transfections, as well as the expression of the podocyte specific marker nephrin, while the expression of the FOXC2-induced podocyte marker podocin was induced in response to the high FOXC2 levels **(Figure 23)**. In addition, p57 expression is significantly increased at 30 h post-transfection indicating cell cycle arrest and thus the end of proliferation and beginning of differentiation, thus signifying a delay in differentiation induction compared to the control samples **(Figure 23)**.

It was deemed important to investigate the prolonged effect of miR-548c-5p on podocytes and how this might affect the differentiation process. This was done by maintaining miR-548c-5p levels through sequential mimic transfections, while the cells were given the stimulus for differentiation induction and observing changes in FOXC2 and other podocyte marker expression. Results suggest that the presence of miR-548c-5p in hPCs affects FOXC2 levels, which in turn may influence their differentiation course. These results exemplify the already established role for FOXC2 as the starting point of podocyte differentiation and introduce miR-548c-5p as an extra monitoring factor of a well-orchestrated process leading to podocyte differentiation. It should be noted that differentiation in immortalised hPCs is only a simulation of the natural reality; the effect observed might be more prominent due to the ongoing proliferation, but the results obtained suggest that it is not random. As this cell line emerged from primary podocytes, cells seem to preserve their identity even when undifferentiated, as they express cell-type specific proteins and present with podocyte-specific characteristics even at an immature state, evident by synaptopodin and nephrin expression data **(Figure 23)**.

Over the past few years several publications have indicated that miRNAs are key components of transcriptional regulation. However, the mechanism by which this regulation is conferred has not yet been deciphered. A possible way has been suggested to be DNA-miRNA interactions. This work provides a proof-of-principle for interactions of miRNAs with DNA regions, as it was sought to delineate their fine-tuning properties in a well-studied biological setting, podocyte differentiation. The use of luciferase constructs established that the miR-548c-5p DNA target site has enhancer activity with seed-region specificity. Thus, there is support of the notion that miRNAs can exert transcriptional enhancement/repression of genes through interaction of the miRNA with its DNA target sequence, by using the example of miR-548c-5p and its predicted target site at 8 kb upstream the *FOXC2* transcription start point. Moreover, this is the first study exhibiting transcriptional regulation of a gene by a miRNA through a DNA target site located as remotely from the gene, giving

the target site region the role of a distant enhancer/repressor element. Therefore, many other miRNAs and especially other members of the MIR-548-family might also have similar properties regarding gene regulation. Based on this premise, the binding properties for predicted extensive target sites located in promoter regions of other MIR-548 family members could be examined in relation to their possible regulatory properties and especially those with very close sequence similarity to miR-548c-5p. It is important to keep in mind that such regulatory elements co-existing with miRNA target sites will not necessarily be located in close proximity to transcriptional start sites. In fact, such sites could be found at distal sites, such as the miR-548c-5p target site investigated in this case. Therefore, a more extensive search for additional miRNA target sites that might influence transcription through regulatory elements/distal target sites should be performed.

Evidently, both the miRNA and its target site are absent from non-primates and miR-548c-5p has no effect on *mFoxc2* expression **(Figure 7B, Figure 7C, Figure 14B)**, rendering the miR-548c-5p/*FOXC2* interaction primate-specific. This implies that miR-548c-5p and presumably other miRNAs are important for tuning cellular processes including differentiation, but are not essential for differentiation to occur, also supported by experiments in dicer knockout mice (Ho et al., 2008). Hence, the evolutionary emergence of similar regulatory elements in primates could be attributed to the increased complexity of mammalian cellular systems and in this case, pinpoints the need for a more defined and controlled gene expression in such a highly differentiated cell type. What also remains to establish is the role of such miRNAs and their respective target regions in podocyte and other cell-type dysfunction and disease.

FOXC2 codes for a transcription factor that belongs to the Forkhead family. As previously stated, *FOXC2* expression is vital for cell fate determination in multiple tissues and organs. More specifically, it has been associated with developmental and tumour angiogenesis through the transcriptional mediation of proteins required for endothelial cell migration, such as CXCR4 and integrin β3 (Kume, 2008, Kume, 2012). In addition, mutations in *FOXC2* cause the autosomal dominant lymphedema distichiasis syndrome (Fang et al., 2000). In the kidney, overexpression of *FOXC2*, following ischemia/reperfusion-initiated differentiation of renal tubular cells, promotes injury recovery and re-differentiation from a transitional mesenchymal type to epithelial cells (Hader et al., 2010). FOXC2 also has a proven role in podocyte differentiation and GBM maturation (Rascle et al., 2007). In *FOXC2* knock-out mice expression of *NPHS2* is reduced and kidneys appear hypoplastic with less glomeruli and dilated capillaries (Takemoto et al., 2006). In *Xenopus* the functional association

between *FOXC2*, *WT1* and Notch signalling, is essential for podocyte development (White et al., 2010).

Taking everything into consideration, it can be concluded that the precise regulation of *FOXC2* expression is vital for cellular functions in human podocytes. Therefore, the influence of miR-548c-5p in regulating *FOXC2* transcription could provide new insights not only into its functional properties, but also into the mechanisms underlying glomerular or other disease development. A possible example of this could be the investigation of an expressional association between *FOXC2* and *RASSF3*, which could subsequently be explored in relation to cancer pathogenesis. FOXC2 has already been associated with poor progression in different types of cancer. The first association between FOXC2 and cancer was identified more than 10 years ago. More specifically, overexpression of FOXC2 was associated with aggressive basal-like breast cancer and the ability of the breast cancer cells to metastasise (Mani et al., 2007). In addition to breast cancer, high levels of FOXC2 have been found to promote metastasis in melanomas as well as colon and prostate cancers and are reversely associated with patient survival and response to therapy (Li et al., 2015, Cui et al., 2015, Borretzen et al., 2019, Hargadon et al., 2019). Interestingly, miR-548c-5p levels have been found to be significantly decreased in tissue from colorectal cancer (CRC) patients compared to samples from healthy controls (Ge et al., 2019). Moreover, serum exosomal miR-548c-5p was shown to hinder colorectal cancer cell metastasis, whereas reduced miR-548c-5p levels in these samples were associated with advanced disease stage and shorter survival rates (Peng et al., 2019). Regarding other types of cancer miR-548c-5p elevated expression was an indicator of good prognosis in patients with Triple Negative Breast Cancer (TNBC) (Boukerroucha et al., 2015). From the studies existing so far regarding FOXC2 and miR-548c-5p in cancer it is evident that increased FOXC2 levels promote cancer progression and metastasis, whereas increased miR-548c-5p levels are associated with a more favourable outcome and appear to be somewhat protective. Therefore, FOXC2 could be a good candidate for targeted therapy and the effect of miR-548c-5p on its expression should be investigated in different types of cancer.

Chapter 6: Conclusions

miRNA prediction analysis revealed a full-length target site for the primate-specific miR-548c-5p at a genomic region >8kb upstream of *FOXC2*. It was hypothesised that the transcription rates of *FOXC2* during podocyte differentiation might be tuned by miR-548c-5p through this target site. Experiments performed have validated that the target site is recognised by miR-548c-5p with seed region specificity and the abundancy of the miRNA influences both FOXC2 mRNA and protein levels during podocyte differentiation. Ago-ChIP and 3C experiments have proved target site occupancy by RISC, which is released to allow the target site to interact with the promoter region of *FOXC2* and ensuing differentiation induction. Taking everything into account, this study depicts the presence of a mechanism by which miR-548c-5p regulates *FOXC2* expression and subsequently influences the process of podocyte differentiation.

Moving forward, the exact way by which miR-548c-5p interacts with the target site could be explored in future experiments, and more specifically whether the miRNA forms a double stranded molecule with the DNA target site. In addition, the composition of the factors bound onto the regulatory element in which the target site belongs could be explored and how this exactly functions in order to promote *FOXC2* transcription.

Overall, this study enhances the role of microRNAs as regulators of transcription as it provides the first evidence of transcriptional regulation of a gene by a microRNA, through a target site located so far away from the gene's transcription start point. Moreover, the complex regulation of *FOXC2* expression by miR-548c-5p adds another layer into the intricate process by which podocyte cells differentiate. As both miR-548c-5p and this specific target site are absent from non-primates the existence of this added level of complexity demonstrates the importance of a delicately balanced and detailed regulation of podocyte differentiation, adding an evolutionary dimension to the modulation of this process.

Chapter 7: References

ABRAHAMSON, D. R., HUDSON, B. G., STROGANOVA, L., BORZA, D. B. & ST JOHN, P. L. 2009. Cellular origins of type IV collagen networks in developing glomeruli. *J Am Soc Nephrol,* 20**,** 1471-9.

ALLO, M., AGIRRE, E., BESSONOV, S., BERTUCCI, P., GOMEZ ACUNA, L., BUGGIANO, V., BELLORA, N., SINGH, B., PETRILLO, E., BLAUSTEIN, M., MINANA, B., DUJARDIN, G., POZZI, B., PELISCH, F., BECHARA, E., AGAFONOV, D. E., SREBROW, A., LUHRMANN, R., VALCARCEL, J., EYRAS, E. & KORNBLIHTT, A. R. 2014. Argonaute-1 binds transcriptional enhancers and controls constitutive and alternative splicing in human cells. *Proc Natl Acad Sci U S A,* 111**,** 15622-9.

AMBROS, V., LEE, R. C., LAVANWAY, A., WILLIAMS, P. T. & JEWELL, D. 2003. MicroRNAs and other tiny endogenous RNAs in C. elegans. *Curr Biol,* 13**,** 807-18.

ARAVIN, A. A., HANNON, G. J. & BRENNECKE, J. 2007. The Piwi-piRNA pathway provides an adaptive defense in the transposon arms race. *Science,* 318**,** 761-4.

ASANUMA, K., KIM, K., OH, J., GIARDINO, L., CHABANIS, S., FAUL, C., REISER, J. & MUNDEL, P. 2005. Synaptopodin regulates the actin-bundling activity of alpha-actinin in an isoform-specific manner. *J Clin Invest,* 115**,** 1188-98.

ATWOOD, B. L., WOOLNOUGH, J. L., LEFEVRE, G. M., SAINT JUST RIBEIRO, M., FELSENFELD, G. & GILES, K. E. 2016. Human Argonaute 2 Is Tethered to Ribosomal RNA through MicroRNA Interactions. *J Biol Chem,* 291**,** 17919-28.

BAI, B., LIU, H. & LAIHO, M. 2014. Small RNA expression and deep sequencing analyses of the nucleolus reveal the presence of nucleolus-associated microRNAs. *FEBS Open Bio,* 4**,** 441-9.

BARTEL, D. P. 2004. MicroRNAs: genomics, biogenesis, mechanism, and function. *Cell,* 116**,** 281-97.

BEREZIKOV, E., CHUNG, W. J., WILLIS, J., CUPPEN, E. & LAI, E. C. 2007. Mammalian mirtron genes. *Mol Cell,* 28**,** 328-36.

BERNSTEIN, E., CAUDY, A. A., HAMMOND, S. M. & HANNON, G. J. 2001. Role for a bidentate ribonuclease in the initiation step of RNA interference. *Nature,* 409**,** 363-6.

BOHNSACK, M. T., CZAPLINSKI, K. & GORLICH, D. 2004. Exportin 5 is a RanGTP-dependent dsRNA-binding protein that mediates nuclear export of pre-miRNAs. *RNA,* 10**,** 185-91.

BORRETZEN, A., GRAVDAL, K., HAUKAAS, S. A., BEISLAND, C., AKSLEN, L. A. & HALVORSEN, O. J. 2019. FOXC2 expression and epithelial-mesenchymal phenotypes are associated with castration resistance, metastasis and survival in prostate cancer. *J Pathol Clin Res,* 5**,** 272-286.

BOUDREAU, R. L., JIANG, P., GILMORE, B. L., SPENGLER, R. M., TIRABASSI, R., NELSON, J. A., ROSS, C. A., XING, Y. & DAVIDSON, B. L. 2014. Transcriptome-wide discovery of microRNA binding sites in human brain. *Neuron,* 81**,** 294-305.

BOUKERROUCHA, M., JOSSE, C., ELGUENDI, S., BOUJEMLA, B., FRERES, P., MAREE, R., WENRIC, S., SEGERS, K., COLLIGNON, J., JERUSALEM, G. & BOURS, V. 2015. Evaluation of BRCA1-related molecular features and microRNAs as prognostic factors for triple negative breast cancers. *BMC Cancer,* 15**,** 755.

BOUTE, N., GRIBOUVAL, O., ROSELLI, S., BENESSY, F., LEE, H., FUCHSHUBER, A., DAHAN, K., GUBLER, M. C., NIAUDET, P. & ANTIGNAC, C. 2000. NPHS2, encoding the glomerular protein podocin, is mutated in autosomal recessive steroid-resistant nephrotic syndrome. *Nat Genet,* 24**,** 349-54.

BRENNECKE, J., STARK, A., RUSSELL, R. B. & COHEN, S. M. 2005. Principles of microRNA-target recognition. *PLoS Biol,* 3**,** e85.
CAI, X., HAGEDORN, C. H. & CULLEN, B. R. 2004. Human microRNAs are processed from capped, polyadenylated transcripts that can also function as mRNAs. *RNA,* 10**,** 1957-66.
CATALANOTTO, C., COGONI, C. & ZARDO, G. 2016. MicroRNA in Control of Gene Expression: An Overview of Nuclear Functions. *Int J Mol Sci,* 17.
CHELOUFI, S., DOS SANTOS, C. O., CHONG, M. M. & HANNON, G. J. 2010. A dicer-independent miRNA biogenesis pathway that requires Ago catalysis. *Nature,* 465**,** 584-9.
CHEN, K., SONG, F., CALIN, G. A., WEI, Q., HAO, X. & ZHANG, W. 2008. Polymorphisms in microRNA targets: a gold mine for molecular epidemiology. *Carcinogenesis,* 29**,** 1306-11.
CHENG, H. & HARRIS, R. C. 2010. The glomerulus--a view from the outside--the podocyte. *Int J Biochem Cell Biol,* 42**,** 1380-7.
CHI, S. W., HANNON, G. J. & DARNELL, R. B. 2012. An alternative mode of microRNA target recognition. *Nat Struct Mol Biol,* 19**,** 321-7.
CHIYOMARU, T., FUKUHARA, S., SAINI, S., MAJID, S., DENG, G., SHAHRYARI, V., CHANG, I., TANAKA, Y., ENOKIDA, H., NAKAGAWA, M., DAHIYA, R. & YAMAMURA, S. 2014. Long non-coding RNA HOTAIR is targeted and regulated by miR-141 in human cancer cells. *J Biol Chem,* 289**,** 12550-65.
COREY, D. R. 2005. Regulating mammalian transcription with RNA. *Trends Biochem Sci,* 30**,** 655-8.
CUI, Y. M., JIAO, H. L., YE, Y. P., CHEN, C. M., WANG, J. X., TANG, N., LI, T. T., LIN, J., QI, L., WU, P., WANG, S. Y., HE, M. R., LIANG, L., BIAN, X. W., LIAO, W. T. & DING, Y. Q. 2015. FOXC2 promotes colorectal cancer metastasis by directly targeting MET. *Oncogene,* 34**,** 4379-90.
DATTA, N., LINDFORS, S., MIURA, N., SALEEM, M. A. & LEHTONEN, S. 2015. Overexpression of transcription factor FOXC2 in cultured human podocytes upregulates injury markers and increases motility. *Exp Cell Res,* 340**,** 32-42.
DENLI, A. M., TOPS, B. B., PLASTERK, R. H., KETTING, R. F. & HANNON, G. J. 2004. Processing of primary microRNAs by the Microprocessor complex. *Nature,* 432**,** 231-5.
DJINOVIC-CARUGO, K., YOUNG, P., GAUTEL, M. & SARASTE, M. 1999. Structure of the alpha-actinin rod: molecular basis for cross-linking of actin filaments. *Cell,* 98**,** 537-46.
DRINNENBERG, I. A., WEINBERG, D. E., XIE, K. T., MOWER, J. P., WOLFE, K. H., FINK, G. R. & BARTEL, D. P. 2009. RNAi in budding yeast. *Science,* 326**,** 544-50.
DWEEP, H. & GRETZ, N. 2015. miRWalk2.0: a comprehensive atlas of microRNA-target interactions. *Nat Methods,* 12**,** 697.
DWEEP, H., STICHT, C., PANDEY, P. & GRETZ, N. 2011. miRWalk--database: prediction of possible miRNA binding sites by "walking" the genes of three genomes. *J Biomed Inform,* 44**,** 839-47.
ELBASHIR, S. M., LENDECKEL, W. & TUSCHL, T. 2001. RNA interference is mediated by 21- and 22-nucleotide RNAs. *Genes Dev,* 15**,** 188-200.
ENGELS, B. M. & HUTVAGNER, G. 2006. Principles and effects of microRNA-mediated post-transcriptional gene regulation. *Oncogene,* 25**,** 6163-9.
FANG, J., DAGENAIS, S. L., ERICKSON, R. P., ARLT, M. F., GLYNN, M. W., GORSKI, J. L., SEAVER, L. H. & GLOVER, T. W. 2000. Mutations in FOXC2 (MFH-1), a forkhead family transcription factor, are responsible for the hereditary lymphedema-distichiasis syndrome. *Am J Hum Genet,* 67**,** 1382-8.
FARAZI, T. A., JURANEK, S. A. & TUSCHL, T. 2008. The growing catalog of small

RNAs and their association with distinct Argonaute/Piwi family members. *Development,* 135**,** 1201-14.
FILIPOWICZ, W., BHATTACHARYYA, S. N. & SONENBERG, N. 2008. Mechanisms of post-transcriptional regulation by microRNAs: are the answers in sight? *Nat Rev Genet,* 9**,** 102-14.
FORMAN, J. J. & COLLER, H. A. 2010. The code within the code: microRNAs target coding regions. *Cell Cycle,* 9**,** 1533-41.
GAGNON, K. T., LI, L., CHU, Y., JANOWSKI, B. A. & COREY, D. R. 2014. RNAi factors are present and active in human cell nuclei. *Cell Rep,* 6**,** 211-21.
GAROVIC, V. D., WAGNER, S. J., PETROVIC, L. M., GRAY, C. E., HALL, P., SUGIMOTO, H., KALLURI, R. & GRANDE, J. P. 2007. Glomerular expression of nephrin and synaptopodin, but not podocin, is decreased in kidney sections from women with preeclampsia. *Nephrol Dial Transplant,* 22**,** 1136-43.
GE, J., LI, J., NA, S., WANG, P., ZHAO, G. & ZHANG, X. 2019. miR-548c-5p inhibits colorectal cancer cell proliferation by targeting PGK1. *J Cell Physiol,* 234**,** 18872-18878.
GODEL, M., OSTENDORF, B. N., BAUMER, J., WEBER, K. & HUBER, T. B. 2013. A novel domain regulating degradation of the glomerular slit diaphragm protein podocin in cell culture systems. *PLoS One,* 8**,** e57078.
GRAHAMMER, F., SCHELL, C. & HUBER, T. B. 2013. The podocyte slit diaphragm--from a thin grey line to a complex signalling hub. *Nat Rev Nephrol,* 9**,** 587-98.
GREGORY, R. I., YAN, K. P., AMUTHAN, G., CHENDRIMADA, T., DORATOTAJ, B., COOCH, N. & SHIEKHATTAR, R. 2004. The Microprocessor complex mediates the genesis of microRNAs. *Nature,* 432**,** 235-40.
GREKA, A. & MUNDEL, P. 2012. Cell biology and pathology of podocytes. *Annu Rev Physiol,* 74**,** 299-323.
GRIMSON, A., FARH, K. K., JOHNSTON, W. K., GARRETT-ENGELE, P., LIM, L. P. & BARTEL, D. P. 2007. MicroRNA targeting specificity in mammals: determinants beyond seed pairing. *Mol Cell,* 27**,** 91-105.
HADER, C., MARLIER, A. & CANTLEY, L. 2010. Mesenchymal-epithelial transition in epithelial response to injury: the role of Foxc2. *Oncogene,* 29**,** 1031-40.
HAMILTON, A., VOINNET, O., CHAPPELL, L. & BAULCOMBE, D. 2002. Two classes of short interfering RNA in RNA silencing. *EMBO J,* 21**,** 4671-9.
HAN, J., LEE, Y., YEOM, K. H., KIM, Y. K., JIN, H. & KIM, V. N. 2004. The Drosha-DGCR8 complex in primary microRNA processing. *Genes Dev,* 18**,** 3016-27.
HANSEN, T. B., VENO, M. T., JENSEN, T. I., SCHAEFER, A., DAMGAARD, C. K. & KJEMS, J. 2016. Argonaute-associated short introns are a novel class of gene regulators. *Nat Commun,* 7**,** 11538.
HARGADON, K. M., GYORFFY, B., STRONG, E. W., TARNAI, B. D., THOMPSON, J. C., BUSHHOUSE, D. Z., JOHNSON, C. E. & WILLIAMS, C. J. 2019. The FOXC2 Transcription Factor Promotes Melanoma Outgrowth and Regulates Expression of Genes Associated With Drug Resistance and Interferon Responsiveness. *Cancer Genomics Proteomics,* 16**,** 491-503.
HARVEY, S. J., JARAD, G., CUNNINGHAM, J., GOLDBERG, S., SCHERMER, B., HARFE, B. D., MCMANUS, M. T., BENZING, T. & MINER, J. H. 2008. Podocyte-specific deletion of dicer alters cytoskeletal dynamics and causes glomerular disease. *J Am Soc Nephrol,* 19**,** 2150-8.
HO, J., NG, K. H., ROSEN, S., DOSTAL, A., GREGORY, R. I. & KREIDBERG, J. A. 2008. Podocyte-specific loss of functional microRNAs leads to rapid glomerular and tubular injury. *J Am Soc Nephrol,* 19**,** 2069-75.
HOLTHOFER, H. 2007. Molecular architecture of the glomerular slit diaphragm: lessons learnt for a better understanding of disease pathogenesis. *Nephrol Dial Transplant,*

22**,** 2124-8.
HU, H. Y., YAN, Z., XU, Y., HU, H., MENZEL, C., ZHOU, Y. H., CHEN, W. & KHAITOVICH, P. 2009. Sequence features associated with microRNA strand selection in humans and flies. *BMC Genomics,* 10**,** 413.
HUANG, V., ZHENG, J., QI, Z., WANG, J., PLACE, R. F., YU, J., LI, H. & LI, L. C. 2013. Ago1 Interacts with RNA polymerase II and binds to the promoters of actively transcribed genes in human cancer cells. *PLoS Genet,* 9**,** e1003821.
HUTVAGNER, G., MCLACHLAN, J., PASQUINELLI, A. E., BALINT, E., TUSCHL, T. & ZAMORE, P. D. 2001. A cellular function for the RNA-interference enzyme Dicer in the maturation of the let-7 small temporal RNA. *Science,* 293**,** 834-8.
HWANG, H. W., WENTZEL, E. A. & MENDELL, J. T. 2007. A hexanucleotide element directs microRNA nuclear import. *Science,* 315**,** 97-100.
JEFFERSON, J. A., ALPERS, C. E. & SHANKLAND, S. J. 2011. Podocyte biology for the bedside. *Am J Kidney Dis,* 58**,** 835-45.
KESTILA, M., LENKKERI, U., MANNIKKO, M., LAMERDIN, J., MCCREADY, P., PUTAALA, H., RUOTSALAINEN, V., MORITA, T., NISSINEN, M., HERVA, R., KASHTAN, C. E., PELTONEN, L., HOLMBERG, C., OLSEN, A. & TRYGGVASON, K. 1998. Positionally cloned gene for a novel glomerular protein--nephrin--is mutated in congenital nephrotic syndrome. *Mol Cell,* 1**,** 575-82.
KETTING, R. F., FISCHER, S. E., BERNSTEIN, E., SIJEN, T., HANNON, G. J. & PLASTERK, R. H. 2001. Dicer functions in RNA interference and in synthesis of small RNA involved in developmental timing in C. elegans. *Genes Dev,* 15**,** 2654-9.
KHVOROVA, A., REYNOLDS, A. & JAYASENA, S. D. 2003. Functional siRNAs and miRNAs exhibit strand bias. *Cell,* 115**,** 209-16.
KIETZMANN, L., GUHR, S. S., MEYER, T. N., NI, L., SACHS, M., PANZER, U., STAHL, R. A., SALEEM, M. A., KERJASCHKI, D., GEBESHUBER, C. A. & MEYER-SCHWESINGER, C. 2015. MicroRNA-193a Regulates the Transdifferentiation of Human Parietal Epithelial Cells toward a Podocyte Phenotype. *J Am Soc Nephrol,* 26**,** 1389-401.
KIM, D. H., SAETROM, P., SNOVE, O., JR. & ROSSI, J. J. 2008. MicroRNA-directed transcriptional gene silencing in mammalian cells. *Proc Natl Acad Sci U S A,* 105**,** 16230-5.
KIM, D. H., VILLENEUVE, L. M., MORRIS, K. V. & ROSSI, J. J. 2006. Argonaute-1 directs siRNA-mediated transcriptional gene silencing in human cells. *Nat Struct Mol Biol,* 13**,** 793-7.
KIRIAKIDOU, M., NELSON, P. T., KOURANOV, A., FITZIEV, P., BOUYIOUKOS, C., MOURELATOS, Z. & HATZIGEORGIOU, A. 2004. A combined computational-experimental approach predicts human microRNA targets. *Genes Dev,* 18**,** 1165-78.
KOUSKOUTI, A. & KYRMIZI, I. 2005. *Chromatin Immunoprecipitation (ChIP) Assay (PROT11)* [Online]. The EPIGENOME Network of Excellence. Available: http://www.epigenome-noe.net/researchtools/protocol.php_protid=10.html [Accessed].
KOUTROUTSOS, K., KASSIMATIS, T. I., NOMIKOS, A., GIANNOPOULOU, I., THEOHARI, I. & NAKOPOULOU, L. 2014. Effect of Smad pathway activation on podocyte cell cycle regulation: an immunohistochemical evaluation. *Ren Fail,* 36**,** 1310-6.
KOZOMARA, A. & GRIFFITHS-JONES, S. 2013. miRBase: annotating high confidence microRNAs using deep sequencing data. *Nucleic Acids Res,* 42**,** D68-73.
KREIDBERG, J. A., SARIOLA, H., LORING, J. M., MAEDA, M., PELLETIER, J., HOUSMAN, D. & JAENISCH, R. 1993. WT-1 is required for early kidney development. *Cell,* 74**,** 679-91.
KUME, T. 2008. Foxc2 transcription factor: a newly described regulator of angiogenesis.

Trends Cardiovasc Med, 18**,** 224-8.
KUME, T. 2012. The Role of FoxC2 Transcription Factor in Tumor Angiogenesis. *J Oncol,* 2012**,** 204593.
LAGOS-QUINTANA, M., RAUHUT, R., LENDECKEL, W. & TUSCHL, T. 2001. Identification of novel genes coding for small expressed RNAs. *Science,* 294**,** 853-8.
LAL, A., NAVARRO, F., MAHER, C. A., MALISZEWSKI, L. E., YAN, N., O'DAY, E., CHOWDHURY, D., DYKXHOORN, D. M., TSAI, P., HOFMANN, O., BECKER, K. G., GOROSPE, M., HIDE, W. & LIEBERMAN, J. 2009. miR-24 Inhibits cell proliferation by targeting E2F2, MYC, and other cell-cycle genes via binding to "seedless" 3'UTR microRNA recognition elements. *Mol Cell,* 35**,** 610-25.
LANDGRAF, P., RUSU, M., SHERIDAN, R., SEWER, A., IOVINO, N., ARAVIN, A., PFEFFER, S., RICE, A., KAMPHORST, A. O., LANDTHALER, M., LIN, C., SOCCI, N. D., HERMIDA, L., FULCI, V., CHIARETTI, S., FOA, R., SCHLIWKA, J., FUCHS, U., NOVOSEL, A., MULLER, R. U., SCHERMER, B., BISSELS, U., INMAN, J., PHAN, Q., CHIEN, M., WEIR, D. B., CHOKSI, R., DE VITA, G., FREZZETTI, D., TROMPETER, H. I., HORNUNG, V., TENG, G., HARTMANN, G., PALKOVITS, M., DI LAURO, R., WERNET, P., MACINO, G., ROGLER, C. E., NAGLE, J. W., JU, J., PAPAVASILIOU, F. N., BENZING, T., LICHTER, P., TAM, W., BROWNSTEIN, M. J., BOSIO, A., BORKHARDT, A., RUSSO, J. J., SANDER, C., ZAVOLAN, M. & TUSCHL, T. 2007. A mammalian microRNA expression atlas based on small RNA library sequencing. *Cell,* 129**,** 1401-14.
LEE, I., AJAY, S. S., YOOK, J. I., KIM, H. S., HONG, S. H., KIM, N. H., DHANASEKARAN, S. M., CHINNAIYAN, A. M. & ATHEY, B. D. 2009. New class of microRNA targets containing simultaneous 5'-UTR and 3'-UTR interaction sites. *Genome Res,* 19**,** 1175-83.
LEE, R. C. & AMBROS, V. 2001. An extensive class of small RNAs in Caenorhabditis elegans. *Science,* 294**,** 862-4.
LEE, Y., AHN, C., HAN, J., CHOI, H., KIM, J., YIM, J., LEE, J., PROVOST, P., RADMARK, O., KIM, S. & KIM, V. N. 2003. The nuclear RNase III Drosha initiates microRNA processing. *Nature,* 425**,** 415-9.
LEE, Y., JEON, K., LEE, J. T., KIM, S. & KIM, V. N. 2002. MicroRNA maturation: stepwise processing and subcellular localization. *EMBO J,* 21**,** 4663-70.
LEE, Y., KIM, M., HAN, J., YEOM, K. H., LEE, S., BAEK, S. H. & KIM, V. N. 2004. MicroRNA genes are transcribed by RNA polymerase II. *EMBO J,* 23**,** 4051-60.
LEEUWIS, J. W., NGUYEN, T. Q., DENDOOVEN, A., KOK, R. J. & GOLDSCHMEDING, R. 2010. Targeting podocyte-associated diseases. *Adv Drug Deliv Rev,* 62**,** 1325-36.
LEWIS, B. P., SHIH, I. H., JONES-RHOADES, M. W., BARTEL, D. P. & BURGE, C. B. 2003. Prediction of mammalian microRNA targets. *Cell,* 115**,** 787-98.
LI, M., ARMELLONI, S., EDEFONTI, A., MESSA, P. & RASTALDI, M. P. 2013. Fifteen years of research on nephrin: what we still need to know. *Nephrol Dial Transplant,* 28**,** 767-70.
LI, Q., WU, J., WEI, P., XU, Y., ZHUO, C., WANG, Y., LI, D. & CAI, S. 2015. Overexpression of forkhead Box C2 promotes tumor metastasis and indicates poor prognosis in colon cancer via regulating epithelial-mesenchymal transition. *Am J Cancer Res,* 5**,** 2022-34.
LIAO, J. Y., MA, L. M., GUO, Y. H., ZHANG, Y. C., ZHOU, H., SHAO, P., CHEN, Y. Q. & QU, L. H. 2010. Deep sequencing of human nuclear and cytoplasmic small RNAs reveals an unexpectedly complex subcellular distribution of miRNAs and tRNA 3' trailers. *PLoS One,* 5**,** e10563.
LIU, J., CARMELL, M. A., RIVAS, F. V., MARSDEN, C. G., THOMSON, J. M., SONG, J. J., HAMMOND, S. M., JOSHUA-TOR, L. & HANNON, G. J. 2004. Argonaute2

is the catalytic engine of mammalian RNAi. *Science,* 305**,** 1437-41.
LIU, J., HU, J., HICKS, J. A., PRAKASH, T. P. & COREY, D. R. 2015. Modulation of Splicing by Single-Stranded Silencing RNAs. *Nucleic Acid Ther,* 25**,** 113-20.
LIU, L., LIN, W., ZHANG, Q., CAO, W. & LIU, Z. 2016. TGF-beta induces miR-30d down-regulation and podocyte injury through Smad2/3 and HDAC3-associated transcriptional repression. *J Mol Med (Berl),* 94**,** 291-300.
LIU, X., FORTIN, K. & MOURELATOS, Z. 2008. MicroRNAs: biogenesis and molecular functions. *Brain Pathol,* 18**,** 113-21.
LUND, E., GUTTINGER, S., CALADO, A., DAHLBERG, J. E. & KUTAY, U. 2004. Nuclear export of microRNA precursors. *Science,* 303**,** 95-8.
M¼LLER-DEILE, J., DANNENBERG, J., LIU, P., THUM, T., LORENZEN, J., NYSTRÖM, J. & SCHIFFER, M. 2017. Identification of Cell-and Disease-Specific Micro RNAs in Glomerular Pathologies. *J Mol Genet Med* [Online], 11.
MAESTRONI, S. & ZERBINI, G. 2018. Glomerular endothelial cells versus podocytes as the cellular target in diabetic nephropathy. *Acta Diabetol,* 55**,** 1105-1111.
MANI, S. A., YANG, J., BROOKS, M., SCHWANINGER, G., ZHOU, A., MIURA, N., KUTOK, J. L., HARTWELL, K., RICHARDSON, A. L. & WEINBERG, R. A. 2007. Mesenchyme Forkhead 1 (FOXC2) plays a key role in metastasis and is associated with aggressive basal-like breast cancers. *Proc Natl Acad Sci U S A,* 104**,** 10069-74.
MATSUI, M., CHU, Y., ZHANG, H., GAGNON, K. T., SHAIKH, S., KUCHIMANCHI, S., MANOHARAN, M., COREY, D. R. & JANOWSKI, B. A. 2013. Promoter RNA links transcriptional regulation of inflammatory pathway genes. *Nucleic Acids Res,* 41**,** 10086-109.
MATZKE, M., AUFSATZ, W., KANNO, T., DAXINGER, L., PAPP, I., METTE, M. F. & MATZKE, A. J. 2004. Genetic analysis of RNA-mediated transcriptional gene silencing. *Biochim Biophys Acta,* 1677**,** 129-41.
MENG, X., JIANG, Q., CHANG, N., WANG, X., LIU, C., XIONG, J., CAO, H. & LIANG, Z. 2016. Small activating RNA binds to the genomic target site in a seed-region-dependent manner. *Nucleic Acids Res,* 44**,** 2274-82.
MINER, J. H. 2012. The glomerular basement membrane. *Exp Cell Res,* 318**,** 973-8.
MODARRESI, F., FAGHIHI, M. A., LOPEZ-TOLEDANO, M. A., FATEMI, R. P., MAGISTRI, M., BROTHERS, S. P., VAN DER BRUG, M. P. & WAHLESTEDT, C. 2012. Inhibition of natural antisense transcripts in vivo results in gene-specific transcriptional upregulation. *Nat Biotechnol,* 30**,** 453-9.
MORRIS, K. V. 2005. siRNA-mediated transcriptional gene silencing: the potential mechanism and a possible role in the histone code. *Cell Mol Life Sci,* 62**,** 3057-66.
MORRIS, K. V., SANTOSO, S., TURNER, A. M., PASTORI, C. & HAWKINS, P. G. 2008. Bidirectional transcription directs both transcriptional gene activation and suppression in human cells. *PLoS Genet,* 4**,** e1000258.
MOTOJIMA, M., KUME, T. & MATSUSAKA, T. 2017. Foxc1 and Foxc2 are necessary to maintain glomerular podocytes. *Exp Cell Res,* 352**,** 265-272.
MOURELATOS, Z., DOSTIE, J., PAUSHKIN, S., SHARMA, A., CHARROUX, B., ABEL, L., RAPPSILBER, J., MANN, M. & DREYFUSS, G. 2002. miRNPs: a novel class of ribonucleoproteins containing numerous microRNAs. *Genes Dev,* 16**,** 720-8.
MUNDEL, P., REISER, J., ZUNIGA MEJIA BORJA, A., PAVENSTADT, H., DAVIDSON, G. R., KRIZ, W. & ZELLER, R. 1997. Rearrangements of the cytoskeleton and cell contacts induce process formation during differentiation of conditionally immortalized mouse podocyte cell lines. *Exp Cell Res,* 236**,** 248-58.
NAUMOVA, N., SMITH, E. M., ZHAN, Y. & DEKKER, J. 2012. Analysis of long-range chromatin interactions using Chromosome Conformation Capture. *Methods,* 58**,** 192-

203.
NISHI, K., NISHI, A., NAGASAWA, T. & UI-TEI, K. 2013. Human TNRC6A is an Argonaute-navigator protein for microRNA-mediated gene silencing in the nucleus. *RNA,* 19**,** 17-35.
NISHIBORI, Y., LIU, L., HOSOYAMADA, M., ENDOU, H., KUDO, A., TAKENAKA, H., HIGASHIHARA, E., BESSHO, F., TAKAHASHI, S., KERSHAW, D., RUOTSALAINEN, V., TRYGGVASON, K., KHOSHNOODI, J. & YAN, K. 2004. Disease-causing missense mutations in NPHS2 gene alter normal nephrin trafficking to the plasma membrane. *Kidney Int,* 66**,** 1755-65.
OBBARD, D. J., GORDON, K. H., BUCK, A. H. & JIGGINS, F. M. 2009. The evolution of RNAi as a defence against viruses and transposable elements. *Philos Trans R Soc Lond B Biol Sci,* 364**,** 99-115.
OHRT, T., MUTZE, J., STAROSKE, W., WEINMANN, L., HOCK, J., CRELL, K., MEISTER, G. & SCHWILLE, P. 2008. Fluorescence correlation spectroscopy and fluorescence cross-correlation spectroscopy reveal the cytoplasmic origination of loaded nuclear RISC in vivo in human cells. *Nucleic Acids Res,* 36**,** 6439-49.
OKAMURA, K., HAGEN, J. W., DUAN, H., TYLER, D. M. & LAI, E. C. 2007. The mirtron pathway generates microRNA-class regulatory RNAs in Drosophila. *Cell,* 130**,** 89-100.
PAPAGREGORIOU, G. 2015. MicroRNAs in Disease. *In:* FELEKKIS, K. & VOSKARIDES, K. (eds.) *Genomic Elements in Health, Disease and Evolution - Junk DNA.* Springer New York.
PATRAKKA, J. & TRYGGVASON, K. 2010. Molecular make-up of the glomerular filtration barrier. *Biochem Biophys Res Commun,* 396**,** 164-9.
PAVENSTADT, H., KRIZ, W. & KRETZLER, M. 2003. Cell biology of the glomerular podocyte. *Physiol Rev,* 83**,** 253-307.
PENG, Z. Y., GU, R. H. & YAN, B. 2019. Downregulation of exosome-encapsulated miR-548c-5p is associated with poor prognosis in colorectal cancer. *Journal of Cellular Biochemistry,* 120**,** 1457-1463.
PETERS, L. & MEISTER, G. 2007. Argonaute proteins: mediators of RNA silencing. *Mol Cell,* 26**,** 611-23.
PHILIPPE, A., NEVO, F., ESQUIVEL, E. L., REKLAITYTE, D., GRIBOUVAL, O., TETE, M. J., LOIRAT, C., DANTAL, J., FISCHBACH, M., POUTEIL-NOBLE, C., DECRAMER, S., HOEHNE, M., BENZING, T., CHARBIT, M., NIAUDET, P. & ANTIGNAC, C. 2008. Nephrin mutations can cause childhood-onset steroid-resistant nephrotic syndrome. *J Am Soc Nephrol,* 19**,** 1871-8.
PIRIYAPONGSA, J. & JORDAN, I. K. 2007. A family of human microRNA genes from miniature inverted-repeat transposable elements. *PLoS One,* 2**,** e203.
PLACE, R. F., LI, L. C., POOKOT, D., NOONAN, E. J. & DAHIYA, R. 2008. MicroRNA-373 induces expression of genes with complementary promoter sequences. *Proc Natl Acad Sci U S A,* 105**,** 1608-13.
POLITZ, J. C., HOGAN, E. M. & PEDERSON, T. 2009. MicroRNAs with a nucleolar location. *RNA,* 15**,** 1705-15.
QUAGGIN, S. E. & KREIDBERG, J. A. 2008. Development of the renal glomerulus: good neighbors and good fences. *Development,* 135**,** 609-20.
RASCLE, A., SULEIMAN, H., NEUMANN, T. & WITZGALL, R. 2007. Role of transcription factors in podocytes. *Nephron Exp Nephrol,* 106**,** e60-6.
REINHART, B. J., SLACK, F. J., BASSON, M., PASQUINELLI, A. E., BETTINGER, J. C., ROUGVIE, A. E., HORVITZ, H. R. & RUVKUN, G. 2000. The 21-nucleotide let-7 RNA regulates developmental timing in Caenorhabditis elegans. *Nature,* 403**,** 901-6.
REYES-GUTIERREZ, P., RITLAND POLITZ, J. C. & PEDERSON, T. 2014. A mRNA

and cognate microRNAs localize in the nucleolus. *Nucleus,* 5**,** 636-42.
RODRIGUEZ, A., GRIFFITHS-JONES, S., ASHURST, J. L. & BRADLEY, A. 2004. Identification of mammalian microRNA host genes and transcription units. *Genome Res,* 14**,** 1902-10.
ROSELLI, S., HEIDET, L., SICH, M., HENGER, A., KRETZLER, M., GUBLER, M. C. & ANTIGNAC, C. 2004. Early glomerular filtration defect and severe renal disease in podocin-deficient mice. *Mol Cell Biol,* 24**,** 550-60.
SALEEM, M. A., O'HARE, M. J., REISER, J., COWARD, R. J., INWARD, C. D., FARREN, T., XING, C. Y., NI, L., MATHIESON, P. W. & MUNDEL, P. 2002. A conditionally immortalized human podocyte cell line demonstrating nephrin and podocin expression. *J Am Soc Nephrol,* 13**,** 630-8.
SASAKI, T., SHIOHAMA, A., MINOSHIMA, S. & SHIMIZU, N. 2003. Identification of eight members of the Argonaute family in the human genome. *Genomics,* 82**,** 323-30.
SCHRAIVOGEL, D., SCHINDLER, S. G., DANNER, J., KREMMER, E., PFAFF, J., HANNUS, S., DEPPING, R. & MEISTER, G. 2015. Importin-beta facilitates nuclear import of human GW proteins and balances cytoplasmic gene silencing protein levels. *Nucleic Acids Res,* 43**,** 7447-61.
SCHRAMKE, V., SHEEDY, D. M., DENLI, A. M., BONILA, C., EKWALL, K., HANNON, G. J. & ALLSHIRE, R. C. 2005. RNA-interference-directed chromatin modification coupled to RNA polymerase II transcription. *Nature,* 435**,** 1275-9.
SEOK, H., HAM, J., JANG, E. S. & CHI, S. W. 2016. MicroRNA Target Recognition: Insights from Transcriptome-Wide Non-Canonical Interactions. *Mol Cells,* 39**,** 375-81.
SHI, S., YU, L., CHIU, C., SUN, Y., CHEN, J., KHITROV, G., MERKENSCHLAGER, M., HOLZMAN, L. B., ZHANG, W., MUNDEL, P. & BOTTINGER, E. P. 2008. Podocyte-selective deletion of dicer induces proteinuria and glomerulosclerosis. *J Am Soc Nephrol,* 19**,** 2159-69.
SHI, S., YU, L., ZHANG, T., QI, H., XAVIER, S., JU, W. & BOTTINGER, E. 2013. Smad2-dependent downregulation of miR-30 is required for TGF-beta-induced apoptosis in podocytes. *PLoS One,* 8**,** e75572.
SHIN, C., NAM, J. W., FARH, K. K., CHIANG, H. R., SHKUMATAVA, A. & BARTEL, D. P. 2010. Expanding the microRNA targeting code: functional sites with centered pairing. *Mol Cell,* 38**,** 789-802.
SMIT, A. F. A., HUBLEY, R. & GREEN, P. 2013-2015. *RepeatMasker Open-4.0* [Online]. Available: http://www.repeatmasker.org [Accessed].
SPENGLER, R. M., ZHANG, X., CHENG, C., MCLENDON, J. M., SKEIE, J. M., JOHNSON, F. L., DAVIDSON, B. L. & BOUDREAU, R. L. 2016. Elucidation of transcriptome-wide microRNA binding sites in human cardiac tissues by Ago2 HITS-CLIP. *Nucleic Acids Res,* 44**,** 7120-31.
STEFANI, G. & SLACK, F. J. 2012. A 'pivotal' new rule for microRNA-mRNA interactions. *Nat Struct Mol Biol,* 19**,** 265-6.
SUBRAMANIAN A, S. E.-H., EMANI M, SAHAKIAN N, VERNON K, ZHOU Y, KOST-ALIMOVA M, WEINS A, SLYPER M, WALDMAN J, DIONNE D, NGUYEN LT, MARSHALL J, ROSENBLATT-ROSEN O, REGEV A, GREKA A 2019. Kidney organoid reproducibility across multiple human iPSC lines and diminished off target cells after transplantation revealed by single cell transcriptomics. *bioRxiv:516807.*
SUGIMOTO, H., HAMANO, Y., CHARYTAN, D., COSGROVE, D., KIERAN, M., SUDHAKAR, A. & KALLURI, R. 2003. Neutralization of circulating vascular endothelial growth factor (VEGF) by anti-VEGF antibodies and soluble VEGF receptor 1 (sFlt-1) induces proteinuria. *J Biol Chem,* 278**,** 12605-8.
SUH, J. H. & MINER, J. H. 2013. The glomerular basement membrane as a barrier to

albumin. *Nat Rev Nephrol,* 9**,** 470-7.
TAKEMOTO, M., HE, L., NORLIN, J., PATRAKKA, J., XIAO, Z., PETROVA, T., BONDJERS, C., ASP, J., WALLGARD, E., SUN, Y., SAMUELSSON, T., MOSTAD, P., LUNDIN, S., MIURA, N., SADO, Y., ALITALO, K., QUAGGIN, S. E., TRYGGVASON, K. & BETSHOLTZ, C. 2006. Large-scale identification of genes implicated in kidney glomerulus development and function. *EMBO J,* 25**,** 1160-74.
VAN DER WEYDEN, L. & ADAMS, D. J. 2007. The Ras-association domain family (RASSF) members and their role in human tumourigenesis. *Biochim Biophys Acta,* 1776**,** 58-85.
VERDEL, A., JIA, S., GERBER, S., SUGIYAMA, T., GYGI, S., GREWAL, S. I. & MOAZED, D. 2004. RNAi-mediated targeting of heterochromatin by the RITS complex. *Science,* 303**,** 672-6.
WANG, Z., WANG, P., WANG, Z., QIN, Z., XIU, X., XU, D., ZHANG, X. & WANG, Y. 2018. MiRNA-548c-5p downregulates inflammatory response in preeclampsia via targeting PTPRO. *J Cell Physiol*.
WEI, Y., LI, L., WANG, D., ZHANG, C. Y. & ZEN, K. 2014. Importin 8 regulates the transport of mature microRNAs into the cell nucleus. *J Biol Chem,* 289**,** 10270-5.
WEINMANN, L., HOCK, J., IVACEVIC, T., OHRT, T., MUTZE, J., SCHWILLE, P., KREMMER, E., BENES, V., URLAUB, H. & MEISTER, G. 2009. Importin 8 is a gene silencing factor that targets argonaute proteins to distinct mRNAs. *Cell,* 136**,** 496-507.
WELSH, G. I. & SALEEM, M. A. 2010. Nephrin-signature molecule of the glomerular podocyte? *J Pathol,* 220**,** 328-37.
WELSH, G. I. & SALEEM, M. A. 2011. The podocyte cytoskeleton--key to a functioning glomerulus in health and disease. *Nat Rev Nephrol,* 8**,** 14-21.
WHITE, J. T., ZHANG, B., CERQUEIRA, D. M., TRAN, U. & WESSELY, O. 2010. Notch signaling, wt1 and foxc2 are key regulators of the podocyte gene regulatory network in Xenopus. *Development,* 137**,** 1863-73.
WU, L., FAN, J. & BELASCO, J. G. 2006. MicroRNAs direct rapid deadenylation of mRNA. *Proc Natl Acad Sci U S A,* 103**,** 4034-9.
YANAGIDA-ASANUMA, E., ASANUMA, K., KIM, K., DONNELLY, M., YOUNG CHOI, H., HYUNG CHANG, J., SUETSUGU, S., TOMINO, Y., TAKENAWA, T., FAUL, C. & MUNDEL, P. 2007. Synaptopodin protects against proteinuria by disrupting Cdc42:IRSp53:Mena signaling complexes in kidney podocytes. *Am J Pathol,* 171**,** 415-27.
YI, R., QIN, Y., MACARA, I. G. & CULLEN, B. R. 2003. Exportin-5 mediates the nuclear export of pre-microRNAs and short hairpin RNAs. *Genes Dev,* 17**,** 3011-6.
YOUNGER, S. T. & COREY, D. R. 2011. Transcriptional regulation by miRNA mimics that target sequences downstream of gene termini. *Mol Biosyst,* 7**,** 2383-8.
YOUNGER, S. T., PERTSEMLIDIS, A. & COREY, D. R. 2009. Predicting potential miRNA target sites within gene promoters. *Bioorg Med Chem Lett,* 19**,** 3791-4.
ZHANG, Z., ZHU, Z., WATABE, K., ZHANG, X., BAI, C., XU, M., WU, F. & MO, Y. Y. 2013. Negative regulation of lncRNA GAS5 by miR-21. *Cell Death Differ,* 20**,** 1558-68.
ZHDANOVA, O., SRIVASTAVA, S., DI, L., LI, Z., TCHELEBI, L., DWORKIN, S., JOHNSTONE, D. B., ZAVADIL, J., CHONG, M. M., LITTMAN, D. R., HOLZMAN, L. B., BARISONI, L. & SKOLNIK, E. Y. 2011. The inducible deletion of Drosha and microRNAs in mature podocytes results in a collapsing glomerulopathy. *Kidney Int,* 80**,** 719-30.
ZHU, J., SUN, N., AOUDJIT, L., LI, H., KAWACHI, H., LEMAY, S. & TAKANO, T. 2008. Nephrin mediates actin reorganization via phosphoinositide 3-kinase in

podocytes. *Kidney Int,* 73**,** 556-66.

Appendix.

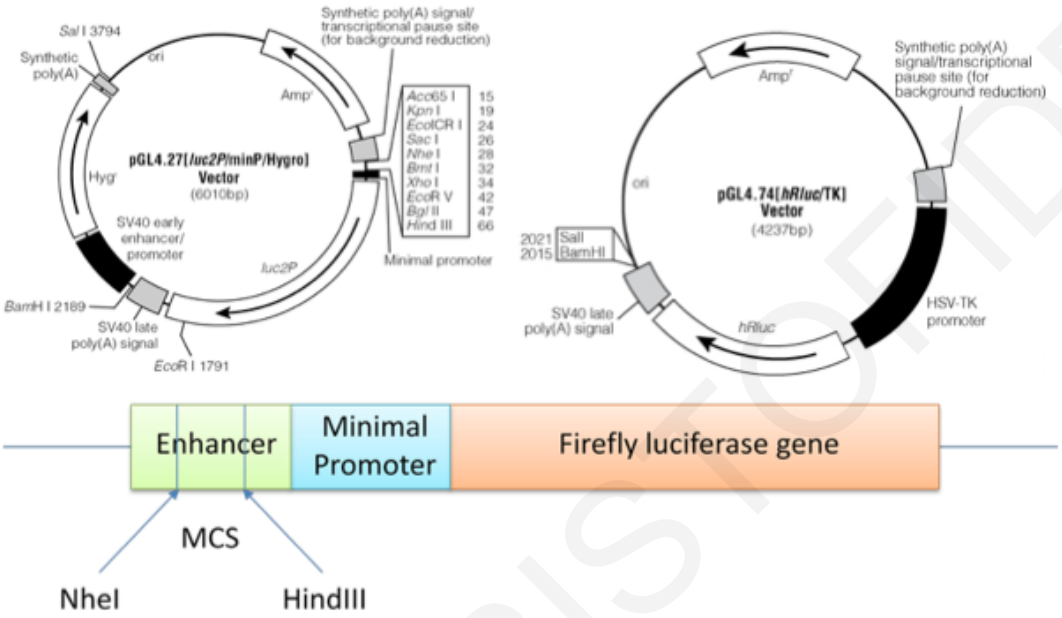

Supp. Figure 1: The plasmid maps for the pGL4.27 firefly and pGL4.74 renilla luciferase vector used in the luciferase reporter assays, as well as an illustration of the multiple cloning site of the pGL4.27 vector in relation to the promoter and the luciferase gene including the restriction enzymes, *Nhe*I and *Hind*III, used for cloning the inserts**.**

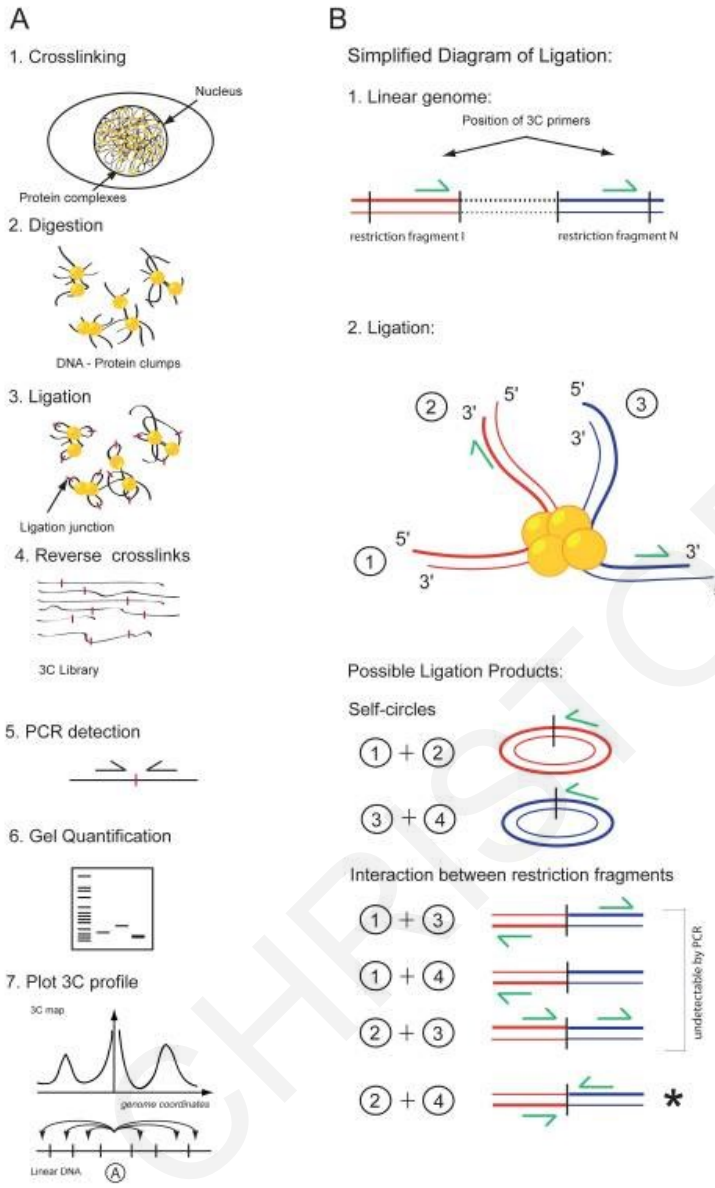

Supp. Figure 2: Chromatin Conformation Capture (3C). **A**. The main steps during 3C comprise of the crosslinking of cells for capturing all interactions inside the cell, followed by lysis and digestion of the crosslinked cells, which allows for the isolation of any protein/DNA complexes present. The digested products are then ligated leading to the formation of new DNA junctions reflecting the proximity of the digested fragments in the sample. Finally, following de-crosslinking and purification, detection and quantification by Real-Time PCR of the resulting products uncover the interactions between the region of interest, known as "anchor", and all other genomic fragments. This is possible because detection primers designed around the restriction sites are all in one direction and thus only in the case of chromatin rearrangement and interaction between two regions a product will be detectable. The results are then compared to a control template, such as a Bacterial Artificial Chromosome (BAC) clone containing the region of interest, within which no conformational rearrangements exist. **B**. Diagram of possible ligation outcomes. Two digestion fragments can be seen in the diagram, red and blue. Fragment ends are labelled 1-4 and the positions of the primers that will be used for detection are depicted as green arrows. Six ligation outcomes are possible, two of which are self-circles. Of the four remaining products, only ligation between fragment end 2 and fragment end 4 is detectable, as only in this case the primers are position appropriately for a PCR product to be detected. [Figure taken from Naumova et al., 2012] (Naumova et al., 2012).

Supplemental data 1: Multiple alignment of miR-548 family members. There are two distinct groups of MIR-548 family members, 5p and 3p microRNAs. Several members of the MIR-548 family share high sequence similarity with some miRNAs being completely identical while others only differ by one or two bases. In the case of miR-548c-5p, two other miRNAs, miR-548am-5p and miR-548o-5p share its mature sequence, but all three miRNAs are derived from separate premature transcripts. The multiple sequence alignment was performed with the ClustalW tool. (https://www.genome.jp/tools-bin/clustalw)

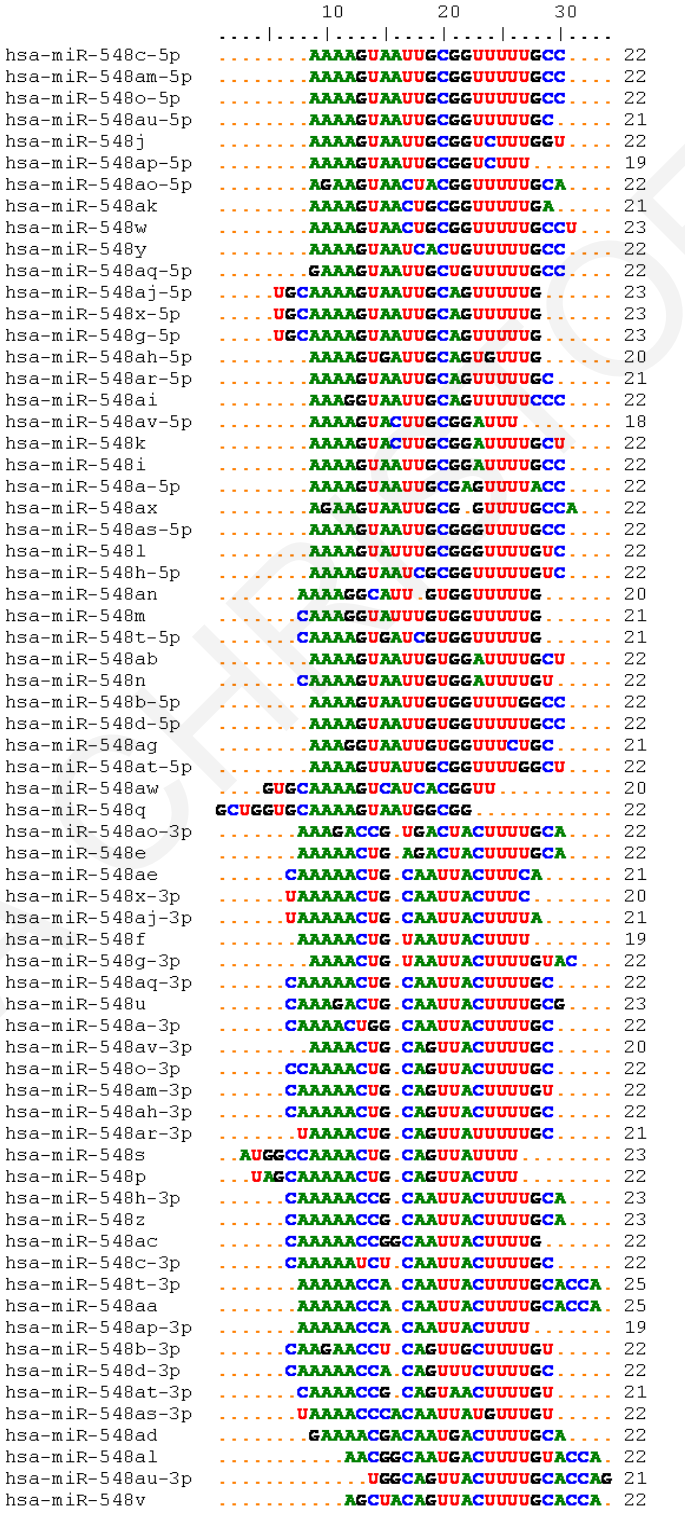

Supplemental data 2: **Made1-type alignment in genes predicted to have miR-548c-5p target sites within their 10kb promoter region.** The sequence depicted represents the sequence including the predicted miR-548c-5p target site and all surrounding nucleotides aligning with the MADE-1 consensus for each predicted target site. The genes highlighted in yellow are the ones whose predicted target site contains <50nt similarity to the Made-1 consensus and thus considered as non-palindromic. Alignment was performed with RepeatMasker (http://www.repeatmasker.org/cgi-bin/WEBRepeatMasker)(Smit et al., 2013-2015), as described in section **3.1.**

FOXC2

```
MADE1#DNA/TcMar-Mariner (1-80nt)

  FOXC2                351 CATTCAAAGTAATGGCAAAAACCGCAATTACTTTTGCACCAACC 394
                             ?
C MADE1#DNA/TcM          47 CATTRAAAGTAATGGCAAAAACCGCAATTACTTTTGCACCAACC 4

Matrix = 20p43g.matrix
Kimura (with divCpGMod) = 0.00
Transitions / transversions = 1.00 (0/0)
Gap_init rate = 0.00 (0 / 43), avg. gap size = 0.0 (0 / 0)
```

ANXA3

```
MADE1#DNA/TcMar-Mariner (1-80nt)

  ANXA3                254 TTTTAATGGCAAAAACCGCAATTACTTTTGCACCAACCTAA 294
                           ?
  MADE1#DNA/TcM         40 TTTYAATGGCAAAAACCGCAATTACTTTTGCACCAACCTAA 80

Matrix = 20p43g.matrix
Kimura (with divCpGMod) = 0.00
Transitions / transversions = 1.00 (0/0)
Gap_init rate = 0.00 (0 / 40), avg. gap size = 0.0 (0 / 0)
```

ATHL1

```
MADE1#DNA/TcMar-Mariner (1-80nt)

  ATHL1                357 GAAAGTAA--GCAAAAACCGCAATTACTTTTGCACCAACCTAA 397
                           ?      --
C MADE1#DNA/TcM          43 RAAAGTAATGGCAAAAACCGCAATTACTTTTGCACCAACCTAA 1

Matrix = 20p43g.matrix
Kimura (with divCpGMod) = 0.00
Transitions / transversions = 1.00 (0/0)
Gap_init rate = 0.03 (1 / 40), avg. gap size = 2.00 (2 / 1)
```

CDC23 - #1

```
MADE1#DNA/TcMar-Mariner (1-80nt)

  CDC23                 26 TTAGGTTGATGCAAAAGTAGTCATGGTTTTTGCCATTAAATGTGATGGCA 75
                               i          i iii             ?  ----------
C MADE1#DNA/TcM          80 TTAGGTTGGTGCAAAAGTAATTGCGGTTTTTGCCATTRAA---------- 41

Matrix = 18p43g.matrix
Kimura (with divCpGMod) = 7.01
Transitions / transversions = 1.00 (5/0)
Gap_init rate = 0.20 (10 / 49), avg. gap size = 1.00 (10 / 10)
```

CDC23 - #2

```
MADE1#DNA/TcMar-Mariner (1-80nt)

  CDC23                372 GTGATGGCAAAAACCGCAATTACTTTTGCACCAACCTAA 410
                             i
C MADE1#DNA/TcM          40 GTAATGGCAAAAACCGCAATTACTTTTGCACCAACCTAA 2

Matrix = 18p43g.matrix
Kimura (with divCpGMod) = 7.01
Transitions / transversions = 1.00 (1/0)
Gap_init rate = 0.00 (0 / 38), avg. gap size = 0.0 (0 / 0)
```

GPR183 (EBI2)
MADE1#DNA/TcMar-Mariner (1-80nt)

```
  EBI2                335 TTAGGTTGGTGGAAAAGTAACTGCAGTTTTTGCC-TTACTTT-AATGGCA 382
                                        v        i   i         -       -
  MADE1#DNA/TcM         1 TTAGGTTGGTGCAAAAGTAATTGCGGTTTTTGCCATTACTTTYAATGGCA 50

  EBI2                383 AAAACCGCAATTACTTTTGCACCAACCTA 411

  MADE1#DNA/TcM        51 AAAACCGCAATTACTTTTGCACCAACCTA 79

Matrix = 18p43g.matrix
Kimura (with divCpGMod) = 2.78
Transitions / transversions = 2.00 (2/1)
Gap_init rate = 0.03 (2 / 76), avg. gap size = 1.00 (2 /
```

FGF23
MADE1#DNA/TcMar-Mariner (1-80nt)

```
  FGF23               107 ATTAAAAGTAATGGCAAAAACCGCAATTACTTTTGCACCGACCT 150
                            ?                                       i
C MADE1#DNA/TcM        46 ATTRAAAGTAATGGCAAAAACCGCAATTACTTTTGCACCAACCT 3

Matrix = 20p43g.matrix
Kimura (with divCpGMod) = 2.38
Transitions / transversions = 1.00 (1/0)
Gap_init rate = 0.00 (0 / 43), avg. gap size = 0.0 (0 / 0)
```

HRK
MADE1#DNA/TcMar-Mariner (1-80nt)

```
  HRK                 171 TTTTTGCCGTTACTTTTAATGGTAAAAACCGCAATTACTTTTGCACCAAC 220
                                    i       ?     i
  MADE1#DNA/TcM        27 TTTTTGCCATTACTTTYAATGGCAAAAACCGCAATTACTTTTGCACCAAC 76

  HRK                 221 CTAA 224

  MADE1#DNA/TcM        77 CTAA 80

Matrix = 20p43g.matrix
Kimura (with divCpGMod) = 3.92
Transitions / transversions = 1.00 (2/0)
Gap_init rate = 0.00 (0 / 53), avg. gap size = 0.0 (0 / 0)
```

LBP - #1
MADE1#DNA/TcMar-Mariner (1-80nt)

```
  LBP                 186 TTAGGTTGGTGCAAAAGTAATTGCGGTTTTTGCCATTACTTTTAAT-GCA 234
                                                                    ?   -
  MADE1#DNA/TcM         1 TTAGGTTGGTGCAAAAGTAATTGCGGTTTTTGCCATTACTTTYAATGGCA 50

  LBP                 235 AAAACCGCAATTAC 248

  MADE1#DNA/TcM        51 AAAACCGCAATTAC 64

Matrix = 20p43g.matrix
Kimura (with divCpGMod) = 0.00
Transitions / transversions = 1.00 (0/0)
Gap_init rate = 0.02 (1 / 62), avg. gap size = 1.00 (1 / 1)
```

LBP - #2
MADE1#DNA/TcMar-Mariner (1-80nt)

```
  LBP                 544 AATCCAGTCTTGGCCGTTACTTTTAATGCCAAAAAAAATAATTACTTTTC 593
                          ------  i  v   i       ?    v      vvii          v
  MADE1#DNA/TcM        25 ------GTTTTTGCCATTACTTTYAATGGCAAAAACCGCAATTACTTTTG 68

  LBP                 594 CATCAACCTAA 604
                            i
  MADE1#DNA/TcM        69 CACCAACCTAA 79

Matrix = 20p43g.matrix
Kimura (with divCpGMod) = 20.84
Transitions / transversions = 1.00 (5/5)
Gap_init rate = 0.10 (6 / 60), avg. gap size = 1.00 (6 / 6)
```

NROB1

```
MADE1#DNA/TcMar-Mariner (1-80nt)

  NROB1                286 TTAGTTTGGTGCAAAAGTAATTGCAGTTTTTGCAATTGAAGGTAATGGCA 335
                             v                   i        v   ?  i
C MADE1#DNA/TcM          80 TTAGGTTGGTGCAAAAGTAATTGCGGTTTTTGCCATTRAAAGTAATGGCA 31

  NROB1                336 AAAACCGCAATTACTTTTGCACCAACCTAA 365

C MADE1#DNA/TcM          30 AAAACCGCAATTACTTTTGCACCAACCTAA 1

Matrix = 18p43g.matrix
Kimura (with divCpGMod) = 4.03
Transitions / transversions = 1.00 (2/2)
Gap_init rate = 0.00 (0 / 79), avg. gap size = 0.0 (0 / 0)
```

NSUN5 - #1

```
MADE1#DNA/TcMar-Mariner (1-80nt)

  NSUN5                 45 TTAGGTTGGTGCAAAAGTAATTGCAGTTTTTGCCATTACTTTTAAAAGTA 94
                                                  i                  ?  vi i
  MADE1#DNA/TcM          1 TTAGGTTGGTGCAAAAGTAATTGCGGTTTTTGCCATTACTTTYAATGGCA 50

  NSUN5                 95 A 95

  MADE1#DNA/TcM         51 A 51

Matrix = 20p43g.matrix
Kimura (with divCpGMod) = 6.51
Transitions / transversions = 3.00 (3/1)
Gap_init rate = 0.00 (0 / 50), avg. gap size = 0.0 (0 / 0)
```

NSUN5 - #2

```
MADE1#DNA/TcMar-Mariner (1-80nt)

  NSUN5                452 TTCAAAGTAATGGCAAAAACCGCAATTACTTTTGAACCAACCTA 495
                             ?                              v
C MADE1#DNA/TcM          45 TTRAAAGTAATGGCAAAAACCGCAATTACTTTTGCACCAACCTA 2

Matrix = 20p43g.matrix
Kimura (with divCpGMod) = 2.37
Transitions / transversions = 0.00 (0/1)
Gap_init rate = 0.00 (0 / 43), avg. gap size = 0.0 (0 / 0)
```

PLAC1

```
MADE1#DNA/TcMar-Mariner (1-80nt)

  PLAC1                530 TTAGGTTGGTGGAAAA-TGATTGCAGTTTTTGCCACTAATTTCAACGGCA 578
                                     v    - i     i          i  v   ?  i
  MADE1#DNA/TcM          1 TTAGGTTGGTGCAAAAGTAATTGCGGTTTTTGCCATTACTTTYAATGGCA 50

  PLAC1                579 AAAACCGCAATTACTTTTGCATCAACCTAA 608
                                           i
  MADE1#DNA/TcM         51 AAAACCGCAATTACTTTTGCACCAACCTAA 80

Matrix = 18p43g.matrix
Kimura (with divCpGMod) = 8.32
Transitions / transversions = 2.50 (5/2)
Gap_init rate = 0.01 (1 / 78), avg. gap size = 1.00 (1 / 1)
```

PSTPIP2

```
MADE1#DNA/TcMar-Mariner (1-80nt)

  PSTPIP2              300 TTACTATTAAAAGTCATGGCAAAAACCGCAATTACTTTTGTACCAATCTA 349
                             i i   ?     v                    i     i
C MADE1#DNA/TcM          51 TTGCCATTRAAAGTAATGGCAAAAACCGCAATTACTTTTGCACCAACCTA 2

Matrix = 20p43g.matrix
Kimura (with divCpGMod) = 11.19
Transitions / transversions = 4.00 (4/1)
Gap_init rate = 0.00 (0 / 49), avg. gap size = 0.0 (0 / 0)
```

PTER

```
MADE1#DNA/TcMar-Mariner (1-80nt)

  PTER                285 TTAGGTTGGTGCAGAAGTAATTGCGGTTTTTGCCATT------------A 322
                                    i                        ------------
  MADE1#DNA/TcM         1 TTAGGTTGGTGCAAAAGTAATTGCGGTTTTTGCCATTACTTTYAATGGCA 50

  PTER                323 AAAACCGCAATTACTTTTGCACCAGC 348
                                                  i
  MADE1#DNA/TcM        51 AAAACCGCAATTACTTTTGCACCAAC 76

Matrix = 18p43g.matrix
Kimura (with divCpGMod) = 3.23
Transitions / transversions = 1.00 (2/0)
Gap_init rate = 0.02 (1 / 63), avg. gap size = 12.00 (12 / 1)
```

RBP4

```
MADE1#DNA/TcMar-Mariner (1-80nt)

  RBP4                304 TTAGGTTGGTACAAAAATAATAGCGATTTTCCCCATTACTTTTAGTGGCA 353
                                  i     i    v   i    iv          ? i
  MADE1#DNA/TcM         1 TTAGGTTGGTGCAAAAGTAATTGCGGTTTTTGCCATTACTTTYAATGGCA 50

  RBP4                354 AAAACCGCAATTACTTTTGTACCAACCTAA 383
                                           i
  MADE1#DNA/TcM        51 AAAACCGCAATTACTTTTGCACCAACCTAA 80

Matrix = 18p43g.matrix
Kimura (with divCpGMod) = 11.05
Transitions / transversions = 3.00 (6/2)
Gap_init rate = 0.00 (0 / 79), avg. gap size = 0.0 (0 / 0)
```

SSH1 - #1

```
MADE1#DNA/TcMar-Mariner (1-80nt)

  SSH1                328 TTAATGACAAAA-CCGCAATTACTTTTGCACCA 359
                           ?    i     -
  MADE1#DNA/TcM        42 TYAATGGCAAAAACCGCAATTACTTTTGCACCA 74

Matrix = 20p43g.matrix
Kimura (with divCpGMod) = 3.33
Transitions / transversions = 1.00 (1/0)
Gap_init rate = 0.03 (1 / 31), avg. gap size = 1.00 (1 / 1)
```

SSH1 - #2

```
MADE1#DNA/TcMar-Mariner (1-80nt)

  SSH1                335 CAAAACCGCAATTAC---TTTTGCACCATTAAAAAAAAAAAAAAATGACAA 381
                             -- i    i ---      --    ?   iv  ------  i
C MADE1#DNA/TcM        69 CAAAA--GTAATTGCGGTTTTTGC--CATTRAAAGTAA------TGGCAA 30

  SSH1                382 AAACCGCAATTACTTTTGCACCAACCTAA 410

C MADE1#DNA/TcM        29 AAACCGCAATTACTTTTGCACCAACCTAA 1

Matrix = 20p43g.matrix
Kimura (with divCpGMod) = 8.23
Transitions / transversions = 4.00 (4/1)
Gap_init rate = 0.15 (11 / 75), avg. gap size = 1.18 (13 / 11)
```

SSH1 - #3

```
MADE1#DNA/TcMar-Mariner (1-80nt)

  SSH1                374 AATGACAAAAACCGCAATTACTTTTGCACCAACCTAA 410
                             i
  MADE1#DNA/TcM        44 AATGGCAAAAACCGCAATTACTTTTGCACCAACCTAA 80

Matrix = 20p43g.matrix
Kimura (with divCpGMod) = 2.78
Transitions / transversions = 1.00 (1/0)
Gap_init rate = 0.00 (0 / 36), avg. gap size = 0.0 (0 / 0)
```

UBQLN2 - #1
MADE1#DNA/TcMar-Mariner (1-80nt)

```
  UBQLN2              326 TTAGGTTGGTGCAAAAGTAATTGCGGTTTTTGCTATTACTTTCAATGGCA 375
                                                          i        ?
  MADE1#DNA/TcM         1 TTAGGTTGGTGCAAAAGTAATTGCGGTTTTTGCCATTACTTTYAATGGCA 50

  UBQLN2              376 AAAACC 381

  MADE1#DNA/TcM        51 AAAACC 56
```

Matrix = 20p43g.matrix
Kimura (with divCpGMod) = 1.85
Transitions / transversions = 1.00 (1/0)
Gap_init rate = 0.00 (0 / 55), avg. gap size = 0.0 (0 / 0)

UBQLN2 - #2
MADE1#DNA/TcMar-Mariner (1-80nt)

```
  UBQLN2              402 CGTTACTTTCAATGGCAAAAACCGCAATTACTTTTGCATCAACCTAA 448
                            i       ?                          i
  MADE1#DNA/TcM        34 CATTACTTTYAATGGCAAAAACCGCAATTACTTTTGCACCAACCTAA 80
```

Matrix = 20p43g.matrix
Kimura (with divCpGMod) = 4.55
Transitions / transversions = 1.00 (2/0)
Gap_init rate = 0.00 (0 / 46), avg. gap size = 0.0 (0 / 0)

ACSM2A
MADE1#DNA/TcMar-Mariner (1-80nt)

```
  ACSM2A              278 TTAGGTTGGTACAAAAGCAATTGCGGTTTTTGCCATTCCTTTTGATGGTA 327
                                  i      i                 v    ?i    i
  MADE1#DNA/TcM         1 TTAGGTTGGTGCAAAAGTAATTGCGGTTTTTGCCATTACTTTYAATGGCA 50

  ACSM2A              328 AAAACCGCAATTACTTTTGCACAAATCTAA 357
                                           v  i
  MADE1#DNA/TcM        51 AAAACCGCAATTACTTTTGCACCAACCTAA 80
```

Matrix = 18p43g.matrix
Kimura (with divCpGMod) = 9.54
Transitions / transversions = 2.50 (5/2)
Gap_init rate = 0.00 (0 / 79), avg. gap size = 0.0 (0 / 0)

ACSM2B
MADE1#DNA/TcMar-Mariner (1-80nt)

```
  ACSM2B              278 TTAGGTTGGTACAAAAGCAATTGCGGTTTTTGCCATTCCTTTTGATGGTA 327
                                  i      i                 v    ?i    i
  MADE1#DNA/TcM         1 TTAGGTTGGTGCAAAAGTAATTGCGGTTTTTGCCATTACTTTYAATGGCA 50

  ACSM2B              328 AAAACCGCAATTACTTTTGCACAAATCTAA 357
                                           v  i
  MADE1#DNA/TcM        51 AAAACCGCAATTACTTTTGCACCAACCTAA 80
```

Matrix = 18p43g.matrix
Kimura (with divCpGMod) = 9.54
Transitions / transversions = 2.50 (5/2)
Gap_init rate = 0.00 (0 / 79), avg. gap size = 0.0 (0 / 0)

C1ORF94
MADE1#DNA/TcMar-Mariner (1-80nt)

```
  C1ORF94             347 TAGGTTGGTACAAAAGTAATTGTGGTTTTTGCCATTGCAAGTGATGGCAA 396
                                  i            i             ?v    i
C MADE1#DNA/TcM        79 TAGGTTGGTGCAAAAGTAATTGCGGTTTTTGCCATTRAAAGTAATGGCAA 30

  C1ORF94             397 AAACCGCAATTACTTTTGCACCAACCTAA 425

C MADE1#DNA/TcM        29 AAACCGCAATTACTTTTGCACCAACCTAA 1
```

Matrix = 18p43g.matrix
Kimura (with divCpGMod) = 4.10
Transitions / transversions = 3.00 (3/1)
Gap_init rate = 0.00 (0 / 78), avg. gap size = 0.0 (0 / 0)

CLYBL - #1

```
MADE1#DNA/TcMar-Mariner (1-80nt)

  CLYBL                214 TTAGGTCGGTGCAAAAGTAATTGTGGGTTTTGCCATTATTTTCAAT 259
                                    i                i  v           i   ?
  MADE1#DNA/TcM          1 TTAGGTTGGTGCAAAAGTAATTGCGGTTTTTGCCATTACTTTYAAT 46

Matrix = 20p43g.matrix
Kimura (with divCpGMod) = 7.28
Transitions / transversions = 3.00 (3/1)
Gap_init rate = 0.00 (0 / 45), avg. gap size = 0.0 (0 / 0)
```

CLYBL - #2

```
MADE1#DNA/TcMar-Mariner (1-80nt)

  CLYBL                372 GTTCTTGCCATTACTTTGAATGGCAAAAACCGCAATTACTTTGGCATGAA 421
                             i           ?                          v   iv
  MADE1#DNA/TcM         26 GTTTTTGCCATTACTTTYAATGGCAAAAACCGCAATTACTTTTGCACCAA 75

  CLYBL                422 CCTAA 426

  MADE1#DNA/TcM         76 CCTAA 80

Matrix = 20p43g.matrix
Kimura (with divCpGMod) = 7.81
Transitions / transversions = 1.00 (2/2)
Gap_init rate = 0.00 (0 / 54), avg. gap size = 0.0 (0 / 0)
```

GPR141 (PGR13)

```
MADE1#DNA/TcMar-Mariner (1-80nt)

  GPR141(PGR13)        385 TTAGGTTGTTGCAAAAGTAATTGCGGTTTTTGTCATTGCTTTGAATGGCA 434
                             v                      i    i    ?
  MADE1#DNA/TcM          1 TTAGGTTGGTGCAAAAGTAATTGCGGTTTTTGCCATTACTTTYAATGGCA 50

  GPR141(PGR13)        435 AAAACCGCAATTACTTTTGCAACAACCTA 463
                                          v
  MADE1#DNA/TcM         51 AAAACCGCAATTACTTTTGCACCAACCTA 79

Matrix = 18p43g.matrix
Kimura (with divCpGMod) = 5.32
Transitions / transversions = 1.00 (2/2)
Gap_init rate = 0.00 (0 / 78), avg. gap size = 0.0 (0 / 0)
```

NLRP11

```
MADE1#DNA/TcMar-Mariner (1-80nt)

  NLRP11               348 TTAGGTTGGTGCAAAAGTAATTGTGGTTTTTGCCATGAAAAA-AATG-CA 395
                                                 i            v?   i-    -
C MADE1#DNA/TcM         80 TTAGGTTGGTGCAAAAGTAATTGCGGTTTTTGCCATTRAAAGTAATGGCA 31

  NLRP11               396 AAAACCGCAATTACTTTTGTACCAACCTAA 425
                                             i
C MADE1#DNA/TcM         30 AAAACCGCAATTACTTTTGCACCAACCTAA 1

Matrix = 18p43g.matrix
Kimura (with divCpGMod) = 4.15
Transitions / transversions = 3.00 (3/1)
Gap_init rate = 0.03 (2 / 77), avg. gap size = 1.00 (2 / 2)
```

OR2T8

```
MADE1#DNA/TcMar-Mariner (1-80nt)

  OR2T8                309 TACTTTCAATGGCAAAAACCGCAATTACTTTTGCACCAATCT 350
                             ?                                      i
  MADE1#DNA/TcM         37 TACTTTYAATGGCAAAAACCGCAATTACTTTTGCACCAACCT 78

Matrix = 20p43g.matrix
Kimura (with divCpGMod) = 2.50
Transitions / transversions = 1.00 (1/0)
Gap_init rate = 0.00 (0 / 41), avg. gap size = 0.0 (0 / 0)
```

ORM1
MADE1#DNA/TcMar-Mariner (1-80nt)

```
  ORM1                236 TTACATTGGTGCCAAAGTAATTGCGGTTTTTGTCATTACTTCTAAATGGC 285
                            vi       v                   i        i?  -
  MADE1#DNA/TcM         1 TTAGGTTGGTGCAAAAGTAATTGCGGTTTTTGCCATTACTTTYAA-TGGC 49

  ORM1                286 AAAAACCGCAATTACTTTGGCACCGACCTAA 316
                                        v     i
  MADE1#DNA/TcM        50 AAAAACCGCAATTACTTTTGCACCAACCTAA 80
```

```
Matrix = 18p43g.matrix
Kimura (with divCpGMod) = 9.47
Transitions / transversions = 1.33 (4/3)
Gap_init rate = 0.01 (1 / 80), avg. gap size = 1.00 (1 / 1)
```